UNIVERSITY OF CALIFORNIA
RIVERSIDE

Plug-in Electric Vehicles: Challenges of Increased Penetration and Optimal Solutions Using Load Modeling, Prediction & Grid Integration

A Dissertation submitted in partial satisfaction
of the requirements for the degree of

Doctor of Philosophy

in

Electrical Engineering

by

Jubair Yusuf

September 2022

Dissertation Committee:
Dr. Sadrul Ula, Co-Chairperson
Dr. Matthew Barth, Co-Chairperson
Dr. Hamed Mohsenian-Rad

The Dissertation of Jubair Yusuf is approved:

_____

_____

Committee Co-Chairperson

_____

Committee Co-Chairperson

University of California, Riverside

ACKNOWLEDGMENT

All the thanks to the Almighty for coming this far in my life and making me able to finish my Ph.D. I would like to thank my supervisor Dr Sadrul Ula for his continuous support and motivation to try relentlessly for more achievements. He has always encouraged me to do more in-depth research and make myself more self-independent in the process. The regular conversations with him have helped me to reshape my approach and become more strategic to any research problems. He has always been willing to help and aware with the current energy related problems that has helped me to look at the bigger picture of my research and its real-life implementation. My Ph.D. journey would not be finished in time without his guidance.

Then, I want to thank Dr. Matthew Barth for his insightful inputs in our regular weekly meetings that has helped me to make this dissertation more thorough. His vast knowledge on sustainable transportation has helped me to have a better understanding on the overlapping areas of transportation and energy. I would also like to thank my dissertation committee member Dr Hamed Mohsenian-Rad for taking time to serve my committee. I would like to mention my lab mate ASM Jahid Hasan. It would not be possible to continue this journey and make all the publications without his help. He has always been there to support me. Special thanks to my other team members, Henry Gomez, Michael Todd, Dr Miroslav Penchev, Luis Enriquez-Contreras, Jacqueline Garrido Escobar, Dr Alfredo Martinez-Morales, Dr Yun Xue, Dr Hao Xin for their support and collaboration in different projects and research papers.

In addition to the aforementioned people, I am also grateful to all the people that worked at SIGI lab at different times. It would not be possible to finish this journey without their help. Even with all the supporting elements available, Ph.D. life gets stressful sometimes. The support from the family and friends become so important at those hard times. I am grateful to my family for their continuous support. My mom Kohinoor Begum and dad Nur Mohammad Miah have sacrificed a lot and always been there to love and support me. My little sister Sumaiya Nur Zahra Nuha has been there to cheer me up with her sweet funny stories of life. My brother Kausar Ismail and sister in law Anika Tabassum have been there encourage me and take care of my parents that has helped to reduce half of my stress.

I am also thankful to all my friends and teachers in my life. My teachers always believe in my ability that boosts my confidence and go for higher studies. I would like to thank my friends: Mustafiz Rahman, Al-Amin Khan, Saiful Islam Sajol, Samin Nur, Dr Ahmed S Arman. On a fine afternoon in Dhaka, a conversation with Arman has motivated me a lot to go for Ph.D. Last but not the least, I am indebted to all my housemates and local community in Riverside. I could not mention all the names but there are more people who contribute to my Ph.D. journey and I feel blessed to have them in my life.

I would also like to acknowledge University of California Electrical and Computer Engineering Department, University of California Office of the President, National Center for Sustainable Transportation (NCST), Esther F. Hays family for partially or fully supporting my Ph.D. study.

The major contents in the dissertation have been published in the Institute of Electrical and Electronics Engineers (IEEE) Transportation Electrification Conference and Expo, North American Power Symposium, IEEE Innovative Smart Grid Technologies North America, IEEE International Conference on Smart Grids and Energy Systems, IEEE Texas Power and Energy Conference, IEEE Kansas Power and Energy Conference, respectively.

DEDICATION

This dissertation is dedicated to my mother Kohinoor Begum, father Nur Mohammad Miah, sister Sumaiya Nur Zahra Nuha and the people I care for.

ABSTRACT OF THE DISSERTATION

Plug-in Electric Vehicle: Challenges of Increased Penetration and Optimal Solution Using Load Modeling, Prediction & Grid Integration

by

Jubair Yusuf

Doctor of Philosophy, Graduate Program in Electrical Engineering
University of California, Riverside, September 2022
Dr. Sadrul Ula, Co-Chairperson
Dr. Matthew Barth, Co-Chairperson

Our sustainable transportation goals have encouraged people to adopt more Plug-in Electric Vehicles (PEVs) in recent times. Incentives and other policies are also encouraging additional PEV penetration. The increasing penetration of PEVs has put new challenges and opportunities in both the transportation and electric grid sectors.

In this dissertation, an optimal framework is introduced to find out the best PEV charging/discharging strategy using microgrids that includes all the Distributed Energy Resources present in a typical modern building microgrid. All the components are modeled and a multi-objective Mixed Integer Linear Programming (MILP) is formulated to minimize both the energy and demand cost. Then, sensitivity analyses are carried out to find out the contributing factors for a PEV Charging Station (CS) selection. A comprehensive techno-economic analysis is executed next and smart charging and discharging strategies are proposed for a combined Light Duty Electric Vehicle (LDEV)

and Heavy Duty Electric Vehicle (HDEV) implementation. A novel data driven methodology is deployed to propose the best investment scenario for an infrastructure owner based on peak reduction, energy cost saving, and minimal payback periods. The influence of fleet size is also shown to validate the model. A real-time Vehicle to Grid (V2G) has also been implemented in both grid-connected and off-grid mode to demonstrate opportunities created by the PEV integration beneficial to the grid.

The user behavior of public PEV charging stations are analyzed next to introduce two utilization factors and predict the electrical load (kW) demand for higher EV penetrations. The success of increased solar production has modified the electrical demand curve in California by shifting peak demand from afternoon to the evening resulting in a "duck curve" requiring rapid ramp-up of thermal generators. The correlation between duck curve and increasing PEV demand is presented to show the PEV impacts on the grid. Then, a customer oriented PEV load modeling is proposed to model the EV load on the grid. Finally, the optimal participation of PEV V2G is explored in a critical demand response event for the grid using a novel framework. The financial benefits for both customers and utilities are presented in PEV V2G participation. The impacts of PEV integration into the grid based on the variety of building load, PEV user behavior and co-simulation are investigated as well.

Table of Contents

List of Tables

List of Figures

1 Introduction

1.1 Background and Motivation

The transportation sector is one of the largest users of energy throughout the world. Population growth, advanced technology, and economic growth are the leading reasons that cause the increase in the transportation sector's energy consumption. According to Statista, 276.49 million vehicles were registered in the U.S in 2019 [1]. The U.S is the largest user of petroleum and the average petroleum consumption in the U.S. was 20.54 million barrels per day in 2019. Sixty-nine percent of this petroleum was consumed in the transportation sector [2]. Alternative fuel technologies are needed to reduce the dependency on petroleum consumption. As renewable energy resources are making inroads in recent years, electrification of transportation will be a major solution towards our sustainable transportation future. The electric power sector in the U.S. uses 37% of primary energy as shown in Figure 1.1 followed by the transportation sector’s energy use of 28% of the total in 2019 [3]. If transportation electrification continues with the increasing number of electric vehicles (EV), then there will be a need for rapid increase in electric power generation. Additional power transmission and distribution capacities will be needed to satisfy this increased demand.

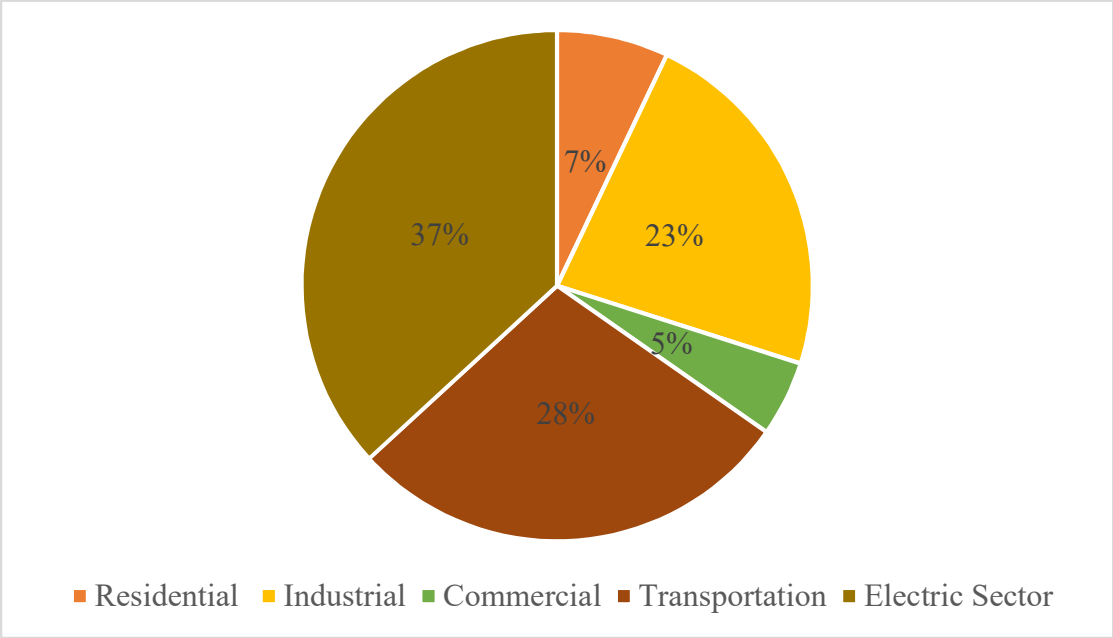

Figure 1.1 Primary Energy Use Share in the US in 2019

EVs are gaining in popularity around the world as a solution to provide a sustainable transportation system, reducing greenhouse gas emissions. The sales of EVs are growing across the world. More than half a million PEVs were sold in the US in 2021 [4] and the number of EVs on the road has already crossed the 3 million mark [5]. Due to the rapid growth of EV usage, the impact on the distribution grid as well as the overall increase in energy consumption is a major concern. Though EVs ensure energy sustainability and clean energy, it also increases the total energy cost when integrated into a building's energy system. Intelligent strategies of EV charging can minimize these building energy costs. Clean energy goals of states like California by 2045 need mass Electric Vehicle (EV) adoption in the transportation sector [6]. Recently, California has set a goal of 5 million Zero-Emission Vehicles (ZEVs) on the roads by 2030 and 250 Thousand

electric vehicle charging stations by 2025 [7] [8]. To cope up with the demand of added energy consumption, optimal charging strategies need to be implemented to minimize the total energy cost. Moreover, the impacts of the building loads and different electricity rates have made the overall EV integration problem more complicated. In addition to that energy optimization problem, EV load modeling is also a concern due to its stochastic nature. The goal of this research is to find these answers: 1) Cost Optimal PEV integration with distributed energy resources and vehicle to grid (V2G) operation; 2) Smart charging and discharging strategies for a heavy-duty and light-duty EV in a workplace setting and implementing V2G to an office building running in off-grid islanded mode; 3) Data-driven PEV load modeling for public PEV charging stations and residential feeders; and 4) Analyzing the grid impacts of PEV integration. This research can help to overcome the challenges associated with mass EV adoption and benefit all the stakeholders (PEV owner, Building/Charging Station owner, and Grid operator).

1.2 Contributions

The key contributions of this dissertation can be summarized as follows:

- An optimal framework is proposed for a distribution level microgrid that helps to find out the best PEV charging/discharging strategy. This also helps the Distribution System Operator (DSO) in PEV Charging Station (CS) selection based on the optimal offline solution impacts and the sensitivity analyses between all the components present in a grid connected commercial building-integrated microgrid.

- An exhaustive cost-benefit analysis has been developed to find out the optimal framework for a combined Light Duty Electric Vehicle (LDEV) and Heavy Duty Electric Vehicle (HDEV) implementation. A novel data-driven methodology is deployed to optimize the overall energy cost that integrates deep learning based prediction model and the PEV availability matrices.
- A novel framework has been proposed to ensure the optimal participation of PEV V2G for a critical demand response event that can be implemented in any Critical Peak Pricing (CPP) rate schedule.
- A rigorous analysis has been made of multifold impacts of PEV integration into the grid based on the variety of building load, feeder types, PEV user behavior and co-simulation. Finally, a real-time Vehicle to Grid (V2G) implementation has been carried out in both grid-connected and off-grid mode

1.3 Organization of the Dissertation Research

The dissertation is organized as follows: Chapter 2 provides the research background and literature review, Chapter 3 describes the cost optimization strategies for PEV operation, Chapter 4 analyzes the PEV load modeling and user behavior, Chapter 5 discusses the PEV impacts on the grid, Chapter 6 shows the real time implementation of V2G in both grid connected and islanded mode, and Chapter 7 concludes the dissertation.

2 Research Background and Literature Review

2.1 Introduction

The number of PEVs on the road are increasing every day that puts unique challenges on the current transportation and electrical distribution infrastructures. The interdependency between both the transportation and grid planners presents impediments that can slow the adoption of electric vehicles. The core challenges of this increased penetration can be divided into three items: 1. PEV Optimal operation, 2. PEV load modeling, and 3. Efficient integration of PEV into the grid. Figure 2.1 shows the overall system infrastructure that represents the increased PEV integration aspects. PEV owners usually charge their PEVs at homes or at their workplaces. These PEV charging stations are the parts of the corresponding building infrastructures. The charging rates of these PEVs can be of four types. 1. Level I charging ($\leq$ 2.4 kW), 2. Level II Charging ($\leq$ 19.2 kW), 3. Level III charging ($\geq$ 50 kW), and 4. Extreme fast charging ($\geq$ 100 kW). Level I and II charging opportunities are the most common charging scenario for residential or commercial buildings. While one PEV charging at these lower rates may not have adverse impact on the overall net demand profile of the building, multiple PEVs can increase the building's net demand significantly. The buildings equipped with distributed energy resources (DERs) may withstand the adverse impact of charging using additional generation from solar or Battery Energy Storage System (BESS). But this scenario highly depends on the solar availability and capacity of BESS. Due to intermittency of these DER resources coupled with the fact that PEV charging activity is highly dependent on the user,

there are multiple areas that require studies for the efficient PEV integration to the system. Modeling the EV load based

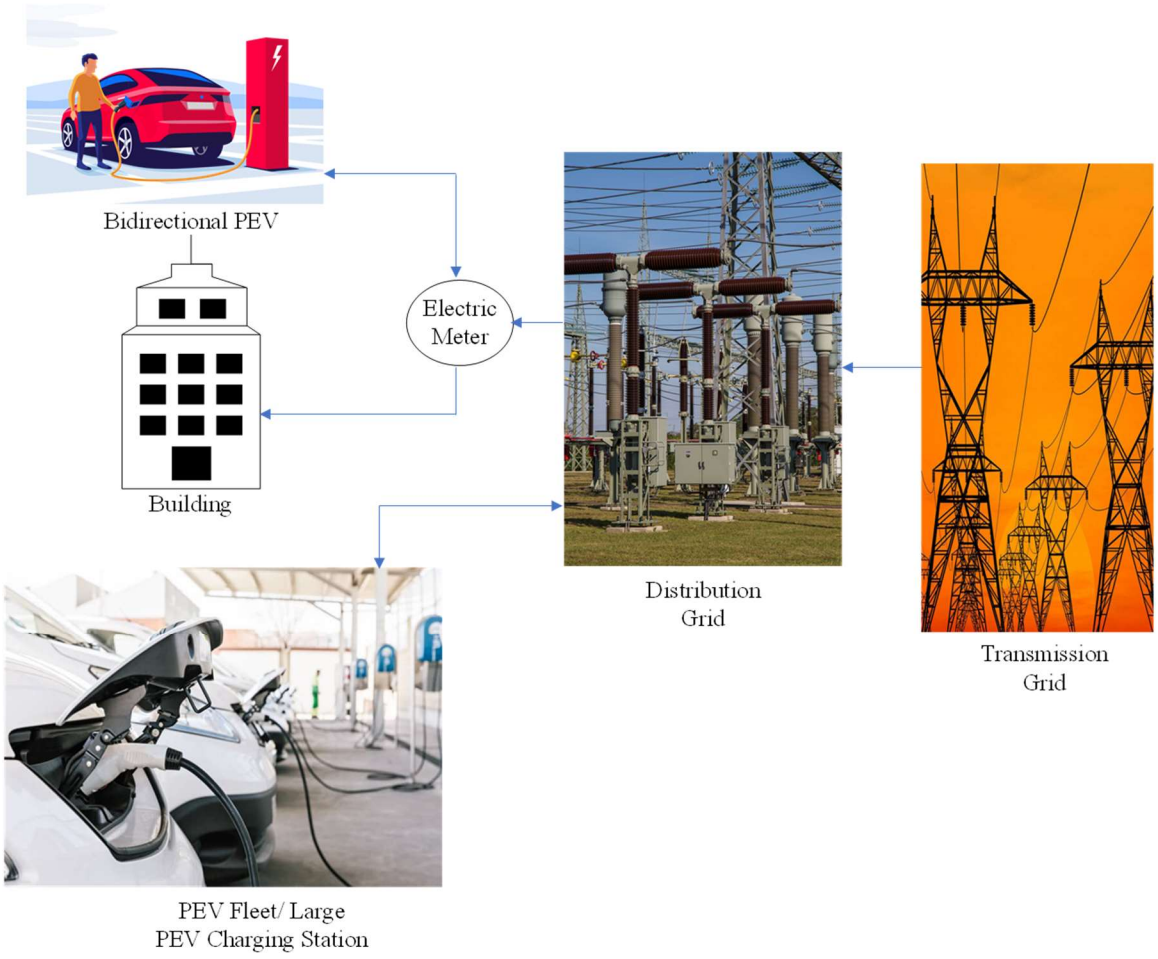

Figure 2.1 PEV Operation and It's Impacts

on their availability and arrival/ departure times and estimating the EV load can help both the building owner and utility planner. Moreover, the optimal scheduling of EV charging can help reduce the peak electrical demands created by EV charging. Based on the availability of level III charging infrastructure, PEV charging at a rate of 50 kW can create

peaks that are 8-10 times higher than the normal peaks that can happen in any regular residential building. This can also be reflected in the electric bill of the building with a very high cost if that building has a demand charge. The availability of V2G enabled vehicle has also made it possible to send energy back to the building. As PEV owner has the freedom to choose if and when to participate in V2G activities, it has also added a new dimension to the optimal operation of PEVs. The building occupants can also contribute to this optimal operation by scheduling their activities which affect their electricity use. A comprehensive modeling of the building loads and implementing the energy reduction opportunities by using the PEV effectively can help solve the interconnected issues of the building and PEV operations.

On the other hand, large public PEV charging stations normally provide charging opportunities for large EV fleets simultaneously. For the large EV fleets in the public charging stations, the charging behavior is different from the charging activities as seen in residential or commercial infrastructures where these depend on the scheduled arrival and departure of the occupants of the buildings. Hence, load modeling is important for the EV fleets at the public charging stations. Moreover, as the number of EVs can be many in the public infrastructure, their combined participation in V2G can help the utility with added energy in times of high demand. The distribution feeder connected to that charging infrastructure may need upgrades as well if there is a need for extreme fast charging capability. The most popular and advanced EV car company Tesla is a good example of the challenges and limitations faced by any fast charging infrastructure. In 2021, Tesla sold 936,000 cars compared to 499,550 in 2020 and 367,500 in 2019 [9]. To make a trip from

Riverside, California to Portland, Oregon with 33 percent of initial SOC for a Tesla car with 82 kWh of capacity, a driver needs to stop 6 times to charge the vehicle as shown by Tesla's trip planner in Figure 2.2. One of the charging stops suggested has 40 charger stalls with 27 of them available at that time as shown in Figure 2.3. The charging capacity available at this location is at a maximum rate of 250 kW. If all the stalls have similar charging capacity and are used at the same time, the total power capacity requirement will be 10 MW. As a typical distribution feeder capacity is 4 MW, it is unlikely that this site has multiple feeders supplying power. If 10 MW capacity is not available at that location and all the stalls are busy at the same time, the charging rates will be lower than 250 kW each. For example, a site in Fremont, CA has 20 stalls with a total capacity of 2 MW, if EVs are plugged in all the stalls, the charging power at each stall will not be more than 100 kW [10]. Similar limitations are true for other locations as well such as in Sequim, WA (8 stalls and transformer capacity is only 300 kW, each stall limited to 37.5 kW when all are being used) [11]. The number of charging stops is another limiting factor for an EV owner to plan for long trips. For example, the distance between Riverside and Portland is 1,015 miles and this model 3 LR has 358 miles of range with one full charge, so there should be maximum of 3 charging stops needed for this trip. But even when one tries to leave with a higher 86 percent initial SOC, the charging stops shown by the Tesla trip planner is 5. This situation gets even worse when these EVCS and any other infrastructure share the same meter or node in a distribution feeder. Hence, advanced modeling is important for both EV and grid for enabling more EV integration and evaluating optimum charging strategies. The coordinated operation can come handy for utilizing the existing limited

capacity as well if costly distribution system upgrade is not possible for that particular node.

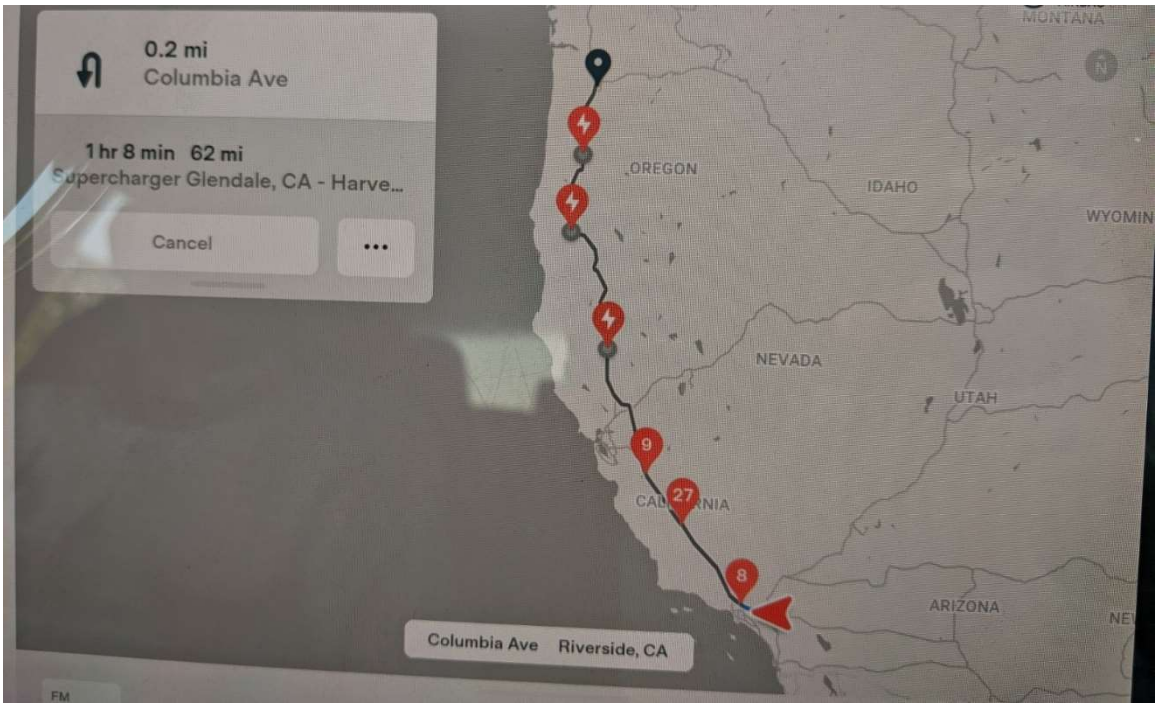

Figure 2.2 Stops Needed for Charging to Make a Trip from Riverside to Oregon with a Tesla 3 LR (initial capacity 33% SOC and capacity 82 kWh, 358 miles)

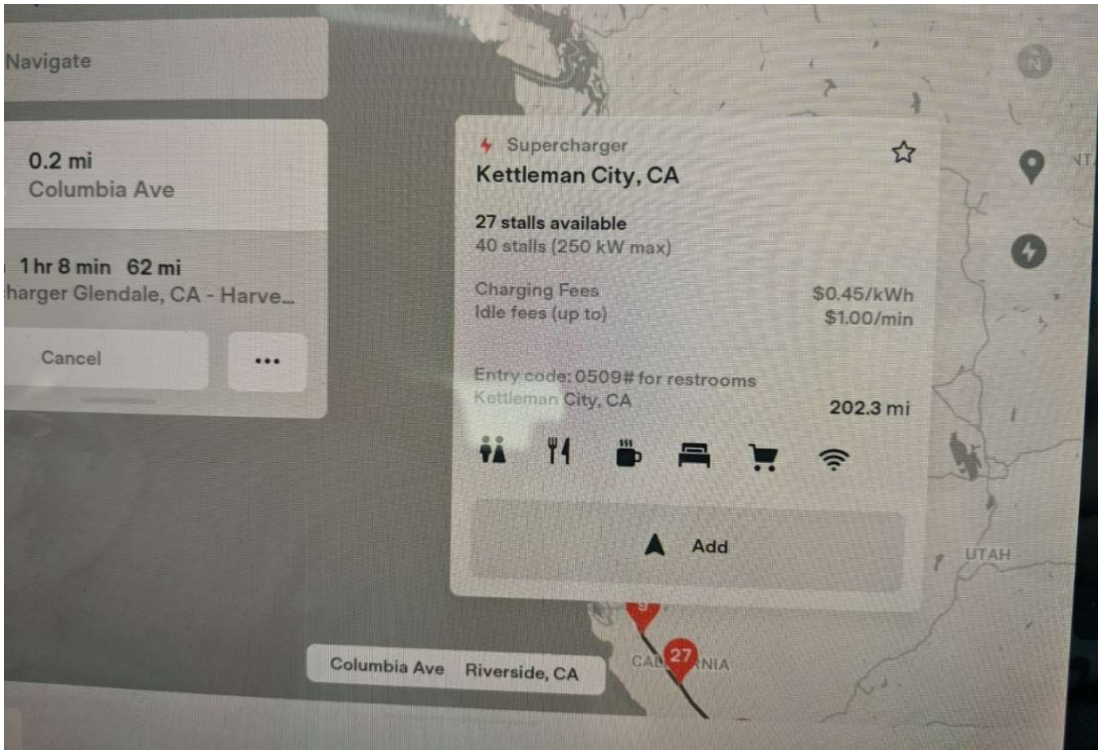

Figure 2.3 A Tesla Supercharger Location with a Maximum Charging Rate of 250 kW

The rapid grid integration of PEV is highly dependent on the capacity of the feeder that is connected to the charging stations or building infrastructures. To determine if any upgrade is needed in the feeder, it is necessary to analyze the current and future impacts of EVs on the grid. These impacts will also be different for feeders serving various types of load. Hence, advanced grid modeling along with the necessary analysis of EV integration scenarios can help the utilities to plan for future expansions. As V2G is becoming more common in the future, a large EV fleet can potentially act as a large battery that can provide the energy back to the grid when needed. Therefore, the analysis of integrated EV impacts is also needed not only on the distribution feeder but also on the transmission and distribution interface.

2.2 PEV Optimal Operation: An Overview

In most cases, PEV charging infrastructure is an integral part of any commercial or residential building. When, the PEV activity and the building share the same electric meter, it requires the optimal PEV operation for the best outcomes in terms of cost for both building and PEV owners. The optimal size of the charging infrastructure is also important for the building or charging infrastructure owner if independent from the building. The availability of HDEVs with higher capacities and higher charging/discharging ratings has created the possibility to invest for a common infrastructure with both LDEV and HDEV implementation.

EV equipped building-integrated microgrids energy use applications have given rise to many modeling and technical studies over the years. Most of the studies focus on optimal planning and operation of a building integrated microgrid irrespective of the presence of renewable and distributed energy resources. The research aspects of these studies can be divided into three categories in general. They are as follows: (a) modeling the building components and using the flexible building loads along with DERs (PV, BESS, PEV, etc.), (b) Optimal scheduling for optimization with different objectives (user comfort, energy reduction, etc.), (c) Types of buildings (residential/commercial). The strategy developed by US DOE energyplus software is more focused on buildings priority zones and fails to capture the dynamic properties of available DERs [12] [13]. In [14] [15] [16] [17] [18] [19] [20] [21], a mixed-integer linear problem is formulated to schedule the energy consumption and minimize the total energy cost of a microgrid along with DERs. The model includes the plug-in loads but avoids the uncertainties associated with the

intermittent energy sources and focuses on the tradeoff between carbon emission and energy cost. Different electricity pricing rates are applied to present various scenarios as well. Issues like BESS and PEV battery degradation have not been taken into consideration in these studies. Stochastic Dual Dynamic Programming is also used to solve the multi-stage stochastic problem that involved the bidirectional PEV approach and solar PV-based hybrid energy storage. But the issues like the level of charging/discharging and lower efficiency of PV-based BESS are ignored during system optimization [22]. In [23], the combination of the thermostat and home energy management system is used for demand response in smart grid applications along with V2G. An optimal charging strategy for residential applications is proposed to shave the peak and reduce the energy cost [24]. In [25], a price-based demand response model is proposed to optimize EV charging and quantify the flexibility of EV charging. An optimization approach is proposed for multi-energy microgrid systems with the vehicle to grid capability and the optimal capacity is estimated [26] [27]. All the studies mentioned here are mainly focused on the temperature modeling of thermal load and use level I and level II charging during any EV integration. The associated vehicle battery systems degradation costs are also not considered on many occasions. The impacts of fast or slow PEV activities on any grid-connected prosumer and their interactions with other controllable loads are still not figured out in the above mentioned literature. While the demand charge is a significant portion of the overall electricity cost, it has not been integrated to the cost functions in any of these references. The framework to find the best charging level for optimal cost is still absent in these

published works. This dissertation attempts to bridge this gap in the literature by offering an optimal framework for the best PEV charging/discharging level selection.

As having optimal charging infrastructure is also an integral part of the PEV optimal operation, this dissertation also tries to find the most cost-effective charging infrastructure for both HDEV and LDEV at the same location. Their optimal operations along with the least payback period can help to find the favorable framework for the building/charging station owners. HDEV and LDEV optimal scheduling have been explored in many studies. Electric buses are often considered as an early example of HDEV implementation around the world. Electric bus CS scheduling is optimized considering an energy storage system and followed by sensitivity analysis [28] [29]. The daily operating cost is minimized but the battery loss model used there to minimize the cost is not conclusive. In [30] [31] , electric bus charging optimization is done under varying operating conditions. Depot charging, end of line charging, and opportunity charging stations are explored to minimize the energy and battery replacement costs. The cost-benefit analysis is executed in [32] to show that a trade-off between the fixed cost and charging cost is needed for the optimal fleet size. In-depot charging has an impact on overall cost minimization and in [33] the cost optimization is carried out for an opportunity charging bus network. While the goal of these studies is optimizing the energy costs for HDEVs, the opportunities of incorporating LDEVs using the same infrastructure, their coordinated operation, and reducing the payback periods are not discussed. Evolutionary algorithms are widely explored by Mixed Integer Programming (MIP) formulation to execute the cost-benefit analysis for mostly LDEVs. In [34], a mixed-integer linear programming (MILP)

problem is formulated to compare the effectiveness of the coordinated and uncoordinated charging strategies where the battery degradation cost is ignored. In [35], evolutionary algorithms are used to reduce electricity costs and battery aging for electric buses. The optimal charging strategy shows improvements in both cost reduction and improving battery life. In [36], a three-stage cooperative energy management system is proposed for a virtual energy hub that provides the minimum operational cost. The virtual energy hub only comprises an electric bus and a simplistic representation of the real test case scenarios. Moreover, the uncertainties are not addressed properly and are more focused on the overall energy management. A bi-objective optimization model is proposed in [37] for battery-electric bus deployment and the trade-off between environmental fairness and resource investment. In [38], an economic evaluation is carried out for adaptive charging algorithm implementation in 16 level-II EVCS and 1 DCFC at the U.S. National Renewable Energy Laboratory. The study mainly focuses on the operation and installation cost along with the reduction in demand charge. The study lacks the detailed modeling of EV and battery degradation. The opportunity for different EVCS, EV, and the payback period of the implementation were not investigated. In [39] , a multi-objective optimization method is applied to find the trade-off between cost and emission aspects of bidirectional EV charging. Next, the reinforcement cost of the grid is determined. Case studies have also been carried out to show the economic benefits of V2G [40] and for different EV charging infrastructure subsidy policies [41]. Cost-benefit analyses were done in smart grid environments for frequency regulation by EV [42] [43], EV grid integration [44] [45] [46] , and privately owned PEV owners [47]. The comparison of cost-efficiency between HDEV

and LDEV implementation at the same infrastructure is still absent in the above mentioned literature. The impacts of net metering on cost optimization for an infrastructure having both HDEV and LDEV are also not analyzed yet. The payback period of different cost-optimal strategies to find the optimal combination of HDEV and LDEV is needed. Therefore, this dissertation also presents a techno-economic comparative analysis for HDEV and LDEV operation to answer some of these concerns.

2.3 PEV Load Modeling: An Overview

To cope with the large number of PEVs and ensure their successful integrations to the grid, modeling the PEV load is important based on the owner's travel schedule and capacity of the distribution feeder. The user behavior and PEV charging scenarios vary for different charging stations (e.g. residential, commercial, public, etc.). Optimal management strategies of these charging stations can ensure the viable growth of electric vehicles. Most of the residential houses and apartments are not equipped with PEV charging stations. Hence, publicly available stations are widely used by PEV users. The behavioral data analysis of these PEV charging stations and modeling the EV load can help the policy makers, charging station providers, and utilities to decide about the necessity of new PEV charging stations' establishment at accessible locations. In addition to the location of charging stations, their management is vital for both CS owners and electric utilities. Uncoordinated charging and unplanned CS management can also lead to distribution network overloading and congestion. Hence, PEV load modeling based on user behavior analysis from public PEV charging stations is highly critical in providing pathways for arriving at strategic optimal decisions. The PEV owner's PEV models and their initial and

final SOC are unknown in most of the cases for the EVCS operators. The unavailability of these two vital information makes policy making decisions and user behavior more difficult to comprehend. Moreover, public PEV charging stations include a variety of PEV users and can differ with the general PEV user behavior for any regular workplace or home. So, general modeling based on regular work or home schedules is unable to model and analyze the fleets distinctly. A lot of studies have been performed on user behavior analysis using collected data from the PEV stations. In general, public PEV charging stations collect the start and end time of the charging sessions and total energy consumption by the respective PEV. Data available in public PEV charging stations are used to model the user behavior with the time of day and CS locations [48] [49] [50]. The PEV load profile is generated using the arrival time information along with the total travelled distance. The load profile was added to regular transformer loading to assess the impact of PEV charging [51]. A general model is proposed for PEV users' charging behavior to reduce congestion and make the CS profitable for the owners [52]. Multinomial logistic regression was done to show the key variables' impacts on charging behavior based on CS data along with environmental effects analysis [53] [54]. Typical data evaluation and analysis is also done to show the opportunity of charging from renewable resources and the impacts of workplace charging on a campus community [55] [56] [57]. A general probabilistic model leading to necessary EV load forecasting is not present in the above mentioned works. A probabilistic EV load model is proposed in this dissertation to forecast the EV load with higher EV penetration to help the utility planners to accommodate more EVs.

While more PEVs on road in the near future is inevitable, their combined charging requirement will also impact the distribution grid. Therefore, EV load modeling based on the feeder type and capacity can help both the utility planners and PEV owners to take decisions on distribution upgrades and charging/discharging sessions, respectively. In recent years, EVs are modeled and their impacts on the distribution feeders have been studied by many researchers. IEEE test feeders are modeled with different EV loadings and evaluated for analyzing the voltage unbalances along with other renewable resources [58] [59]. In [60], Electric Vehicle Charging Station (EVCS) is considered as the main load where only level II charging is considered and its impacts are studied with a combination of smart inverters and their power factor flexibilities. The quantification of the techno-economic impact of hosting capacity increase of Distributed Energy Resources (DERs) and electric vehicles (EVs) on the distribution feeders has been evaluated in [61].In [62], charging coordination is done to increase the maximum EV penetration and reduce grid congestion. System voltage-based local controller and frequency-based decentralized control mechanisms are recommended to neutralize EV integration impacts [63] [64]. The existing literature analyzes the EV integration impacts from the point of view that how many megawatts or percentage of total load are representing EV load in a particular node or feeder. This perspective ignores the fact that the number of EVs that exist in a locality or are connected to a node depends on the number of EVs owned by each household or customer and it may not be an identical value for each node. Customer-oriented EV estimation is important for the utility to decide on necessary system upgrades. The number of EVCS required at a certain locality is coherent with the EV to Customer Ratio (EVCR)

for the nodes of the feeder of that locality. Moreover, the diversity in EV capacities due to different makes and models along with their daily travel profiles distinct from the various owners are not taken into account in most of the studies. To analyze the requirements for the distribution system upgrading, a comprehensive and realistic detailed distributed EV load modeling in a given feeder is needed.

The accuracy of the modeling can also help to estimate the current EV hosting capacity. In addition to that, the existing works mostly focus on feeders where a fixed fraction of the total feeder load is assigned to each node which may include EV chargers. The proposed centralized control mechanisms in existing works do not consider the voltage dependency at the local nodes based on their different EVCRs. Decentralized algorithms often follow frequency-based control mechanisms and ignore the relationship between the voltage distribution and EVCR at the local nodes. The statistical distribution of the voltage unbalance scenarios at the local nodes can help to demonstrate the EV integration impacts on the voltage at the customer level. This sensitivity analysis will allow the distribution utility to find out the exact locations of real congestion and offer maximum opportunities to utilize available grid flexibility.

2.4 PEV Grid Integration: An Overview

In recent years, both investor-owned utilities and public utilities have introduced various energy rates to the consumers depending on their regular usage of maximum power and energy consumption. In addition to the usual on-peak, mid-peak, and off-peak pricing, Critical Peak Pricing (CPP) is the latest addition to such electricity rates in which consumers are given the flexibility to control their usage to reap monetary rewards from

the grid operators. Based on different studies of residential customers on CPP rates, it was reported that customers reduced more load than other Time of Use (TOU) rates with very high critical peak prices ($.50/kWh or higher). For those small and medium businesses that have demand in the range of 300-500 kW, CPP can be highly effective for demand response. On average 13 percent of energy use reduction was estimated for the US on critical peak days [65]. It also helps to reduce the transmission and distribution congestion and defer new additional generation needing peaker plants. The frequency of CPP events is not usually that many. They normally take place in peak usage periods during the summer days. On CPP event days, consumers get rewards/credits for each kW reduction and get penalized for high usage of energy. After comparing eight different studies that modeled the benefits of specific types of demand response mechanisms it was concluded that CPP provided the highest gross benefit as 6.67$/kW-yr amount [65] [66]. On a given day, if it is not possible to reduce the overall building load, then V2G capability adds another bidirectional dimension by providing energy back to the grid to effectively lower demand when needed.

Charging of PEVs may be a significant load in small and medium buildings. In response to CPP, stopping the ongoing PEV charging will reduce load considerably. In addition to that, activating the V2G mode will provide additional power to the Point of Common Coupling (PCC). After providing for local building load, any additional power can go back to the grid to further reduce the peak demand of a feeder. In states like California where solar PV installations rapidly increased in recent years, afternoon peak demands have been replaced by early evening peaks due to the absence of solar. On a

cloudy day, sudden removal of large solar production during the daylight hours can also result in a reduction in the net generation on the grid triggering CPP. A sufficient number of consumers responding to CPP may be able to reduce overall demand and result in restoring the balance between net generation and load. Flex alert is also similar to CPP events in terms of relevance but may be issued at a short notice. CPP events are normally issued by local utilities whereas Flex alert is issued by the California Independent System Operator (CAISO) [67].

Advancement in technology and enabling state policies are offering opportunities for the vehicle to grid energy delivery. The newer models of EVs are more likely to have a longer range and higher battery energy storage capacity (e.g. 226 miles range with 62 kWh) [68]. Therefore, vehicle owners may be more comfortable in providing a portion of the battery energy back to the grid and still have enough range left for required driving. Level II EVs have a maximum charging/discharging power of between 6 and 15 kW, whereas level III EVs have a charging /discharging power of 50 kW. As the charging power rate is higher for level III EVs, they offer better opportunities for bidirectional operation and provide both demand and energy services to the grid [18] .

A substantial amount of work has been done on electricity pricing related to EVs. Electricity tariff highly affects EV customers' load profile by their ability to choose when to charge or discharge [69] . Optimal pricing and routing policies have also been proposed for electric vehicle public charging station networks [70] . Other recent studies have used fuzzy logic-based models which included EV charging load along with critical peak pricing events [71] [72]. Behavioral analysis is also included in a study which shows that higher

charging cost during a CPP event may be avoided if alternative transportation choices were available [73]. The beneficial opportunity of providing EV energy back to the grid at CPP periods has not been widely explored yet. This dissertation investigates the opportunity of electric vehicles' participation during any CPP event by activating vehicle to grid (V2G) mode of operation. A novel framework is developed to make vehicle to grid (V2G) operation efficient with a goal of reducing the overall cost for any EV owning consumer. A Mixed Integer Linear Programming (MILP) problem is formulated and solved to reduce the energy cost for a small commercial building that has two on-site PEVs. A range of pricing is modeled to show the effectiveness of this strategy along with all the usual constraints. The financial benefits of both the consumer and the utility operator are also discussed for this CPP handling strategy.

The analysis of EV integration on both distribution and transmission grid is needed. This work focuses on analyzing the impacts on both the system. While, the impacts analysis on the distribution grid are straightforward, co-simulation approaches are applied to analyze the dynamics of EV on Transmission & Distribution (T&D) interface. Several T&D interfacing techniques are compared and their interaction schemes are explored to choose the best T&D co-simulation framework [74] . In [75] [76] [77], different analytical approaches are carried out to solve the non-linear equations of T&D interfacing for both balanced and unbalanced systems. Newton's method provides better rates of convergences over the Fixed Point Iteration (FPI) method. It is also shown that the system frequency response can be interpreted in a better way with the proposed co-simulation framework. The impacts of bulk Volt-Var control on the transmission system are also analyzed using

the co-simulation framework [78]. The impacts of distributed Photovoltaic systems on bulk power systems are carried out by using two IEEE test systems (Transmission and distribution respectively) and a co-simulation platform [79]. Distributed PV penetration impacts are analyzed on transmission system voltage and power using the co-simulation approach. [80] [81]. In [82], different co-simulation frameworks are proposed and their advantages over each other are presented. All the above-mentioned literature focused on the development of co-simulation methodology and validation of them. Even though the impacts of PV systems are thoroughly investigated during co-simulation approach, the interactions of EV loads are not properly addressed yet.

3 Modeling and Cost Optimization Strategies for PEV Operation

3.1 Introduction

The higher level of EV penetration is not viable without optimal cost benefit for all the key role players in the EV industry. As discussed in Section 2.3 all the relevant works lack a rigorous analysis of different levels of bidirectional PEV impacts on a commercial building-integrated microgrid. One can raise a number of questions regarding PEV integration: 1. How will the fast or slow PEV charging/discharging impact any grid-connected commercial building consumer? 2. How will it interact with other controllable loads present in the building? 3. How will it impact the distribution grid while optimizing the savings of the customers behind the meter? 4. What happens to the bidirectional strategy when demand charge is integrated? 5. Which one is the best charging level for optimal cost and how much greater savings are possible in comparison to other charging/discharging levels? This chapter tries to find the answers to all these questions and attempts to bridge this gap in the literature by offering an optimal framework for the best PEV charging/discharging level selection.

From Section 2.2, we can also see that while there are many studies done that evaluate the pros and cons of residential and public PEV charging strategies, workplace charging strategies have not been widely analyzed. Moreover, as people spend a significant amount of time at their workplace, workplace charging strategies are very important from both the user and building owner's perspective. The ability of PEVs to do bidirectional

charging and vehicle-to-building operation, vehicle-to-grid services are not implemented widely yet. All the studies discussed above have been mostly focused on LDEV or HDEV optimization separately. The combined benefits possible from operating both at the same workstation have not yet been explored. A comprehensive cost-benefit analysis considering the infrastructure and implementation cost is still absent in the literature which will be very important for mass deployment of HDEV and LDEV in the near future. Further, in all the discussions in the literature a comprehensive cost-benefit analysis to determine the optimal framework for LDEV and HDEV implementation in a distribution-level microgrid is lacking. One can raise several questions regarding the LDEV and HDEV integration at the same workstation: 1) How cost-efficient is HDEV implementation in comparison to LDEV implementation? 2) What is the optimal cost including both HDEV and LDEV integration? 3) How much energy savings are possible while V2G initiatives are taken? 4) How does the battery degradation impact the overall cost-benefit of the microgrid owner? 5) What happens to the cost-benefit depending on the PEV owner behaviors? 6) Does net metering affect cost optimization? 7) What is the payback period of different cost-optimal strategies?

Along with answers to the aforementioned questions, this chapter also tries to show the impacts of different stakeholders on cost optimization strategies. PEV owner preferences, their availability and the integrated building loads are the key parts in terms of successful PEV integration.

3.2 Key Factors in PEV Optimal Cost

Several factors play key roles to find the optimal cost strategy for PEV operation. PEV owner strategy and PEV availability for any charging/discharging activities determines it's participation for any strategy selection. In addition to that, PEV charging station stays integrated with any building/ infrastructure in most cases. The loads of the infrastructure also make impacts on optimal cost operation.

3.2.1 Impacts of Building Loads

3.2.1.1 System Description

In this work, each of the buildings is considered to be equipped with an EV charging port and vehicle to grid operation is available for both of these ports. The PEV receives power in grid to vehicle operation and feeds power back to the grid during bidirectional operation. For each building-EV pair, the building and the EV share the same meter for calculating energy cost. Load data from two different campus buildings are used for simulation purposes. Nissan Leaf E Plus version is used for PEV specifications. Figure 3.1 and Figure 3.2 show the unidirectional and bidirectional operation of an EV integrated building microgrid, respectively.

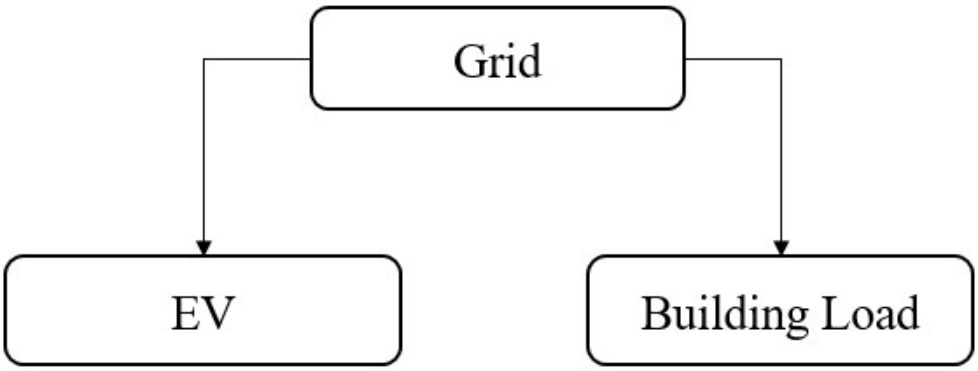

Figure 3.1 Unidirectional Operation: The PEV Acts Only as a Load

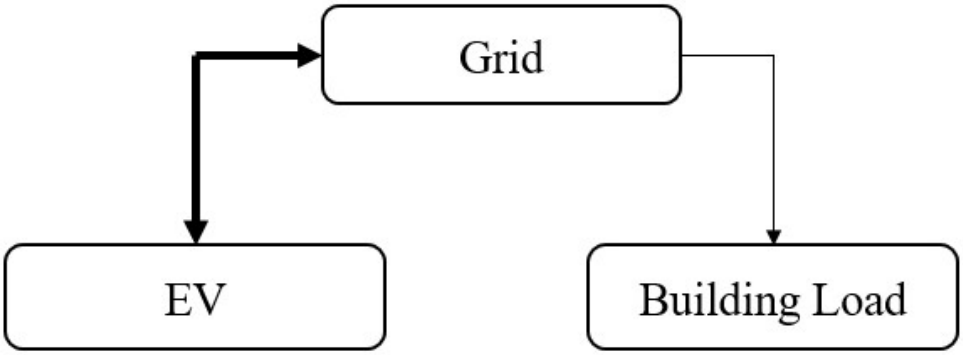

Figure 3.2 Bidirectional Operation: The PEV can Both Consume and Supply Power Based on Operating Procedure

3.2.1.2 Load Characteristics

The two buildings are located at University of California Riverside campus. The plugged-in time used for simulation is from 5 am to 3 pm to capture a typical working day load profile variation. Figure 3.3 shows the 15-minute rolling average demand (kW) for both the buildings over this time period. The daily load of building 1 does not fluctuate sharply with time. The maximum load for the first building always stays below 30 kW. On the other hand, the daily load of building 2 fluctuates sharply with time. The maximum load of this building is approximately 785 kW whereas the minimum load is 275 kW. The load of the second building can be categorized into three distinct sections. From 5 am to 7 am it remains below 300 kW, then the demand increases and remains around 500 kW from 8 am to 1:15 pm. Finally, it reaches the peak value of 758 kW at 1.30 pm. The demand fluctuates by 65 percent from low usage period to high usage period

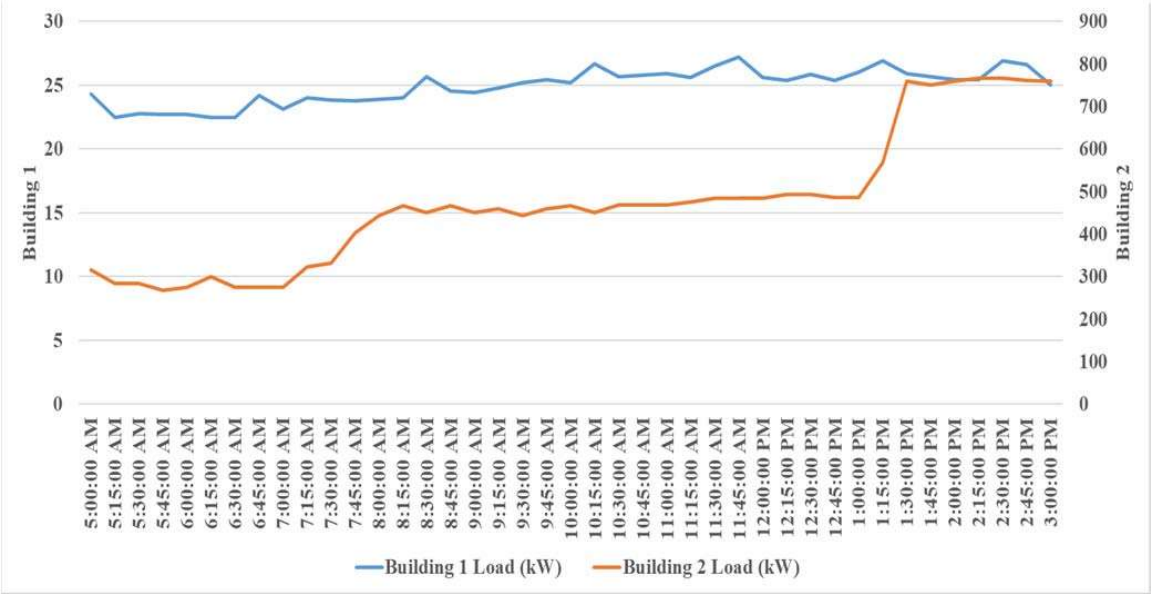

Figure 3.3 Demand Profile for Building 1 and Building 2

3.2.1.3 PEV Characteristics

The EV profile used for simulation is from Nissan Leaf E Plus version whose specifications are given in Table 3-1. The battery capacity is 64 kWh and the rate of charging is between 11kW and 22 kW, depending on user preference [83] [84]. The maximum charging and discharging rate used in the simulation is 15 kW and the minimum rate is greater than zero. The EV charging starts with a 20% State of Charge (SOC) at 5 am. The SOC characteristics of the EV is assumed linear for the simulation purposes.

Table 3-1 PEV Specification

Type	Spec
Model	Nissan Leaf E-Plus
Range (miles)	225
Battery (kWh)	64
Maximum Charging Power (kW)	15

3.2.1.4 Energy Price

The energy price used for the cost optimization problem is a Time of Use (TOU) based energy price for a commercial building sharing the same meter for EV charging. The energy rates used for simulation are: (1) Southern California Edison (SCE), an Investor Owned Utility (IOU), and (2) Riverside Public Utility (RPU), a Public Municipal Utility. SCE rate is divided into three tiers such as on-peak, mid peak and off-peak. On the other hand, RPU has only two tiers of energy rates such as off-peak and mid peak for the load

profile month of winter used in this work. The plugged-in time for EV is selected in such a way so that it can reflect all different energy prices for a day. Table 3-2 summarizes the energy rates for the simulation periods in a day.

Table 3-2 TOU Based Energy Charge [85]

Time	SCE Energy Charge ($/kWh)
5 am - 8 am	0.13
8 am - 2 pm	0.16
2 pm - 3 pm	0.25

Time	RPU Energy Charge ($/kWh)
5 am - 6 am	0.1413
6 am -3 pm	0.1696

3.2.1.5 Notations

The problem formulation and constraints are represented by various notations as summarized below in Table 3-3.

Table 3-3 Summary of Notations

Notation	Notation Description
i	index of a time slot in the billing cycle
e_i	energy cost in slot i
n	total number of slots
P_i	energy price for billing cycle in slot i
$G2V_i$	total power drawn from grid to vehicle in slot i
L_i	total building load in slot i
SOC_i	State of charge of PEV battery in slot i
$V2G_i$	total power delivered from vehicle to grid in slot i
$\eta_{charging}$	PEV battery's charging efficiency
$\eta_{discharging}$	PEV battery's discharging efficiency
SOC_{max}	PEV battery's maximum SOC
SOC_{min}	PEV battery's minimum SOC

Notation	Notation Description
$G2V_{max}$	maximum power drawn from grid to vehicle
$V2G_{max}$	maximum power delivered from vehicle to grid
$L_{maxallowed}$	maximum possible load
μ	time interval for each energy cycle

3.2.2 Problem Formulation and Constraints

The problem to minimize the electricity cost is an optimization problem with required total power, PEV and building load constraints.

3.2.2.1 Objective Function

The objective of our problem is to minimize the energy cost of PEV charging associated with any building. In order to minimize the energy cost, we need to solve the following equation.

$$minimize \sum_{i=1}^{n} e_i \quad \textbf{3.1}$$

3.2.2.2 Constraints

The constraints for this optimization problem can be classified according to the direction of power transfer. As the power transfer can be both unidirectional and bidirectional, the total load equation and SOC constraints will vary accordingly. The constraints for the vehicle to grid power transfer will also be added for bidirectional

operation. The first to fifth constraints stand for unidirectional power transfer, while the rest are used for bidirectional power transfer.

$$e_i = P_i \times (G2V_i + L_i) \times \mu \quad \textbf{3.2}$$

$$SOC_i = \begin{cases} SOC_{Primary}; i = 1 \\ SOC_{i-1} + \eta_{charging} \times G2V_i \times \mu; i > 1 \end{cases} \quad \textbf{3.3}$$

$$0 \leq G2V_i \leq G2V_{max} \quad \textbf{3.4}$$

$$G2V_i + L_i \leq L_{max\ allowed} \quad \textbf{3.5}$$

$$SOC_{min} \leq SOC_i \leq SOC_{max} \quad \textbf{3.6}$$

$$e_i = P_i \times (G2V_i - V2G_i + L_i) \times \mu \quad \textbf{3.7}$$

$$SOC_i = \quad \textbf{3.8}$$

$$\begin{cases} SOC_{Primary}; i = 1 \\ SOC_{i-1} + \eta_{charging} \times G2V_i \times \mu - \eta_{discharging} \times V2G_i \times \mu; i > 1 \end{cases}$$

$$0 \leq V2G_i \leq V2G_{max} \quad \textbf{3.9}$$

$$G2V_i - V2G_i + L_i \leq L_{max\ allowed} \quad \textbf{3.10}$$

The first constraint denotes that the total energy cost at any time will be equal to the summation of the building energy consumption and EV energy consumption cost. The second constraint calculates the SOC of EV battery at any instant of time. Here the SOC indicates the stored energy in the battery. At any instant the stored energy in the battery must be equal to the energy stored at the previous time slot plus the energy supplied from grid to the vehicle. We assume that initially the SOC is 20% which is 12.8 kWh for Nissan Leaf E-Plus version. The third constraint states that the power supplied from grid to vehicle must be greater than zero and will be less than or equal to the maximum charging power; whereas the fourth constraint denotes that the sum of charging power supplied from the grid, and building load will be less than the maximum possible load for that building. The fifth constraint shows that SOC should be within the allowable limit. The constraints from 3.7-3.10 are the additional constraints for bidirectional operation. The sixth constraint shows that the energy transferred from vehicle to grid needs to be subtracted to find the net energy charge. The seventh constraint denotes that the discharging energy is subtracted to find the SOC of the battery. Finally, the eighth constraint determines the limit for vehicle to grid power transfer and the ninth constraint describes that the net power must be less than the maximum demand for the building.

3.2.2.3 Convex Optimization

The formulated objective function is linear which is convex. Similarly, the constraints used here are also linear and convex. Therefore, the optimization problem itself is convex. MATLAB CVX tool [86] has been used to solve this convex optimization problem

3.2.3 Simulation Results

Both unidirectional and bidirectional operations are studied for both of the buildings and the energy rate profiles. The detailed results are discussed below.

3.2.3.1 Unidirectional Operation

The grid to vehicle charging profile is shown in Figure 3.4 for all possible cases in unidirectional operation. For small and less fluctuating building load (building 1), the optimization scheme requires charging power consumption to be higher for SCE energy rate at the earlier hours as SCE energy rate is less than RPU rate at that time. But with time, the EV consumes more power from the grid for RPU rates in comparison to SCE rates. For large and high fluctuating building load (building 2), the difference between energy rates is not creating significant impact on charging profile for EV. This is due to relatively small size of 15 kW EV charging rate compared to minimum building load of 275 kW along with building's inherent large load variation.

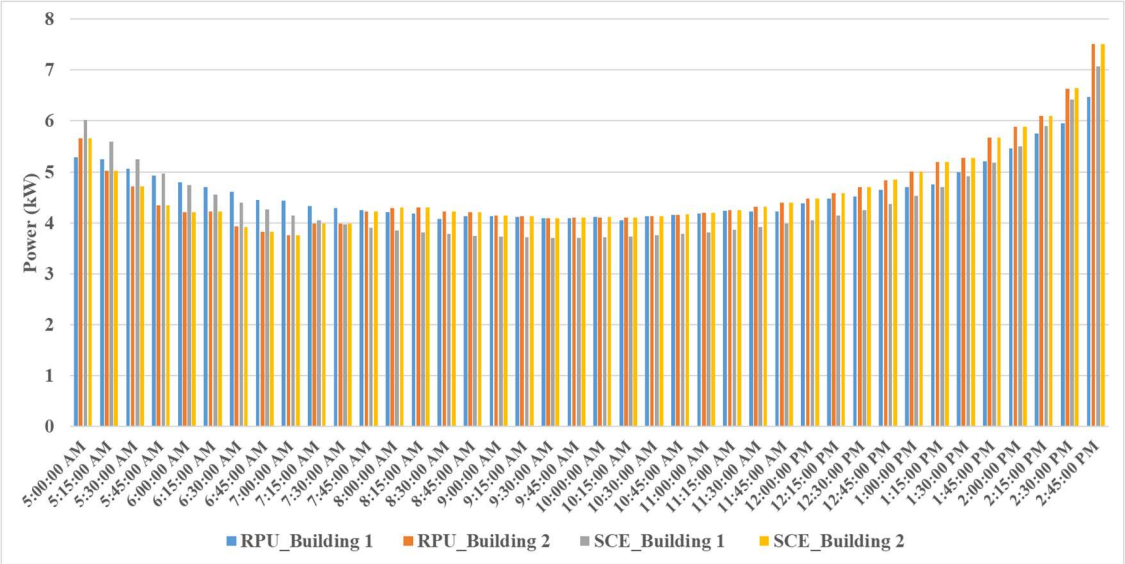

Figure 3.4 Unidirectional Operation : Charging Profile for EV

Figure 3.5 shows the impact of various charging scenarios on overall building load profiles. The impacts of building loads are insignificant for unidirectional PEV operation as the optimization solution tries to provide the best optimal cost.

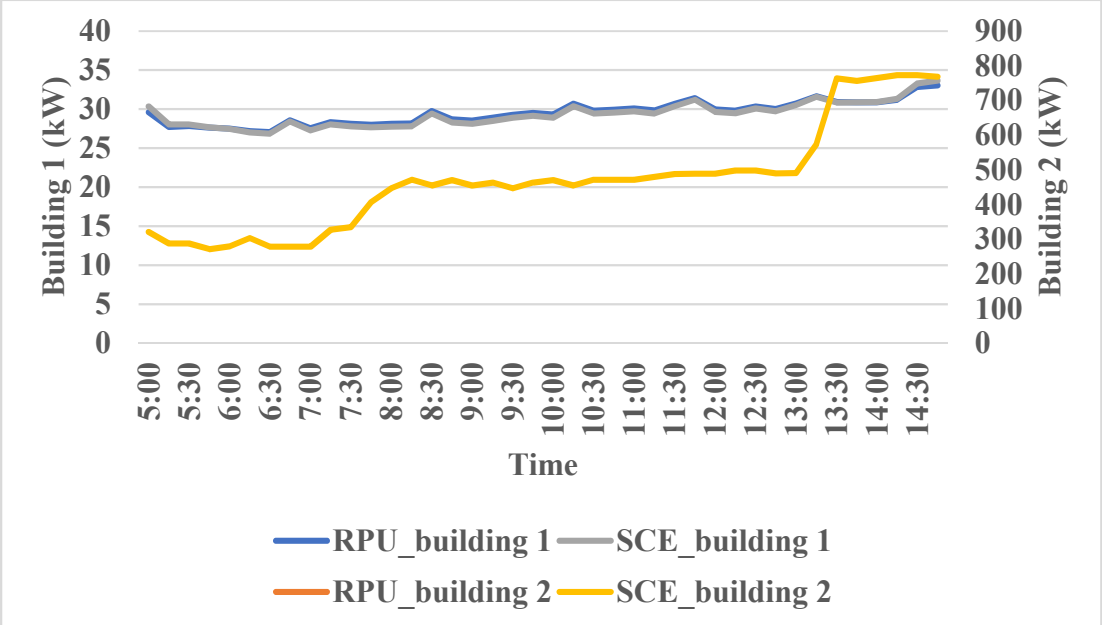

Figure 3.5 Total Building Loads with an EV in Unidirectional Operation

3.2.3.2 Bidirectional Operation

The bidirectional charging profile is shown in Figure 3.6 for all possible cases. For small and less fluctuating building load (building 1), the EV feeds more power back to the grid for SCE rates as compared to RPU rates. The EV acts in a similar way for the second building too. As RPU energy rate increases after 6 am, EV operates in V2G mode after this period to facilitate the maximum reduction in energy cost. On the other hand, SCE rate increases after 8 am, making the PEV to begin V2G operation later for this energy rate as compared to RPU's rate. It also shows another drop in power consumption after 2 pm for SCE energy rate, as the energy rate increases again after 2 pm. For building 2, the PEV starts discharging later while RPU rate is activated. In case of SCE rates, at first the PEV feeds more power back to the grid for the first building, later on, it does the opposite.

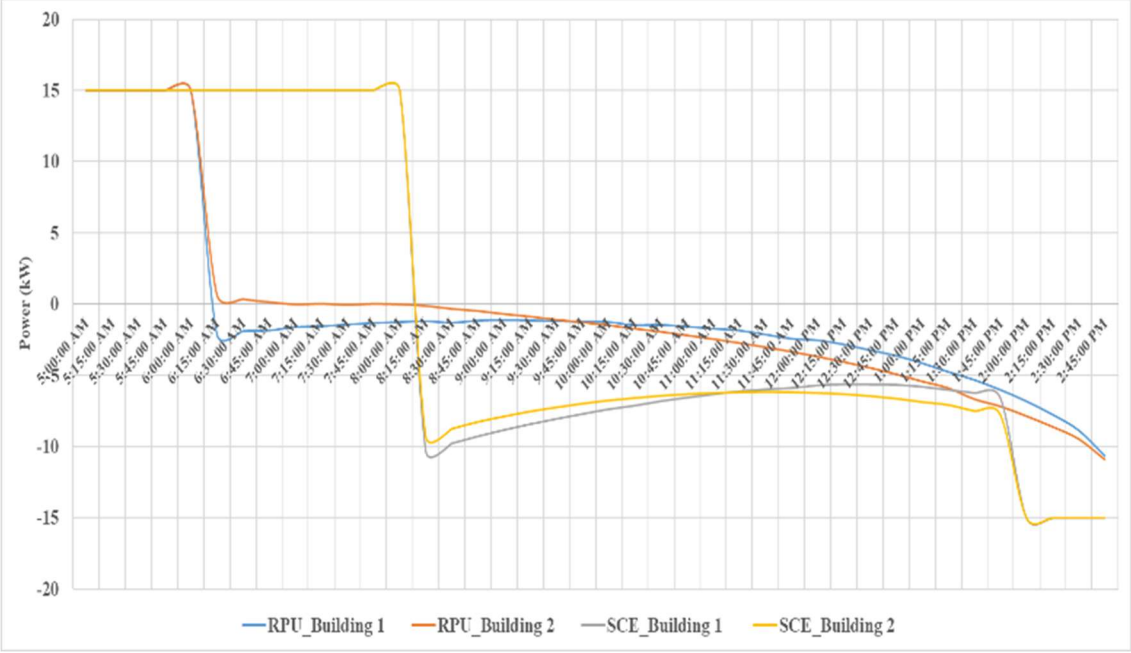

Figure 3.6 Bidirectional Operation : Charging Profile for EV

Figure 3.7 shows the bidirectional charging scenarios on the different building load profiles and battery SOC is depicted in Figure 3.8. The SOC increases up to 93% for SCE energy rate for both buildings whereas the SOC does not reach more than 49% for RPU energy rate. As the goal is to minimize the energy cost, the SOC starts decreasing to provide the maximum power to the grid and hence reduces the energy cost. Large building loads result in better SOC in comparison to small building loads which means the EV feeds less power back to the grid for large building loads. For complete recovery of SOC, EV should be charged during low cost off-peak hours.

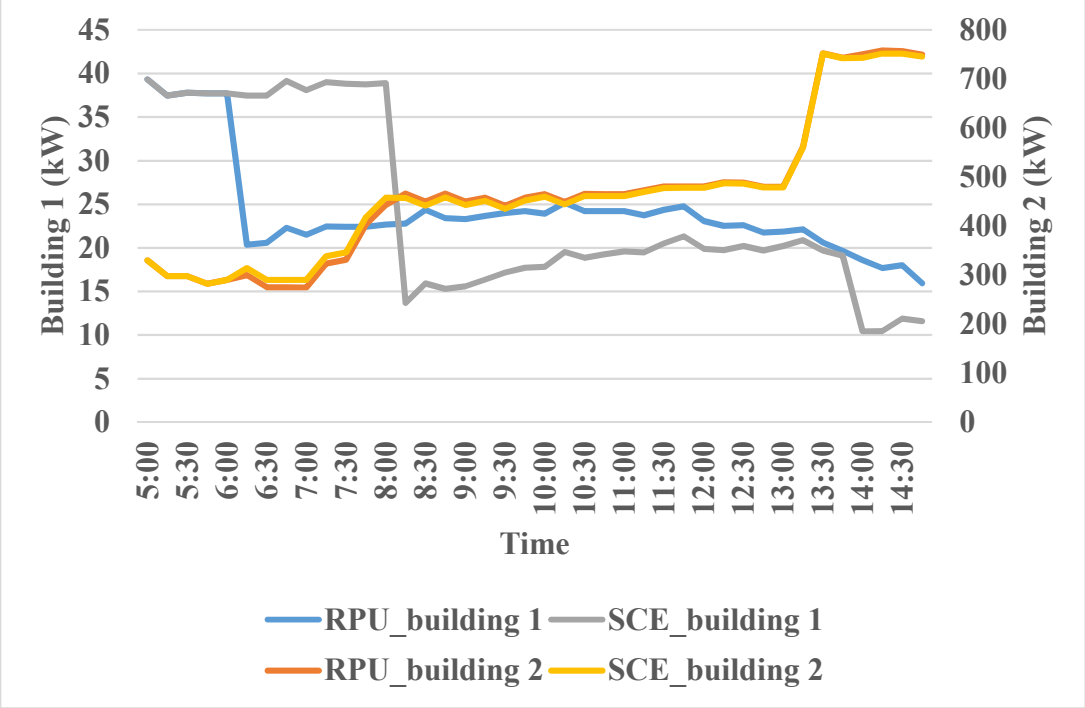

Figure 3.7 Total Building Loads with an EV in Bidirectional Operation

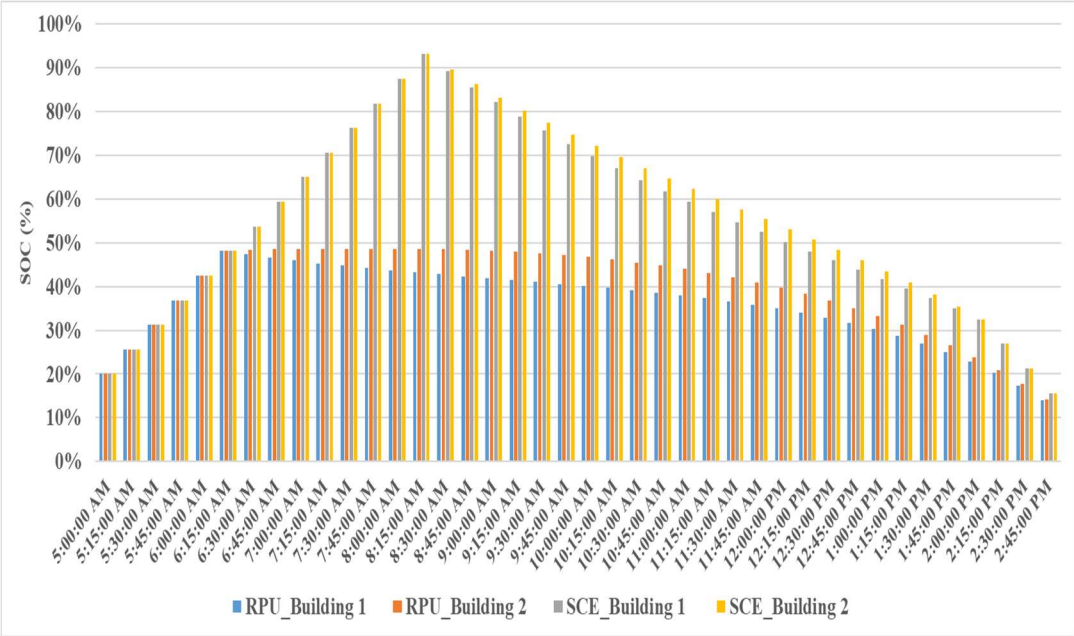

Figure 3.8 Bidirectional Operation : SOC Profile for EV

3.2.4 Cost Analysis

The simulation results show more reduction in energy cost for bidirectional operation. Though the percentage of cost reduction in bidirectional operation is large for the building with smaller average loads, the cost minimization is small for the building with larger average loads due to the EV charging power being very small compared to the building load itself. The cost reduction also depends on energy rates. RPU energy rate is both low and difference between on-peak and off-peak is smaller compared to SCE energy rates. When the building load is small, the total cost is lower for SCE rates in both operation. On the other hand, the total cost is lower for RPU rates in case of a large integrated building load. Figure 3.9 and Figure 3.10 show the total cost for all scenarios.

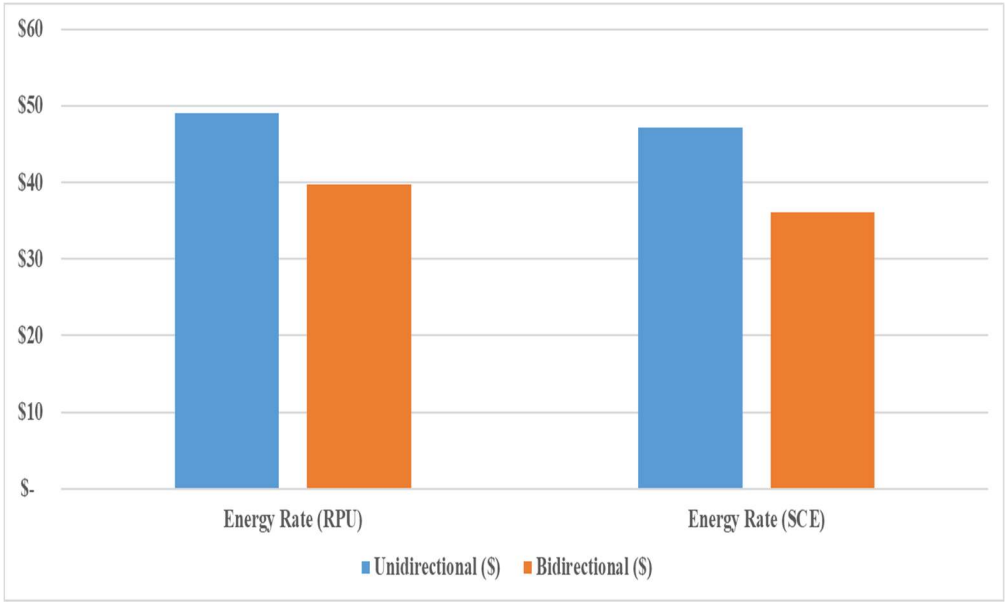

Figure 3.9 Cost Comparison Per Day: Small Building Load with one EV(Building 1)

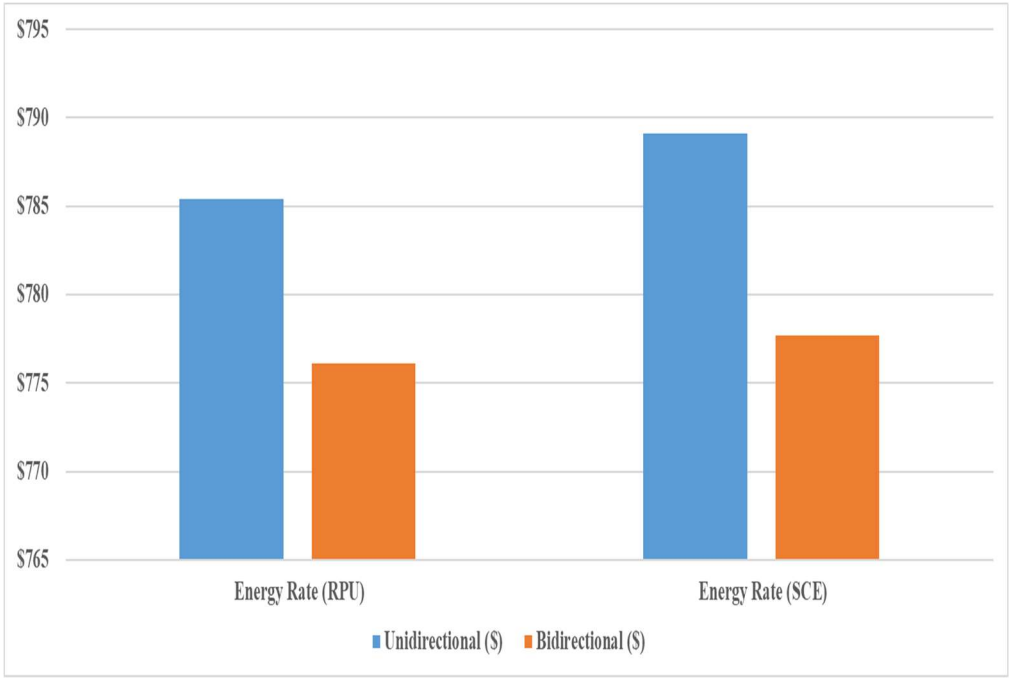

Figure 3.10 Cost Comparison Per Day: Large Building Load with One EV (Building 2)

This study shows that 18.9-23.5% cost reduction is possible for small building loads whereas 1.2-1.4% cost reduction is possible for large building load when using a single level 2 EV charger. Table 3-4 shows the estimated daily savings in bidirectional operation for all possible cases.

Table 3-4 Cost Savings in Bidirectional Operation

Building Type	Rate and Load	Savings in Bidirectional Operation (%)
Building 1 (Small Average Load)	Energy Rate (RPU)	18.9%
	Energy Rate (SCE)	23.5%
Building 2 (Large Average Load)	Energy Rate (RPU)	1.2%
	Energy Rate (SCE)	1.4%

Any similar EV with equal or less charging power capability will act in similar manner for the given building loads and energy rates. Another verification was done by applying this methodology to a Nissan Leaf 2nd Generation EV with maximum charging power of 6 kW, where it showed similar results except one scenario. This EV model can not optimize the cost for large building loads in bidirectional mode due to its lower charging rate being dominated by inherent large building load variations.

3.2.5 Impacts of Probability Distribution and PEV Owner Strategies

3.2.5.1 Problem Formulation

The goal is to optimize the energy cost purchased from the grid considering the randomness of PEV parameters in mind. Hence, it involves the expected amount of energy available after PEV charging/discharging activities. There are two light duty electric vehicles that are available for the employees or researchers of this building for short to medium distance travels for attending meetings. Both light duty PEVs are 2013 Nissan Leaf electric vehicles having the capability of vehicle to grid (V2G) operation. Both have 24 kWh battery capacity with a capability of fast charging/discharging given that fast charging bidirectional EV stations are available. The recent models of Nissan Leaf have a 40 kWh or 62 kWh battery capacity [87]. Hence, 40 kWh battery capacity is used to minimize the cost function. As one of the two vehicles is dedicated to research coupled with a fact that there is only one bidirectional charger available, one light duty PEV is considered in optimizing the overall cost. The same approach could be extended to consider multiple vehicles and charger configurations.

$$\text{minimize } \sum_{t=1}^{T}\left[\left\{P_{building}(t) + Prb_{EV}(t) \times \left(\eta_{\text{ch,B}} \times \mathrm{P_{G2V}(t)} - \mathrm{P_{V2G}(t)}/\eta_{\text{disch,B}}\right)\right\} \times \Delta t \times E_p(t)\right] \quad \textbf{3.11}$$

Equation 3.11 states the optimization problem, where, $P_{building}\ (t)$ is the building power usage (kW) at any time t. $\mathrm{P_{G2V}}\ (t)$ and $\mathrm{P_{V2G}(t)}$ are the charging and discharging power (kW) by the PEV at time t. $Prb_{EV}(t)$ represents the probability of PEV being available at

any time instant. $E_p(t)$ and Δt is the energy price and time interval, respectively. T is the total period which is 13 hours for this cost optimization as EV is unavailable for any activities for the rest of the period. $E_p(t)$ is a Time of Use (TOU) pricing rate from a Public Owned Utility which is shown in Table 3-5.

Table 3-5 Energy Price

Time	Energy Price ($/kWh)
On-peak (4 pm - 9 pm)	0.1079
Off-peak (9 am - 4 pm) (9 pm -10 pm)	0. 0874

3.2.5.2 Constraints

The constraints for the formulated expected value optimization are annotated by equations 3.12-3.17. The equation 3.12 calculates the State of Charge of available PEV at any time t where SOC_{EV}, $\eta_{ch,EV}$, $\eta_{disch,EV}$ denote the remaining energy, charging efficiency, and discharging efficiency of PEV, respectively. The next two equations stand for physical limitations for the charging and discharging activities of PEV. The available Coritech bidirectional charger in Figure 3.27 can charge/discharge at a maximum rate of 30 kW. Equation 3.15 ensures that the charging and discharging events will not take place at the same time. The next constraint states that e_1 and e_2 are binary variables. Equation 3.18 is used to maintain the overall power balance in the system. The summation of purchasing power from the grid and discharging power of PEV will be equal to the

combined total power required for building and G2V activities. The final constraint indicates that the probability of PEV availability will be always between 0 and 1. for ∀t∈T,

for ∀t∈T

$$SOC_{EV}(t)=SOC_{EV}(t-1)+\left(\eta_{ch,EV} \times P_{G2V}(t) - P_{V2G}(t)/\eta_{disch,EV}\right)/ Cap_{init} \times \Delta t \quad \textbf{3.12}$$

$$0 < P_{G2V}(t) \leq e_1(t) \times P_{G2V\,max} \quad \textbf{3.13}$$

$$0 < P_{V2G}(t) \leq e_2(t) \times P_{V2G\,max} \quad \textbf{3.14}$$

$$e_1(t) + e_2(t) = 1 \quad \textbf{3.15}$$

$$e_1(t), e_2(t) \in \{0,1\} \quad \textbf{3.16}$$

$$SOC_{min,EV} \leq SOC_{EV}(t) \leq SOC_{max,EV} \quad \textbf{3.17}$$

$$P_{grid}(t) + P_{V2G}(t) = P_{building}(t) + P_{G2V}(t) \quad \textbf{3.18}$$

$$Prb_{EV}(t) = [0,1] \quad \textbf{3.19}$$

3.2.5.3 Optimization

The cost function along with its constraints is a Mixed Integer Linear Programming (MILP) problem. The problem is solved in Gurobi [88] with a work station having i-7 core and 16 GB RAM.

3.2.6 Simulation Results

3.2.6.1 Impacts of Probability Distribution

EV availability distribution is mostly considered as normal distribution in literature [89] which is evident for a large EV fleet. But in reality, small and medium commercial buildings who own their PEVs, their usage doesn't follow a normal distribution. Hence, models based on normal distribution might be inappropriate for PEV owners whose PEV usage is also a part of their regular office work. To investigate the impacts of the probability distribution on cost optimization strategy, real time probability distribution, and random distribution of PEV availability are compared. Figure 3.11 and Figure 3.12 are showing the impacts of PEV availability distribution on purchased grid power, charging, and discharging power. For the random normal distribution, all charging events are distributed normally with a standard deviation of 1 and the mean value at 3 pm. The normal distribution considers the peak probability at a certain period which results in the highest cost reduction opportunity only at that time using the bidirectional capability. This causes fewer V2G events during the on-peak period. No strategy is being considered for the PEV owner for these scenarios and it is assumed as the base case.

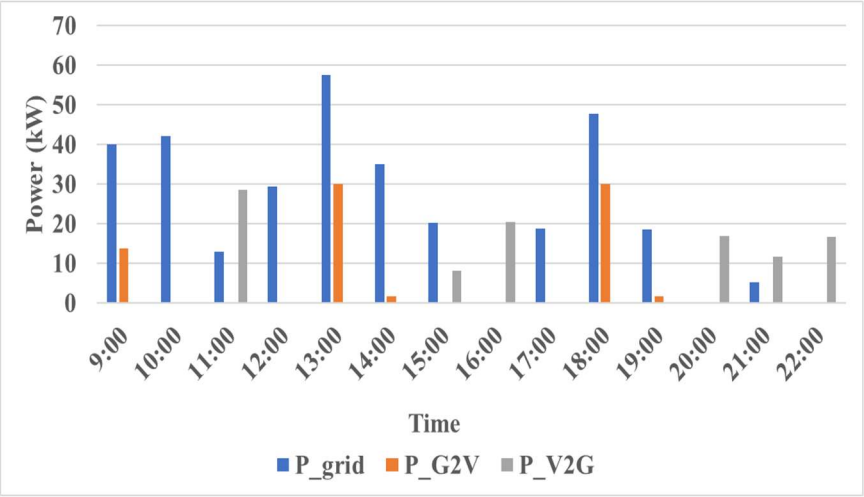

Figure 3.11 Grid Power, G2V and V2G Power for Actual PEV Availability: Initial Mid-Range SOC

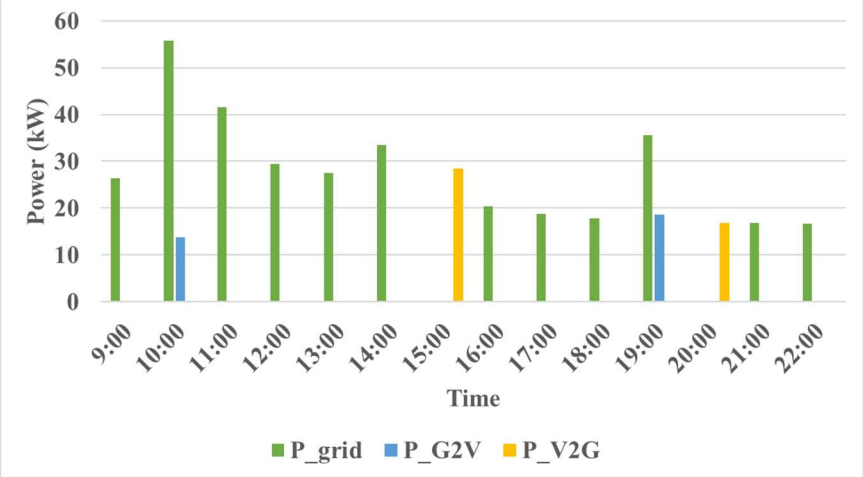

Figure 3.12 Grid Power, G2V and V2G Power for Normal PEV Distribution: Initial Mid-Range SOC

3.2.6.2 Impacts of PEV Owner Strategies

The bidirectional operation of PEV is highly dependent on PEV owner behavior. Discharging to the grid can also affect the battery life of PEV along with providing uncertainty for battery SOC to make a reasonable trip successfully. Hence, two PEV owner strategies are considered to show the impacts on overall electricity cost optimization. The

first strategy is that the PEV owner will be willing to do V2G if the final SOC level is equal to their initial SOC before the G2V or V2G event starts. The second strategy is that the PEV owner wants to have a comfortable SOC level after the charging or discharging event takes place. As Figure 3.29 indicates that the maximum change of SOC level is 22.5 percent which occurred rarely. In general, for this PEV model with a 30 kWh/100 mi rating it can finish a round trip of at least 26 miles with the comfortable SOC level at the starting and finishing the trip with 20 percent SOC left [90] . Therefore, for this particular optimization, we can consider the PEV owner will be satisfied with a 40 percent SOC level of the total capacity.

Strategy 1: Final SOC Equals to Initial SOC.

Strategy 2: Final SOC Equals to Acceptable SOC.

Strategy 1 is the worst-case scenario when the PEV owner leaves the car at the charging station with a lower SOC level as mentioned in the categories for simulation. Figure 3.13 and Figure 3.14 are showing the grid power, charging, and discharging power along with the energy left in PEV at any instant for having a mid-range initial SOC of 50-80 percent of the total. As for mid-range initial SOC: the initial SOC is even higher than the acceptable SOC value, therefore more V2G events take place during the on-peak periods in the second strategy. This scenario does not hold for lower level initial SOC. The figures are presented for mid-range SOC as this is the most common scenario depicted in Figure 3.31. In these figures, E represents the stored energy in PEV.

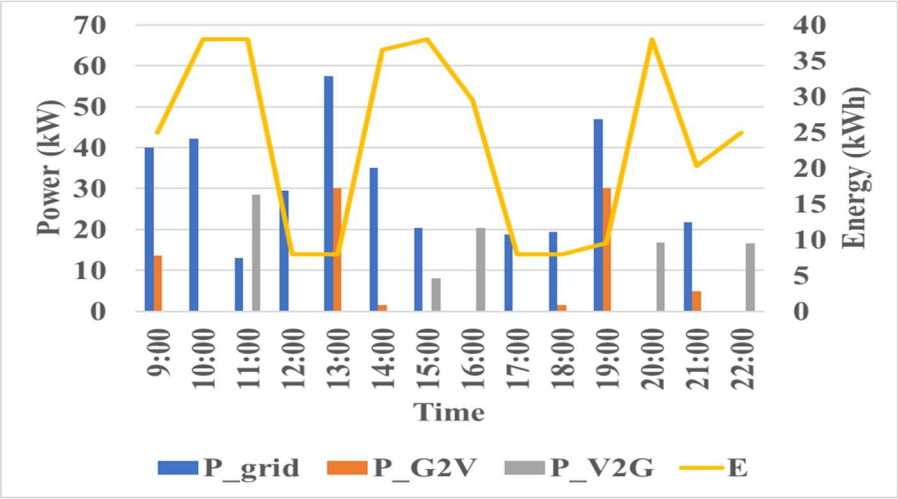

Figure 3.13 Grid Power, G2V, V2G Power and Energy for Strategy 1

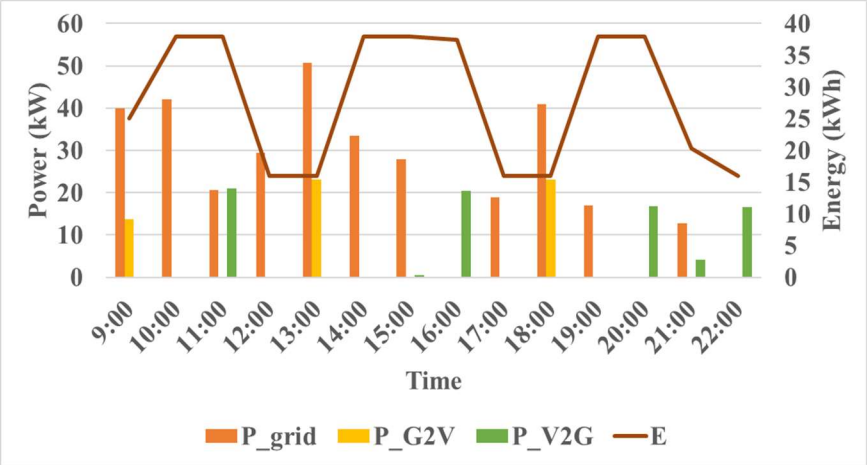

Figure 3.14 Grid Power, G2V, V2G Power and Energy for Strategy 2

3.2.6.3 Cost Analysis

The simulation results show that cost reduction is possible for any consumer with PEV ownership while he adopts net metering and V2G. Between 2.5 and 2.8 percent, energy cost reduction is possible using a Nissan Leaf in comparison to no PEV ownership by the building owner. Higher initial SOC at the start of PEV activity gives more flexibility

in cost reduction. Table 3-6 shows the comparison of cost and savings for the two different probability distributions considered.

Table 3-6 Cost Comparison for Different Probability Distribution

Initial SOC Level	Base Case with Data Driven Probability Distribution		Base Case with Normal Probability Distribution	
	Savings	Cost ($)	Savings	Cost ($)
20-50%	2.5%	32.23	3.2%	31.99
50-80%	2.6%	32.17		
80-100%	2.8%	32.12		

Figure 3.15 and Figure 3.16 depict the impacts of owner strategies on cost optimization function. Strategy 1 always provides less energy cost regardless of their initial SOC level. Between 2 and 2.6 percent cost savings are possible for any strategy in comparison to having no PEV at the facility. Making more PEVs available and having more bidirectional PEV chargers can result in higher cost savings.

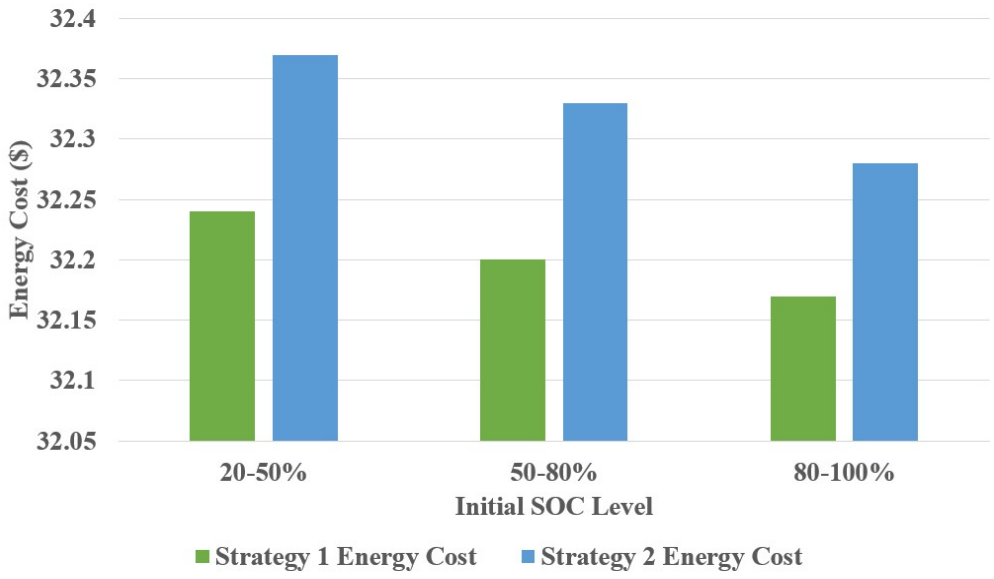

Figure 3.15 Energy Cost Comparison Based on PEV Owner Strategies

Figure 3.16 Percentage of Savings Based on PEV Owner Strategies

3.3 Centralized Optimization Approach

3.3.1 System Description and Modeling

3.3.1.1 System Details

The testbed building is located at the College of Engineering – Center for Environmental Research & Technology (CE-CERT) at the University of California Riverside. This building has offices for research faculty, staff, students along with administrative offices and conference rooms. It is 21,352 sqft in size and serves as a distribution level microgrid for the existing utility feeder. It is equipped with 180 kW solar PV, a 500 kWh/100 kW BESS and, five EV charging stations. Four of the chargers are for level II charging (6 kW) while the fifth one is a level III charger (50 kW). To perform a vehicle to grid (V2G) operation, there is a specialized bidirectional fast EV charger mounted on a trailer testbed. EVs can send power back to the grid through this charger in addition to the usual charging mode of operation. This building consists of an open working space which means that there are no different thermal zones. The pattern of energy use of this building is similar to a regular office building and is usually unoccupied during weekends and holidays. As energy-efficient measures are more needed when the building is occupied, a weekday has been selected to co-ordinate various loads and optimize the overall system. Figure 3.17 is showing the schematic of the system and available DERs.

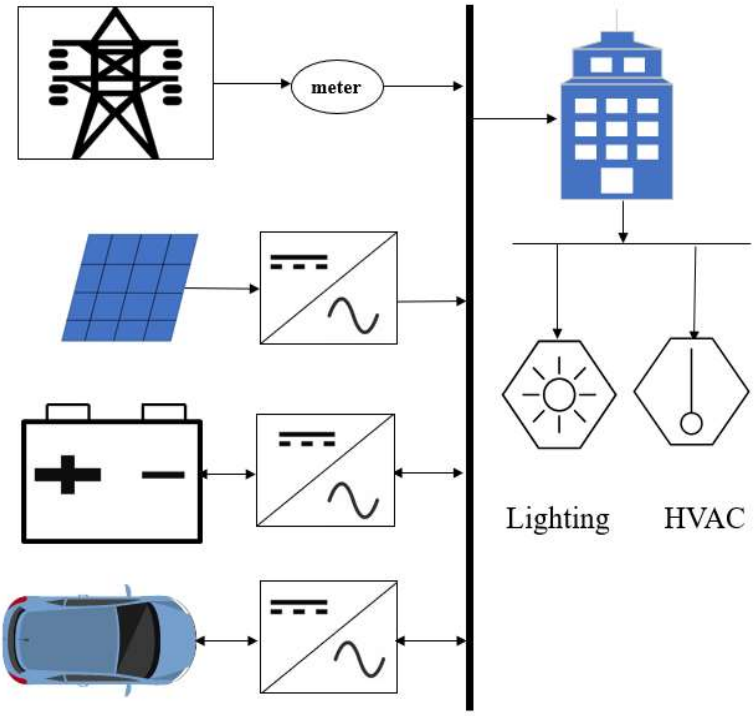

Figure 3.17 Building Schematic with Behind the Meter DER Components

3.3.1.2 Notations

NOMENCLATURE

Continuous Variable

Index and Set

t	Time slot index
T	Set of Total time

Decision Variables

P_{grid}	Power from the grid to the building (kW)
$P_{ch,B}$	BESS charging power (kW)
$P_{disch,B}$	BESS discharging power (kW)
P_{G2V}	Power collected from the grid to vehicle (kW)
P_{V2G}	Power transferred from vehicle to grid (kW)
SOC_B	State of Charge of BESS (kWh)
SOC_{EV}	State of Charge of EV (kWh)
P_{HVAC}	Power consumed by HVAC (kW)
$P_{lighting}$	Power consumed by lighting (kW)
φ	Lighting power consumed per area (kW/ft^2)
$T_{setpoint}$	Setpoint temperature for building (degree C)

Input Parameters and Continuous Variables

P_{PV}	Power (kW) available from the solar PV array
T_{out}	Outside temperature (degree C)
C_e	Price of energy from the grid ($/kWh)
GHI_{PV}	Global Horizontal Irradiance (GHI) of PV array (kW/m^2)

Input Parameters and Constants

Δt	Time interval
η_{PV}	Solar PV array efficiency
A_{PV}	Area (m^2) of the solar PV array
ξ_{PV}	PV array parameter co-efficient
T_a	Ambient temperature (degree C)
$SOC_{min,B}$	Minimum SOC for BESS (kWh)
$SOC_{max,B}$	Maximum SOC for BESS (kWh)
$\eta_{ch,B}$	BESS charging efficiency
$\eta_{disch,B}$	BESS discharging efficiency
$P_{ch,B\ max}$	Maximum charging power for BESS (kW)
$P_{disch,B\ max}$	Maximum discharging power for BESS (kW)
$SOC_{min,EV}$	Minimum SOC for EV (kWh)
$SOC_{max,EV}$	Maximum SOC for EV (kWh)
$\eta_{ch,EV}$	EV charging efficiency
$\eta_{disch,EV}$	EV discharging efficiency
$P_{G2V\ max}$	Maximum charging power for EV (kW)
$P_{V2G\ max}$	Maximum discharging power for EV (kW)
φ_{min}	Minimum lighting power consumed per area (kW/ft^2)
φ_{max}	Maximum lighting power consumed per area (kW/ft^2)
$A_{Building}$	Area (ft^2) of the building
$\eta_{lighting}$	Lighting efficiency
$T_{setpoint\ min}$	Minimum setpoint temperature for the building
$T_{setpoint\ max}$	Maximum setpoint temperature for the building
P_{misc}	Power consumed by miscellaneous building load
$C_{d,B}$	Cost associated with battery activities ($/kWh)
$C_{d,EV}$	Cost associated with EV activities ($/kWh)
C_{dep_daily}	Daily depreciation cost ($/day)
E_{dep_daily}	Daily depreciation energy (kWh/day)
K_{dep}	Global coefficient of depreciation
E_{BESS}	BESS Stored Capacity (kWh)
E_{EV}	EV Stored Capacity (kWh)

Binary Variables

b_1	Charging decision binary variable for BESS
d_1	Discharging decision binary variable for BESS
e_1	Charging decision binary variable for EV
e_2	Discharging decision binary variable for EV

3.3.1.3 PV Modeling

There are different steady state models for solar power estimation. Solar PV model based on temperature and irradiance provides most accuracy and hence widely used [91] [92]. Solar PV power output is calculated from equation 3.20 . Global Horizontal Irradiance is used as it includes Direct Normal Irradiance (DNI), Diffuse Horizontal Irradiance (DHI) and ground reflected radiation

$$\mathrm{P_{PV}(t)} = \eta_{\mathrm{PV}} \times \mathrm{A_{PV}} \times \mathrm{GHI_{PV}} \times \{1 - \xi_{\mathrm{PV}}\,(\mathrm{T_{out}(t)} - \mathrm{T_a})\} \text{ for } \forall t \in T \qquad \textbf{3.20}$$

3.3.1.4 BESS Modeling

The Battery Energy Storage System (BESS) used for optimization problem is modeled by the equations given later in this section As SOC profile is unavailable for this BESS, equation 3.21 calculates the remaining energy stored in the battery, after any charging or discharging cycle, is used for SOC evaluation of this BESS. Equation 3.3 ensures that BESS charging rate always lies between the maximum and minimum charging limit whereas discharging rate is limited by 3.23. Equations 3.24 and 3.25 ensure that BESS will not charge and discharge at the same time. BESS SOC limit is maintained by 3.26. Initial SOC is assumed to be 70 percent whereas minimum and maximum SOC are assumed to be 40 and 100 percent, respectively. The battery spec is 150 kwh/50 kW rating with a 95 percent charging/discharging efficiency.

for $\forall t \in T$

$$SOC_B(t)=SOC_B(t-1)+\left(\eta_{ch,B} \times P_{ch,B}(t) - P_{disch,B}(t)/\eta_{disch,B}\right)/ \quad \textbf{3.21}$$

$$Cap_{init} \times \Delta t$$

$$0 < P_{ch,B}(t) \leq b_1(t) \times P_{ch,B\,max} \quad \textbf{3.22}$$

$$0 < P_{disch,B}(t) \leq d_1(t) \times P_{disch,B\,max} \quad \textbf{3.23}$$

$$b_1(t) + d_1(t) = 1 \quad \textbf{3.24}$$

$$b_1(t), d_1(t) \in \{0,1\} \quad \textbf{3.25}$$

$$SOC_{min,B} \leq SOC_B(t) \leq SOC_{max,B} \quad \textbf{3.26}$$

3.3.1.5 EV Modeling

The EV charging characteristics and stored energy calculation are given from 3.27-3.32. Equation 3.27 denotes the energy left in EV after any charging or discharging activities. G2V and V2G operation are limited by 3.28-3.29. The constraints from 3.30-3.31 ensure the prevention of G2V and V2G operations simultaneously, while Equation 3.32 provides the SOC limit for EV battery. Two EV specs have been considered for simulation: one is Nissan Leaf E-plus with 64 kWh/7 kW and the other one is Tesla X with 100 kWh/50 kW rating. It is assumed that both have an initial SOC of 60 percent. The minimum and maximum SOC for both are 40 and 100 percent, respectively.

for $\forall t \in T$

$$SOC_{EV}(t)=SOC_{EV}(t-1)+\left(\eta_{ch,EV} \times P_{G2V}(t) - P_{V2G}(t)/\eta_{disch,EV}\right)/ \quad \textbf{3.27}$$

$$Cap_{init} \times \Delta t$$

$$0 < P_{G2V}(t) \leq e_1(t) \times P_{G2V\,max} \quad \textbf{3.28}$$

$$0 < P_{V2G}(t) \leq e_2(t) \times P_{V2G\,max} \quad \textbf{3.29}$$

$$e_1(t) + e_2(t) = 1 \quad \textbf{3.30}$$

$$e_1(t), e_2(t) \in \{0,1\} \quad \textbf{3.31}$$

$$SOC_{min,EV} \leq SOC_{EV}(t) \leq SOC_{max,EV} \quad \textbf{3.32}$$

3.3.1.6 HVAC Modeling

HVAC load of any building is closely related to room temperature. As room temperature is not available for this building and it varies with outside temperature, the later one is used to model HVAC load. Factors like cooling load, types of HVAC also have impacts on power consumed by HVAC. For this optimization model, to generate the most simplified expression for HVAC load estimation, HVAC data of this building has been collected using Fluke meter for a regular weekday. The data collected from this smart meter is fitted by Matlab curve fitting tool. Hence, a linear expression is generated to find the relation between HVAC power and the difference of HVAC setpoint and outside temperature. HVAC power for this building can be described by 3.33.

for ∀t∈T

$$P_{HVAC}(t) = -.2186 \times \left(T_{setpoint}(t) - T_{out}(t)\right) + 5.86 \quad \textbf{3.33}$$

3.3.1.7 Lighting Modeling

Consumption of lighting highly depends on the application of building. Light intensity of any area can be measured in lux. The recommended lux for warehouse and work area are .1 and .15 kW/m2 respectively [93] . Equation 3.34 has been used to estimate the lighting power of the building and light intensity has been controlled by 3.35.

$$P_{lighting}(t) = (.0929 \times \varphi(t) \times A_{Building})/\eta_{lighting} \quad \text{for } \forall t \in T \quad \textbf{3.34}$$

$$\varphi_{min} < \varphi(t) < \varphi_{max} \qquad \text{for } \forall t \in T \qquad \textbf{3.35}$$

3.3.1.8 Temperature Comfort Modeling

The ideal room temperature is 25 degree Celsius. To control the thermal comfort of the building, 3.36 is deployed where the minimum and maximum temperature setpoint for HVAC are 24 and 26 degree respectively.

$$T_{setpoint\ min} < T_{setpoint}(t) < T_{setpoint\ max} \qquad \text{for } \forall t \in T \qquad \textbf{3.36}$$

3.3.1.9 Energy Price Modeling

The energy rate used for simulation is from an Investor Owned Utility (IOU) called Southern California Edison (SCE). It is assumed that the electric vehicle is plugged in between 9am-9pm. As it is a Time of Use (TOU) energy rate, it charges consumers more between 4-9 pm. Table 3-7 summarizes the energy cost for these time periods.

Table 3-7 TOU Based Energy Charge

Time	SCE Energy Charge ($/kWh)
9 am – 4 pm	0.22
4 pm – 9 pm	0.41

3.3.1.10 Degradation Cost Modeling

The depreciation cost for any li-ion battery is dynamic and depends on several factors such as daily usage, temperature, operation scenarios. The depreciation cost can be modeled using the equation 3.37 and it can vary from 0.08-0.13 $/kWh [94].

$$C_d = \frac{C_{dep\_daily}}{E_{dep\_daily}/K_{dep}} \quad \textbf{3.37}$$

3.3.1.11 Power Balance Modeling

Equation 3.38 describes the power balance equation for different energy providers. The sum of power provided to building by grid, solar PV, BESS and EV will be equal to power required for BESS charging, EV charging, HVAC, lighting and miscellaneous loads for this building.

$$\mathrm{P}_{grid}(\mathrm{t}) + \mathrm{P}_{\mathrm{PV}}(\mathrm{t}) + \mathrm{P}_{\mathrm{disch,B}}(\mathrm{t}) + \mathrm{P}_{\mathrm{V2G}}(\mathrm{t}) = \mathrm{P}_{ch,B}(\mathrm{t}) + \mathrm{P}_{\mathrm{G2V}}(\mathrm{t}) + \mathrm{P}_{\mathrm{HVAC}}(\mathrm{t}) + \mathrm{P}_{\mathrm{lighting}}(\mathrm{t}) + \mathrm{P}_{\mathrm{misc}}(\mathrm{t}) \text{ for } \forall \mathrm{t} \in \mathrm{T} \quad \textbf{3.38}$$

3.3.2 Problem Formulation and Constraints

3.3.2.1 Objective Function

The objective functions of the optimization problem are stated by 3.39 and 3.40. The first equation is needed to be solved for minimizing the energy cost and degradation cost resulted from BESS and PEV activities and the second equation also integrates the demand cost.

Objective 1:

$$\text{Minimize } \sum_{t=1}^{T}\Big\{\big(P_{grid}(t)\times\Delta t\times C_e(t)\big)+\Big(\eta_{\text{ch,B}}\times \text{P}_{\text{ch,B}}(\text{t})+ \tag{3.39}$$

$$\text{P}_{\text{disch,B}}(\text{t})/\eta_{\text{disch,B}}\Big)\times C_{d,B}(t)\times\Delta t+(\eta_{\text{ch,EV}}\times \text{P}_{\text{G2V}}(\text{t})+\text{P}_{\text{V2G}}(\text{t})/\eta_{\text{disch,EV}})\times$$

$$C_{d,EV}(t)\times\Delta t\Big\}$$

Objective 2:

$$\text{Minimize } \Big[\max P_{grid}\times\ C_d+\sum_{t=1}^{T}\Big\{\Big(P_{grid}(t)\times\Delta t\times C_e(t)\Big)+ \tag{3.40}$$

$$\Big(\eta_{\text{ch,B}}\times \text{P}_{\text{ch,B}}(\text{t})+\text{P}_{\text{disch,B}}(\text{t})/\eta_{\text{disch,B}}\Big)\times C_{w,B}(t)\times\Delta t+\Big(\eta_{\text{ch,EV}}\times \text{P}_{\text{G2V}}(\text{t})+$$

$$\text{P}_{\text{V2G}}(\text{t})/\eta_{\text{disch,EV}}\Big)\times C_{w,EV}(t)\times\Delta t\Big\}\Big]$$

3.3.2.2 Constraints

All constraints for the formulated optimization problem are described by equations (1)-(19).

3.3.2.3 Optimization

The objective functions and all the equations used as constraints are linear. Both continuous and binary variables exist in the sets of constraints' variables. Therefore, this optimization problem is a MILP problem. Gurobi Python [88] environment has been used to model and solve this optimization problem. The workstation used to solve it is of core-i7 with 16 GB RAM.

3.3.3 Simulation Results & Discussions

3.3.3.1 Base Case

The base case used to solve this optimization problem considers the availability of a regular good sunny day for maximum solar generation. Maximum thermal comfort is induced to make the temperature level varying in a very tight range. The plug-in load is considered constant for this building. As battery degradation cost is considered for both BESS and PEV, so higher energy charges such as the California IOU energy rates are used to figure out the actual impacts of all the controllable and non-controllable loads and sources available. The specifications of all the base case variables are noted in Table 3-8.

Table 3-8 Base Case Description

Base Case	
Solar PV	Sunny Day
BESS	150 kWh/50 kW
PEV	64 kWh/7 kW
Lighting	50% of Total Building Area
Temperature	24℃≤T≤26℃
Energy Price	Investor Owned Utility
Miscellaneous	Constant

3.3.3.2 Slow and Fast G2V/V2G Impacts on the Base Case

Solar power was mostly available from 9-3 pm for the given day. During the base case scenario, PEV operates in charging mode to reach the highest level of SOC while solar is abundant. Later, it shifts to discharging state and discharges power at a constant rate of 7 kW to reduce the total cost associated with G2V and V2G activities. This results in a sharp declination of PEV SOC and maintains the desired final SOC level at the end of the on-peak period. The lower capacity of PEV is the reason behind the constant discharging operation during on-peak periods. BESS acts in a similar way and discharges during off-peak periods. Figure 3.18 shows the impacts of all charging/discharging scenarios for PEV to optimize the energy cost.

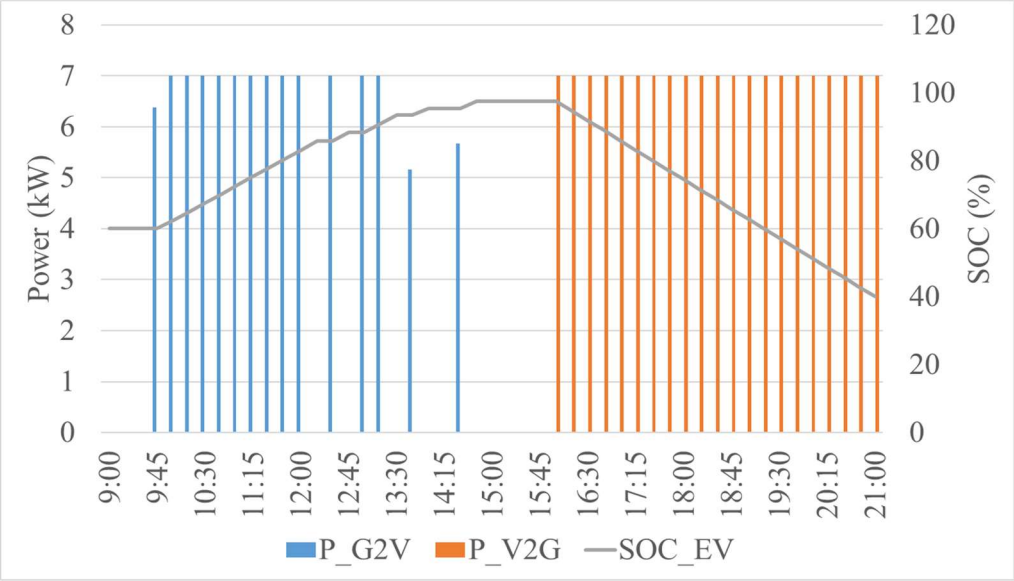

Figure 3.18 Base Case with Nissan Leaf E Plus: EV Charging Profile Along With SOC

In the case of fast charging/discharging impacts analysis, the available EV is capable of DC fast charging with 480 V three-phase ac power connection and up to 50 kW G2V/V2G rate. Both EV and battery charging/discharging take place at the same time in the case of level II charging. In contrast, the PEV and battery charging/discharging activities do not happen simultaneously in this case. If the charging/discharging events take place less, the battery life for BESS and PEV will sustain more. So, the charging and discharging events for BESS occur when EV is not in action and vice versa. The G2V and V2G profiles for PEV along with relevant SOC and solar generation are shown in Figure 3.19. Level III EV activities provide the higher cost-benefit for both objectives shown in Table 3-9. As no constraint is imposed upon the maximum demand that can be provided by the grid, so the optimal scheduling is the same for both objectives. The rest of the sensitivity analyses discussed in the latter sections are based on the first objective.

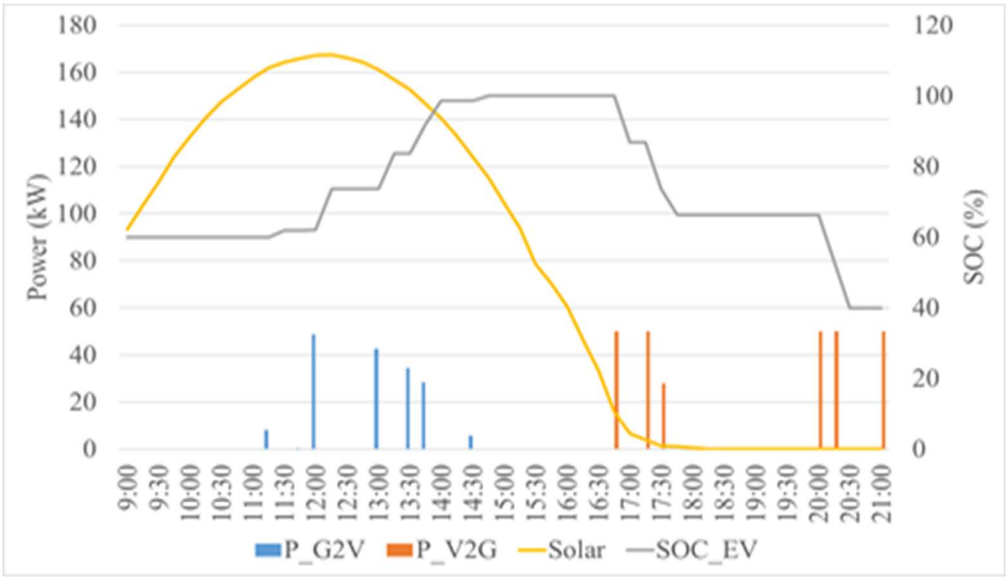

Figure 3.19 Base Case with Tesla X: Solar and EV Charging Profile Along With SOC

Table 3-9 Base Case Daily Cost Comparison

Type	Objective 1	Objective 2	Percentage of Savings (%) (Objective 1)	Percentage of Savings (%) (Objective 2)
Heuristic Solution	273.34	457.18	–	–
Nissan Leaf: Level II	217.27	401.112	20.5	12
Tesla X: Level III	210.49	394.33	23	14

3.3.3.3 Effects of Lighting Variation

Lighting is one of the highest energy consumer loads present in buildings. To analyze the lighting impacts on the optimization strategy, lighting intensity is varied within a permissible limit. Advanced control systems help to vary the lighting of a place depending on its occupancy. Occupancy sensors and motion sensors are the most common control types of equipment for lighting variation. Centralized building automation control algorithms can include lighting control along with control of HVAC and other DER resources. The effects on the maximum peak and energy cost due to lighting variation are studied and documented. Figure 3.20 shows the impacts of lighting variation on cost optimization strategy and maximum peak. Level III charging/discharging capable electric

vehicles always results in achieving minimum energy cost. Higher battery capacity and a higher rate of charging/discharging offer the best opportunity to charge/discharge at the right time. As expected, energy cost increases when the lighting level increases. In the case of a level II G2V/V2G charger, for an increase of 40 to 60 percent lighting level, the maximum peak increases by 43 percent while energy cost increases by 59 percent.

On the other hand, a higher charging rate causes a higher maximum peak occur with level III EV charging as expected. Though the change in maximum peak (40%) is lower in comparison to level II activities, the difference in energy cost increment is 63% higher than that of level II .

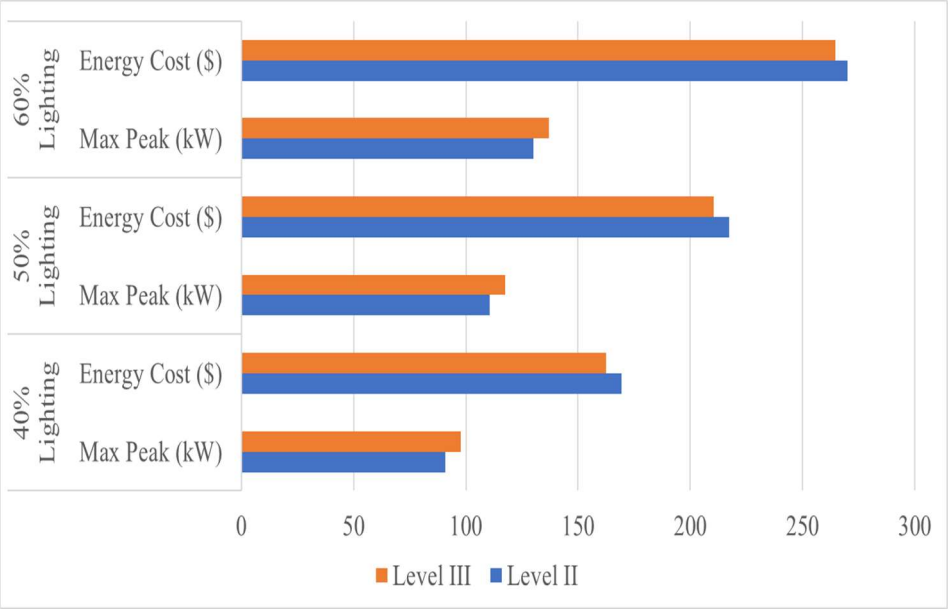

Figure 3.20 Impacts on Energy Cost and Maximum Peak for Lighting Variation

Figure 3.21 is showing the charging/discharging power of BESS and PEV along with their SOC for lighting level variation with fast charging. While a lower lighting level is selected

for optimization, both BESS and PEV can work one at a time and provide maximum and longer energy support to the building. When a higher lighting level (60%) is required, then neither BESS nor PEV can fully provide charging during high solar availability. They are also incapable of providing energy during on-peak hours for a longer period.

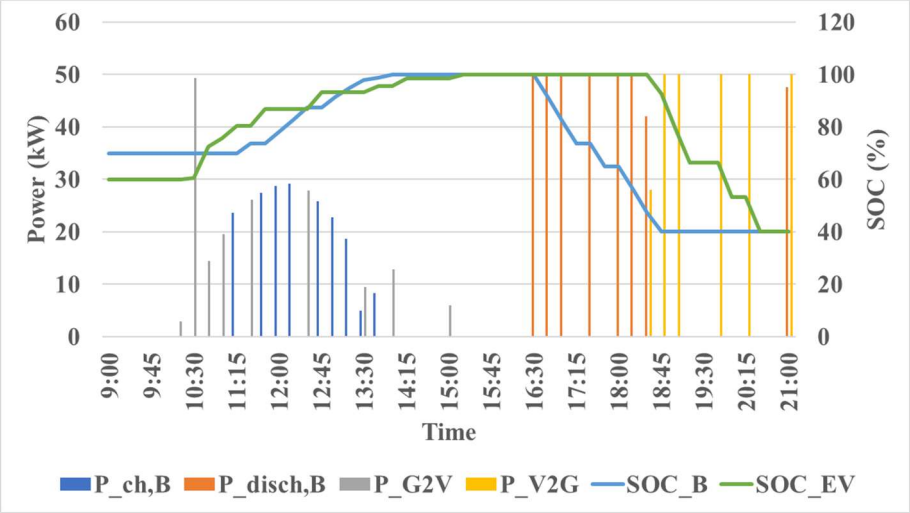

Figure 3.21 Base Case with Level III Charging and 40% Lighting: BESS & PEV Power and SOC Profile

3.3.3.4 Effects of Electricity Price

The pricing structure is a large motivating factor in the cost optimization strategy for any building integrated with DERs. If the price varies a little or does not vary at all over time, then the evaluation of decision variables gets more sophisticated. The pricing of energy largely depends on the size and average electricity usage by the building occupants. Typically, users of most small or medium-size buildings do not pay any demand (kW) charge. However, their energy (kWh) charges are significantly higher making energy cost optimization more important. Large energy consumers usually are on Time of Use (TOU)

rates and must pay various demand charges in addition to the typically lower energy charges.

Two pricing structures from local Municipal Utility are used to test the impacts of pricing on our comprehensive optimization solution. The energy price per kWh is lower than the BESS and EV degradation cost on the first case and the on-peak energy cost is slightly higher than the off-peak energy charge. Later on, a flat energy charge is also used to find out the significance of optimal strategy for all the controllable resources available. The various energy charges for the hours of interest (9 am- 9 pm) of the public municipal utility are shown in Table 3-10.

Table 3-10 Public Municipal Utility Charge

Type	Time	Energy Charge ($/kWh)
TOU	9 am – 4 pm	0.0874
	4 pm – 9 pm	0.1079
Flat Rate	9 am – 9 pm	0.1684

When this TOU rate is used for the optimization model, the BESS and PEV do not charge or discharge at all. As their degradation cost per kWh for any charging or discharging activities is higher than the energy cost, they don't take part in any energy minimization from the grid. Only other available controllable loads such as HVAC and lighting help to minimize the overall energy cost. On the other hand, with a flat energy

price higher than the degradation cost, BESS and PEV do not take part in charging or discharging because of a lack of time-varying pricing opportunities. Their only usages are for managing the demand and intermittent solar production. Flat pricing provides 25.6% and 26.0% cost savings for level II and III charging, respectively. This compares with the cost saving results of TOU prices of 20.5% and 23% for level II and level III charging, respectively.

3.3.3.5 Effects of Temperature Variation

Keeping tight constraints on temperature settings results in very comfortable and stable indoor temperatures. But it limits the opportunity for varying HVAC loads to contribute towards operational cost reduction. In this scenario, relying on the thermal mass of the building, the temperature is varied to a larger extent during the low occupancy period. The optimization problem is solved with a lower bound of 22 degrees and an upper bound of 28 degrees Celsius (25 +/- 3 °C). This larger temperature variation gives a slightly better economic benefit (20.9%-23.4%) compared to the base case. Raising the temperature limits further especially in extreme cases can result in more economic benefits, for example during critical grid events such as Flex Alert in California [67]. Flex alert is issued by the local utility when consumers respond to reduce their energy usage and help the grid operators prevent possible blackouts and brownouts.

Figure 3.22 is showing the comparison of HVAC power consumption with the base case for level II charging activities. HVAC power consumption gets lower throughout the day for a wider range of temperature settings as expected during slow charging. It generally follows the same trend during fast charging activities.

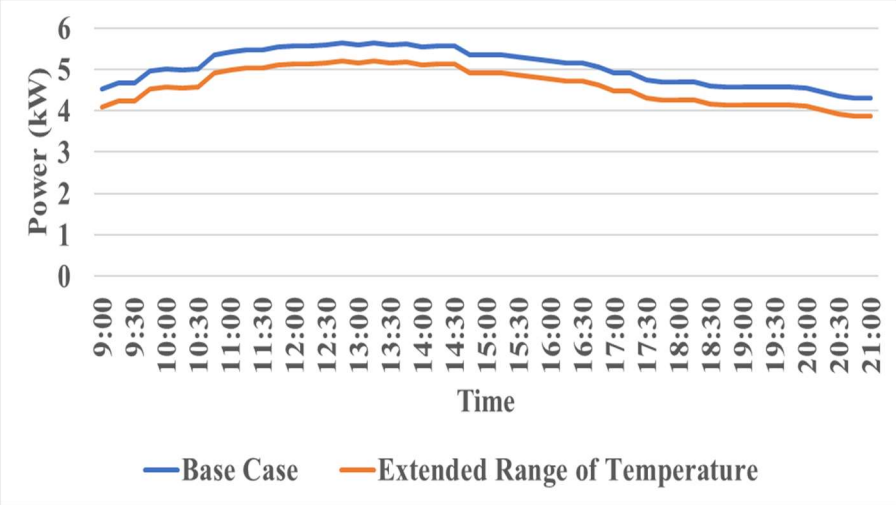

Figure 3.22 HVAC Power Consumption with Level II Activities: Base Case & Extended Range of Temperature

Figure 3.23 is showing the charging and discharging profile for BESS and PEV in case of extended variation in temperature and fast PEV activities. In this mode of operation, as expected lesser number of charging and discharging incidents occur resulting in more savings.

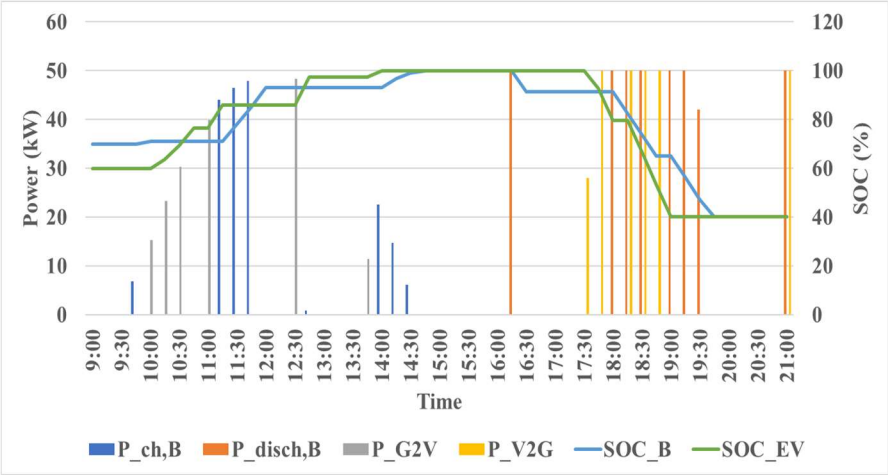

Figure 3.23 Temperature Variation with Extended Range & Level III Activities: BESS & PEV Power and SOC Profile

3.3.3.6 Cloudy Day Impacts

The BESS and PEV must get fully charged before the more expensive on-peak period on a sunny day so that they can discharge while needed. But when there is not enough solar during the daytime on a cloudy day, the situation gets worse. To evaluate the impacts of a cloudy day on the regular operation of the building with DERs, a cloudy day temperature, and solar irradiance profiles are used. The amount of savings possible for a cloudy day is much lower than a regular sunny day. A maximum of 6.1 percent energy cost reduction is possible for a cloudy day. A level III charger is better again in the case of energy cost optimization compared to a level II and provides 1.2 percent more savings. Figure 3.24 and Figure 3.25 are showing the net power imported from the grid for a typically sunny and cloudy day while the base case is considered. Cloudy day results in a 4.38 percent increase in peak during level II activities compared to a sunny day. On the other hand, a cloudy day results in a 1.75 percent decrease in peak demand for level III activities. The difference in peaks is due to the individual chargers' capacities. As solar is

intermittent throughout the cloudy day, the BESS and PEV are not being charged up to their 100 percent capacity. Only a few discharging events take place during on-peak periods.

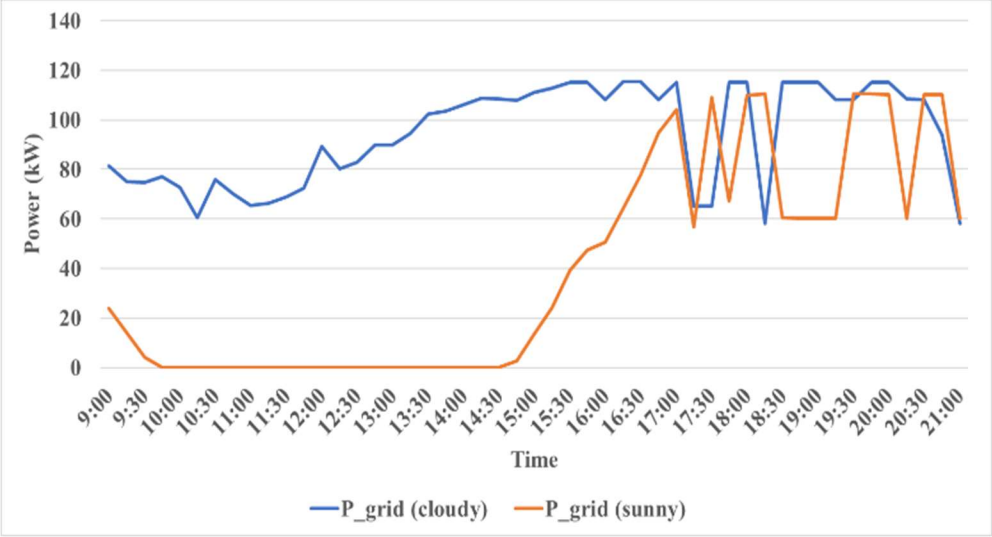

Figure 3.24 Cloudy Day & Level II Activity: Power Purchased from Grid

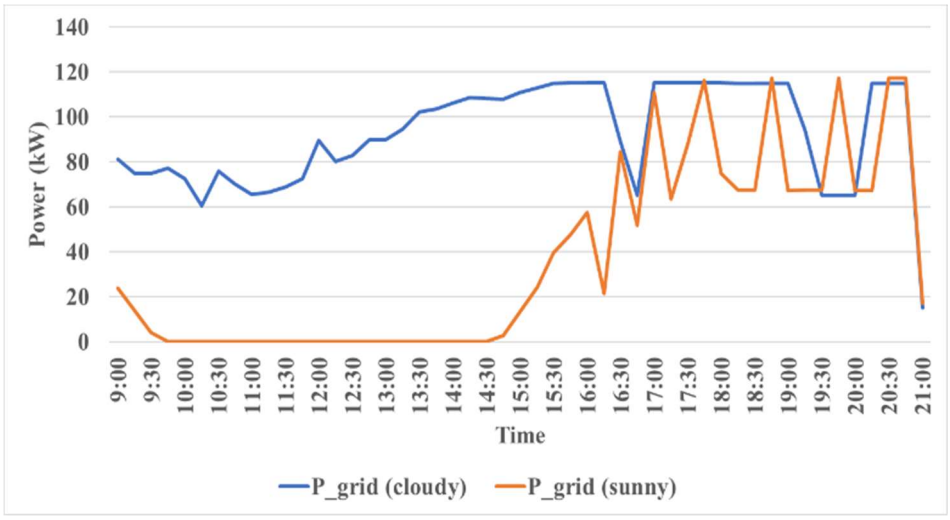

Figure 3.25 Cloudy Day & Level III Activity: Power Purchased from Grid

3.3.3.7 Impacts on Distribution Feeder

To analyze the DER impacts on the low voltage distribution grid, IEEE 13 bus system is chosen and modified to adopt the coordinated DERs integrated into the system. This is a relatively highly loaded 4.16 kV feeder equipped with spot loads [95]. To model the test feeder, PV and BESS are connected to node no 671 on phases A and C, respectively. PEV is connected to node 611. HVAC, lighting, and miscellaneous loads are considered to be integrated on node 675 where grid purchased power is added. The nodes are chosen proportionately with maximum power capabilities of different DERs to investigate the real impacts on the feeder. All DERs and building loads are added as additional loads to their respective nodes along with the base spot load values. The modified test feeder is shown in Figure 3.26.

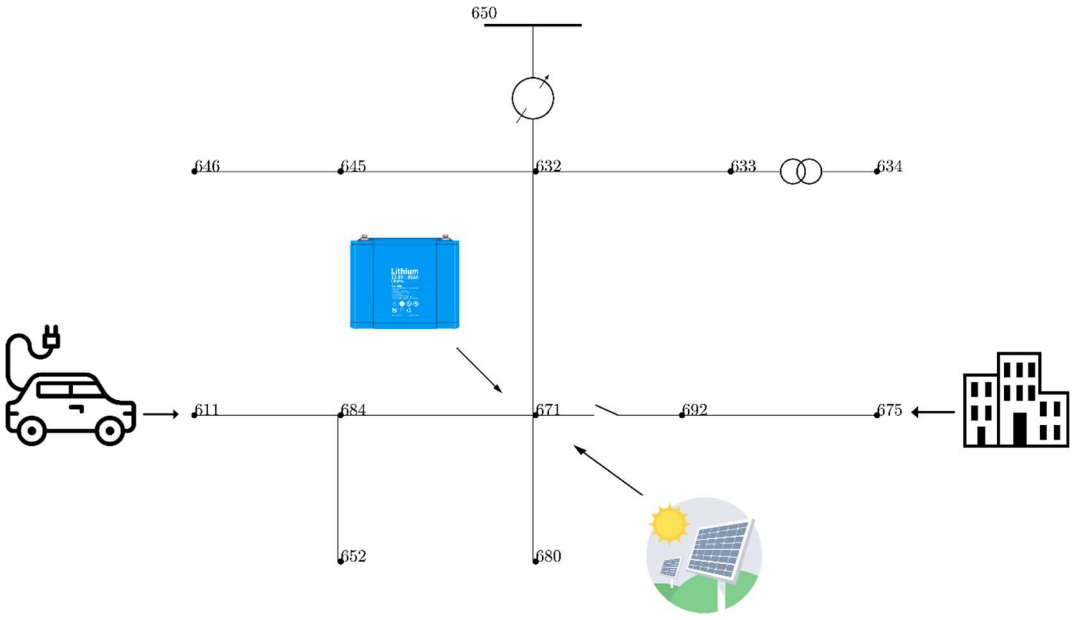

Figure 3.26 Modified IEEE-13 Bus Test Feeder

In distribution systems, the addition of DERs can make the grid unstable because of their intermittent nature and unoptimized scheduling. To evaluate the DER impacts on a distribution level test feeder, voltage profile study at the respective DER buses is a reliable indicator. Hence, the voltage profiles are analyzed at nodes 611, 671, and 675. To make the BESS, PEV, and PV impacts on the distribution grid explicit, they have been integrated as distributed control equipment instead of connected to the same node. OpenDSS is used to solve the power flow equation and evaluate the DER impacts on the test feeder. Newton method is used to solve the power flow equation in OpenDSS [96].

Voltage Deviation Index (VDI) is highly recommended to show the overall voltage unbalance scenario for the whole simulation period. VDI is formulated as the root mean square voltage deviation from the nominal voltage magnitudes of the buses with time depicted in equation 3.41. V_t is the per unit (pu) voltage at time t for any node. The nominal voltage is considered as 1 pu. Hence, the voltage deviation is monitored for each time slot in the nodes where DERs are applied and used for VDI calculation.

$$\text{VDI} = \sqrt{\sum_{t=1}^{T}(V_t - V_{nominal})^2 / T} \qquad \textbf{3.41}$$

Table 3-11 shows the VDI for all case scenarios at 611, 671, and 675 nodes. Level III ensures fewer voltage deviations for the building, BESS, and PEV nodes whereas level II results in less VDI for the PV node. Level II activities result in 18% higher VDI for PEV and 13% higher VDI for building nodes respectively. VDI captures the voltage deviation for the total simulation period, there is more bidirectional power flow for the level III PEV

node that makes the VDI lower for level III activities. On the other hand, level III results in 24% higher VDI at the PV node.

Table 3-11 Voltage Deviation Index

Cost Objective	PEV level	Building	PV	BESS	PEV
Energy+BESS degradation +PEV degradation	Level II	0.03392	0.0279	0.07035	0.0777
	Level III	0.0296	0.0357	0.07	0.0644

3.3.3.8 Computation Time

The computational time is a factor in solving any real-time optimization problem. The mathematical modeling done here provides all linear equations to analyze the characteristics of controllable components such as BESS, PEV, HVAC. The linearity provides the flexibility for the solver to solve it quickly and makes it practical for real-time optimization. It takes an average of 0.05 seconds to solve the problems in most of the cases which is a lot faster than any other type of machine learning-based non-linear model.

3.4 Data Driven Optimization

3.4.1 Nomenclature

t	Time slot index
T	Total time period
n_{ld}	light duty PEV index
n_{hd}	heavy duty PEV index
l_1	charging decision binary variable index
l_2	discharging decision binary variable index
N_{ld}	Set of light duty PEVs
N_{hd}	Set of heavy duty PEVs
L_{ch}	Set of charging binary variables
L_{disch}	Set of discharging binary variables
Δt	Time interval
b_1	Charging decision binary variable for BESS
d_1	Discharging decision binary variable for BESS
SOC_{EV}	State of Charge of EV
$SOC_{min,EV}$	Minimum SOC for EV
$SOC_{max,EV}$	Maximum SOC for EV

$\eta_{ch,EV}$	EV charging efficiency
$\eta_{disch,EV}$	EV discharging efficiency
$P_{ins,EV}$	Instantaneous power consumption by any EV
r_m	Resistance of EV motor
D_{tire}	Diameter of the EV tires
k_a	Armature constant
φ	Magnetic flux
m_{EV}	Total mass of the EV
a	Acceleration of EV while driving
k_{aero}	Aerodynamic drag coefficient
v	Velocity while EV on a trip
f_{rl}	Rolling friction coefficient
g	Acceleration due to gravity
$P_{EV,ch}$	Power transferred from grid to each vehicle (kW)
$P_{EV,disch}$	Power generated from each vehicle to grid (kW)
$P_{EV,ch\ max}$	Maximum charging power for EV (kW)
$P_{EV,disch\ max}$	Maximum discharging power for EV (kW)

P_{grid}	Power from grid to building
P_{solar}	Power generated from solar
$P_{building}$	Power consumption for the building
$P_{EV,disch,total}$	Total Power transferred from vehicle to grid (kW)
$P_{EV,ch,total}$	Total Power collected from grid to vehicle (kW)
$A_{EV,n_{ld}}$	Availability matrix for light duty EV
$A_{EV,n_{hd}}$	Availability matrix for heavy duty EV
C_e	Price of energy purchased from grid ($/kWh)
$C_{battery}$	Cost of Li-ion battery ($/kWh)
Cap_{init}	Initial Capacity of the EV battery
Cap_{useful}	Useful Capacity of the EV battery
$Deg_{calendar}$	Calendar degradation of the EV battery
Deg_{cycle}	Cycle degradation of the EV battery
DOD	Depth of Discharge
a,b,c	Fitting parameters for cycle degradation

3.4.2 Methodology

As an example location for this analysis, we consider the transportation-based microgrid at the College of Engineering – Center for Environmental Research & Technology (CE-CERT) at the University of California Riverside. One of the CE-CERT buildings (Building 1084) is used for administrative activities and another (Building 1200) is used for research activities. The CE-CERT microgrid consists of a 180 kW solar PV system at each building [97] . The electrical load of the 1084 building follows a regular office load pattern whereas the electrical load of 1200 building is relatively larger with a more uncertain pattern. The regular work hours are from 8 am to 5 pm on weekdays. The testbed for PEV operation is shown in Figure 3.27.

Figure 3.27 Testbed for Bidirectional Cost Optimization

3.4.2.1 Predicting Building and Solar Data

The building load pattern depends on the occupancy along with the solar generation being intermittent due to weather. The energy cost is calculated based on the 15-minute rolling average energy consumption by the electric utilities. Hence, 15-minute ahead

building load and solar prediction are done for each of the buildings. Statistical approaches such as ARIMA don't provide a good estimation for the short-term time series prediction [98]. Long Short-Term Memory (LSTM) network is applied for the 15-minute ahead time series prediction. The network is applied on the Keras platform using Tensorflow at the backend [99]. A rolling-horizon approach is implemented to predict the data. The input data are updated for each time slot. 30 days of data are used for training the model initially. Then the 1st timestamp data of the next day is predicted. The Adam optimizer is used [100], and the batch size, number of layers, and number of epochs have been tuned to find the best fit for the fitted model. The prediction results do not change much with a higher number of layers and epochs. A typical summer month data is used for the prediction. Figure 3.28 is showing the predicted data for the 31st July for both of the buildings and Table 3-12 is showing the error metrics for the prediction which shows that solar generation is predicted with a very low root mean square error (RMSE). The prediction is good enough to follow the building load pattern but the RMSE increases with a high load deviation for the 1200 building.

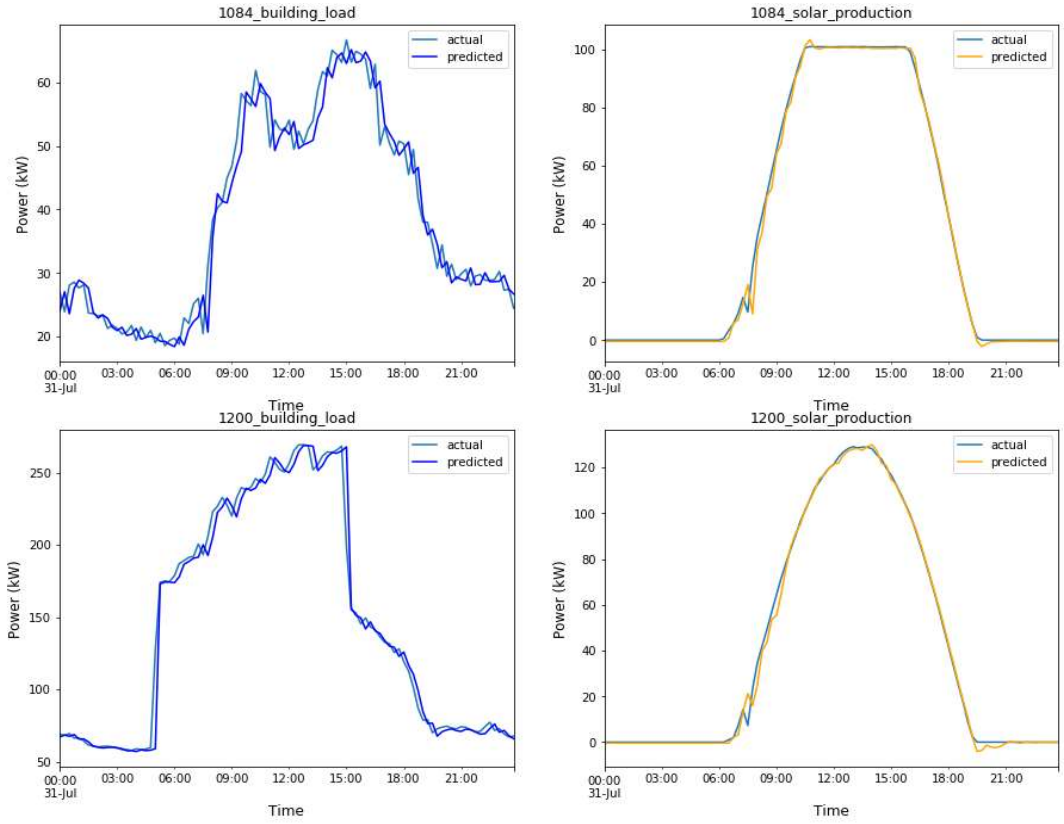

Figure 3.28 Predicting Building Load and Solar Generation for Both of the Buildings

Table 3-12 Error Metrics for Prediction

Prediction (kW)	**RMSE**	**Prediction (kW)**	**RMSE**
1084 building load	3.14	1084_solar	2.39
1200_building_load	11.12	1200_solar	2.57

3.4.2.2 Heavy Duty PEV Data

When considering HDEV activity, we utilize data from an electric trolley bus that operates on a fixed route around UC Riverside. The battery pack used in the electric trolley is composed of 540 cylindrical lithium iron phosphate cells arranged in a 5P108S (5 parallel, 108 series) pattern that provides 345.6 V and a capacity of 155.52 kWh nominal. The cells are laid out across 12 ventilated enclosures, with each enclosure featuring its own battery management system (BMS) modules. The on-board charger takes in AC voltage from the utility grid and converts it to the necessary DC voltage to charge the battery pack. The charger is currently configured to charge at one of three selectable levels corresponding to 33, 67, and 100 ADC and allows a maximum of 40 kW power level. The bus has been tested along a specific route (Route 51) as part of the Riverside Transit Agency schedule [101]. The total route is 9.3 miles long with an additional stop at CE-CERT. To measure the average kWh needed per mileage, the bus is tested for multiple days with both loaded and unloaded conditions. The average energy consumption is 1.48 kWh/mi and 1.15 kWh/mi for loaded and unloaded conditions, respectively. Using the same route every day is similar to the schedule of school buses. It is assumed that the bus will complete two round trips each day as school buses do one in the morning and one in the afternoon. The energy consumption per trip can be estimated by using the following equations. The instantaneous power consumed by an EV is extracted from [102] and modified as follows.

$$P_{ins,EV} = \frac{r_m \times D_{tire}^2}{4 \times k_a^2 \times \varphi^2}(m_{EV}a + k_{aero}v^2 + f_{rl}m_{EV}g + \quad \textbf{3.42}$$

$$m_{EV}gsin\theta)2+v(k_{aero}v^2 + f_{rl}m_{EV}g + m_{EV}gsin\theta) + m_{EV}av$$

The first two terms in 3.42 are the power losses from motor and travel resistance, respectively. The last term is the power generated from acceleration/deceleration. The integral of this instantaneous power consumption throughout the whole trip will result in 3.43.

$$E_{total\ per\ trip} = \int_{t=1}^{T} P_{ins,EV}(t)dt \quad \textbf{3.43}$$

3.4.2.3 Light Duty PEV Data

For our LDEV analysis, we consider two light-duty electric vehicles that are available for the employees of these buildings for short to medium-distance travels for attending meetings. Both light-duty PEVs are 2013 Nissan Leaf electric vehicles that have the capability of vehicle to grid (V2G) operation. Both have 24 kWh battery capacity with a capability of fast charging/discharging given that fast charging bidirectional EV stations are available. The recent models of Nissan Leaf have a 40 kWh or 62 kWh battery capacity [87] . As 40 kWh battery capacity PEV is the most common one used by the consumers, this is used to minimize the cost function. Because the travel routes and meeting times do not follow a regular schedule, the pattern of PEV usage is different in comparison to any regular commute travel profile. The diurnal energy requirements for any PEV largely

depend on its regular activities. To capture the usual activities of the available PEVs, two commercial data loggers were used inside of each vehicle. The parameters of initial consideration included Vehicle Speed, Charge Status, Battery Level (% and Wh), Battery Voltage, Battery Current, Battery Temperature, Motor Torque, and Motor Speed. Travel patterns and profiles have been generated using the available parameters in combination with GPS tracking of the vehicle. As the charging characteristics cannot be inferred in real-time, hence they are translated from prior travel data and charging events. If any change in SOC occurred between turning on and off the vehicle, that can be evaluated using subsequent trip data [103] . Extracted travel data is used for Figure 3.29 - Figure 3.31.

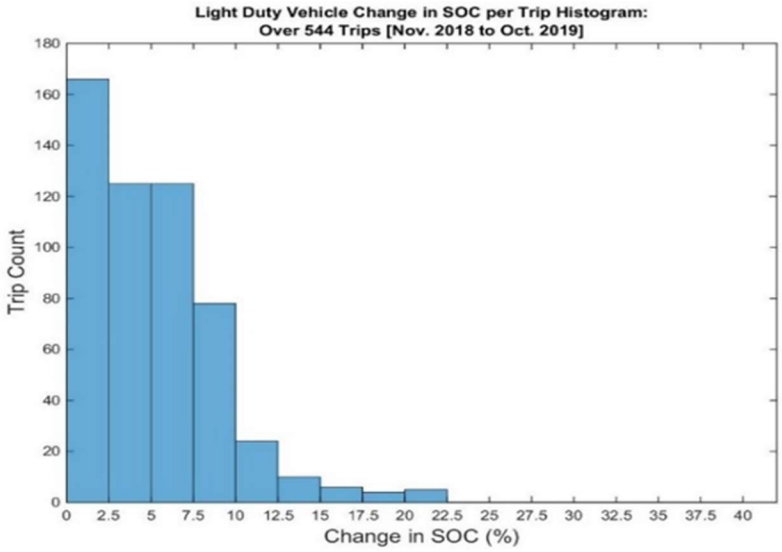

Figure 3.29 Change in SOC Per Trip for Both PEVs

Figure 3.29 shows the change in SOC per trip. Most of the trips involve short distance travel for attending meetings and covering distances of 6 to 8 miles for a round trip, so the resulting change in SOC is small. The maximum change in SOC observed for a few occasions is 22.5%. Figure 3.30 shows the charging events for both PEVs and Figure

3.31 shows initial SOC before the trips were made. A total of 544 trips were made with the two light-duty PEVs from Nov 2018 to Oct 2019. Initial SOC mostly lies between 60-80% of the total capacity of the available PEVs.

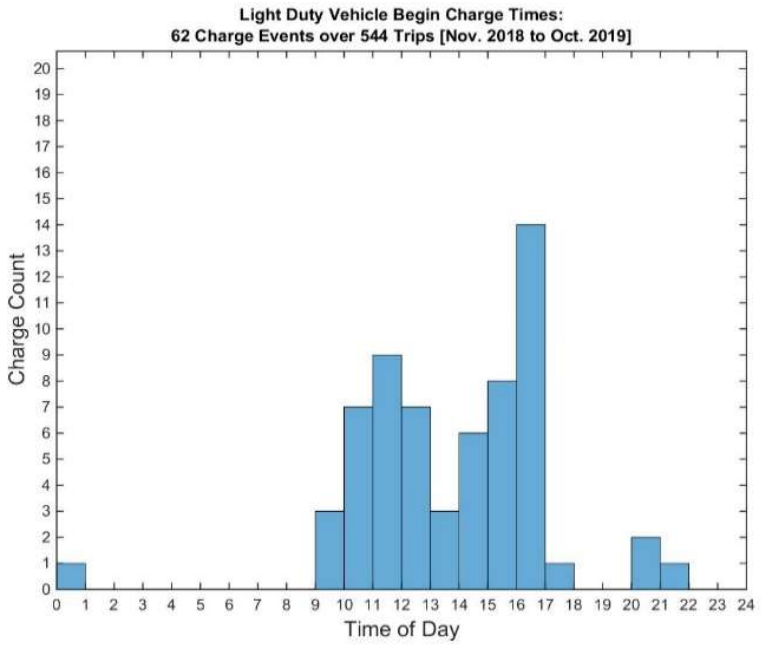

Figure 3.30 Charging Events of Both PEVs

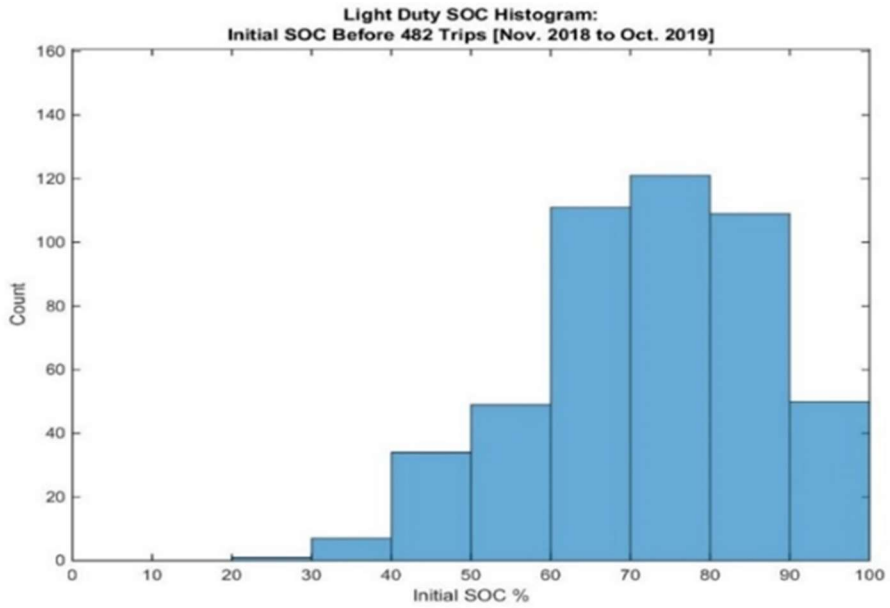

Figure 3.31 Initial SOC Per Trip for Both PEVs

3.4.3 Problem Formulation & Constraints

3.4.3.1 Problem Formulation

The goal is to minimize the overall cost for EV operation in this specific workplace-integrated microgrid. This overall cost includes the total cost of energy and battery degradation.

$$\text{minimize (Energy Cost} + \text{ Battery Degradation Cost)} \qquad \textbf{3.44}$$

3.4.3.2 Energy Cost

The first objective of this multi-objective problem is minimizing the cost of energy purchased from the grid. The total energy cost can be described by 3.45. Equation 3.46 shows the sum of delivering power from grid, solar and EV is equal to the sum of power required by EV and the building. The total charging and discharging power by EV are

calculated by 3.47 and 3.48. The EV SOC, charging, and discharging rates are constrained by 3.49-3.52. The charging and discharging decision variables are binary which are imposed by 3.53-3.54.

$$\text{Energy Cost} = \sum_{t=1}^{T} P_{grid}(t) \times \Delta t \times C_e\,(t) \quad \textbf{3.45}$$

$$P_{grid}(t) + P_{EV,disch,total}(t) + P_{solar}(t) = P_{EV,ch,total}(t) + P_{building}(t) \quad \textbf{3.46}$$

$$P_{EV,ch,total}(t) = \sum_{n_{ld}=1}^{N_{ld}} A_{EV,n_{ld}}\,(t) \times P_{EV,ch,n_{ld}}\,(t) + \sum_{n_{hd}=1}^{N_{hd}} A_{EV,n_{hd}}\,(t) \times P_{EV,ch,n_{hd}}\,(t) \quad \textbf{3.47}$$

$$P_{EV,disch,total}(t) = \sum_{n_{ld}=1}^{N_{ld}} A_{EV,n_{ld}}\,(t) \times P_{EV,disch,n_{ld}}\,(t) + \sum_{n_{hd}=1}^{N_{hd}} A_{EV,n_{hd}}\,(t) \times P_{EV,disch,n_{hd}}\,(t) \quad \textbf{3.48}$$

for $\forall t \in T$, $\forall n_{ld} \in N_{ld}$, $\forall n_{hd} \in N_{hd}$, $\forall l_1 \in L_{ch}$, $\forall l_2 \in L_{disch}$,

$$\text{SOC}_{\text{EV}}(t) = \text{SOC}_{\text{EV}}(t\text{-}1) + \left\{\left(\eta_{\text{ch,EV}} \times \text{P}_{EV,ch}(t) - \text{P}_{EV,disch}(t)/\eta_{\text{disch,EV}}\right)/ Cap_{init}\right\} \times \Delta t \quad \textbf{3.49}$$

$$\text{SOC}_{\text{min,EV}} \leq \text{SOC}_{\text{EV}}(t) \leq \text{SOC}_{\text{max,EV}} \quad \textbf{3.50}$$

$$0 \leq \mathrm{P}_{EV,ch}(\mathrm{t}) \leq l_1(t) \times \mathrm{P}_{EV,ch\,\max} \quad \textbf{3.51}$$

$$0 \leq \mathrm{P}_{EV,disch}(\mathrm{t}) \leq l_2(t) \times \mathrm{P}_{EV,disch\,\max} \quad \textbf{3.52}$$

$$l_1(t) + l_2(t) = 1 \quad \textbf{3.53}$$

$$l_1(t), l_2(t) \in \{0,1\} \quad \textbf{3.54}$$

3.4.3.3 Battery Degradation Cost

The EV battery degradation depends on multiple factors such as temperature and operating conditions. The battery degradation cost can be described by the eqn. 3.55 [104] [105]. The impact of yearly degradation is highly dependent on the operating temperature and negligible in comparison to the cycle degradation. Hence, only cycle degradation is used to compute the daily battery degradation cost.

Battery Degradation Cost= **3.55**

$$\sum_{t=1}^{T} C_{battery} \times \frac{(Deg_{calendar} + Deg_{cycle})}{(Cap_{init} - Cap_{useful})}$$

$$Cap_{useful} = 0.8 \times Cap_{init} \quad \textbf{3.56}$$

$$Deg_{cycle} = a \times DOD^3 + b \times DOD^2 + c \times DOD \quad \textbf{3.57}$$

To make it quadratic and solve it by the off the shelf solvers like Gurobi [88], an auxiliary variable is introduced. If $y' = DOD^2$, then the above equation can be written as

$$Deg_{cycle} = a \times y' \times DOD + b \times y' + c \times DOD \quad \textbf{3.58}$$

3.4.3.4 Cost-Benefit Analysis

The following parameters are used to execute the cost benefit analysis.

$$\text{Payback Period} = \frac{Total\ Operational\ and\ Installation\ Cost}{Yearly\ Savings} \quad \textbf{3.59}$$

$$Total\ Operational\ and\ Installation\ Cost = \text{Equipment cost} + \text{Installation cost} + \text{Annual recurring fees} \quad \textbf{3.60}$$

$$Yearly\ Savings = 365 \times \text{Daily savings from optimized EV operation} \quad \textbf{3.61}$$

3.4.3.5 Optimization

The cost function along with its constraints is a Mixed Integer Programming (MIP) and a non-convex problem. The problem is solved in Gurobi optimization solver with a work station having i-7 core and 16 GB RAM [88].

3.4.4 Results and Discussions

The current infrastructure allows the electric bus to be plugged into any of the buildings through an inverter stationed in a 500 kWh stationary battery energy storage trailer. There are five EVCS connected to the 1084 building electrical distribution panel.

The daily solar production in 1084 building is more than the average load consumption whereas the average load consumption is higher in the 1200 building. 1084 building is a Tier 1 (maximum demand < 100 kW) building and 1200 building is Tier 4 (maximum demand is 250-500 kW) building [106]. Multiple use cases are considered to analyze the cost benefits available from LDEV and HDEVs.

3.4.4.1 Optimal Scheduling of EVs

Case I: Only HDEV is Present

The first case explores the opportunity of cost optimization by the electric trolley in this commercial building-integrated microgrid. The electric trolley is available for charging and discharging anytime outside the morning (before 8:30) and afternoon (between 14:00 and 15:00) scheduled trip times. Both 1084 and 1200 buildings are considered for this scenario and the cost opportunity is examined for both on-board and off-board charger activities. It is assumed that the on-board charger in the bus allows a maximum of 40 kW and the off-board charger allows a maximum of 100 kW for charging/discharging. Though the actual electric bus does not allow bidirectional charging with the on-board charger (40 kW), 100 kW bidirectional power transfer is possible through the inverter mounted on the mobile trailer. Figure 3.32 and Figure 3.33 show the grid-to-vehicle (G2V) and vehicle-to-grid (V2G) activities by the electric trolley on both of the buildings for different charger configurations, respectively. The 1084 building is enriched with surplus solar production during the daytime. Hence, the charging events take place when solar is available despite the on-peak hours (12 pm – 6 pm), and the bus discharges when solar goes down in the afternoon. Despite the capacity of charging at 100

kW rates, the HDEV charges slowly to balance the net power at 1084 building with off-board configurations. Though the solar is abundant from 14:00-15:00, no charging takes place due to unavailability of the HDEV. During the late evening hours, the on-board charger triggers more discharging events due to its low discharging capacity of 40 kW. When degradation cost is included, higher DoD leads to higher degradation. Hence, the bus charging/discharging activities are lower compared to the activities without the effort to minimize the degradation cost. The charging/discharging rates are also lower when degradation cost is included. Solar production in the 1200 building is not enough to compensate for all the building loads. More discharging events take place during the day and the discharging rate is also maximum. The inclusion of degradation cost leads to a moderate charging/discharging profile for a longer period to extend the battery life.

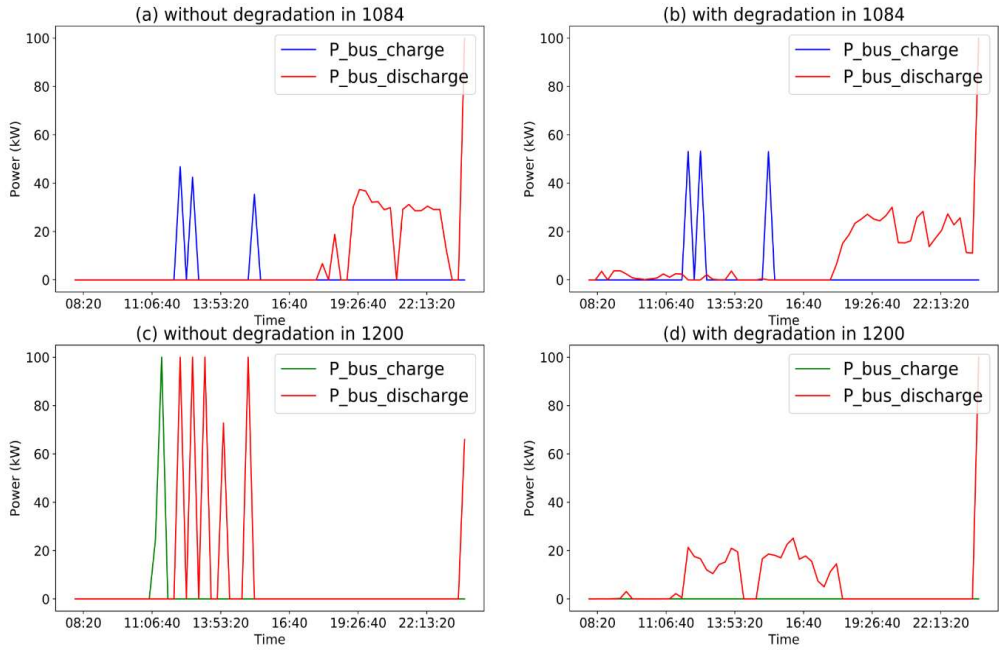

Figure 3.32 Case I: HDEV Activities in Different Buildings with Off-board Charging; HDEV was Unavailable Before 8.30 and Between 14:00 and 15:00

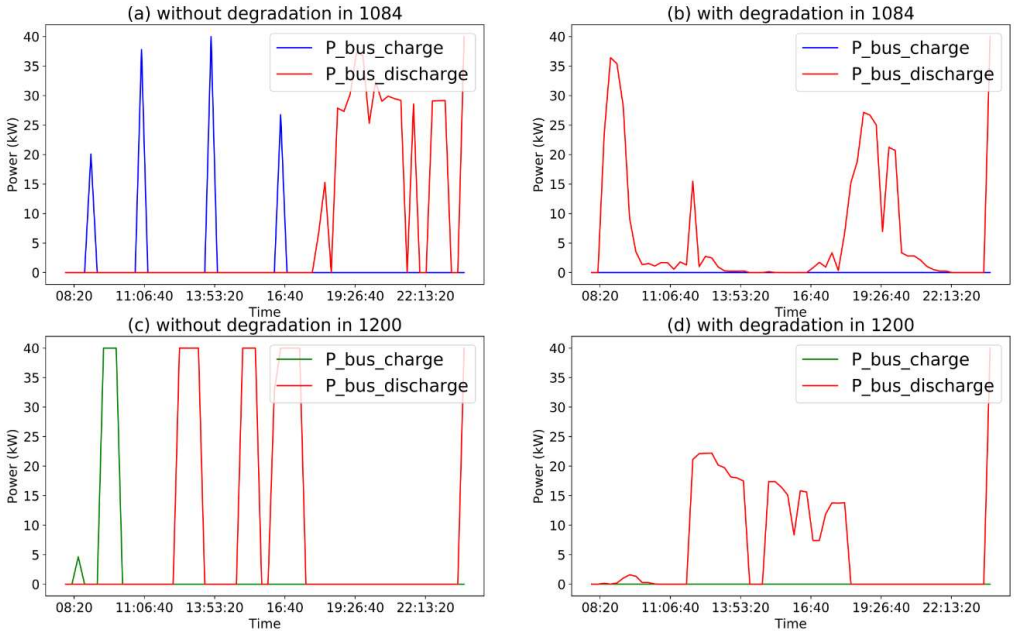

Figure 3.33 Case I: HDEV Activities in Different Buildings with On-board Charging; HDEV was Unavailable Before 8.30 and Between 14:00 and 15:00

Case II: Only LDEV is Present

LDEVs are assumed to be available for energy optimization in the second case. It is assumed that all the LDEVs are identical and the capacity of each is 40 kWh. All the off-board chargers are bidirectional and the maximum bidirectional capability of each charger is 30 kW. The on-board chargers in the LDEVs are assumed to be bidirectional and the power rating of 6.6 kW is representative of level II EV charging/discharging. The availability of LDEVs depends on the regular work schedules. They are unavailable during the lunch period and out of work hours (after 5 pm). As Figure 3.29 indicates that the maximum change of SOC level is 22.5 percent which only occurs rarely. In general, for this LDEV model with a 30 kWh/100 mi rating, a round trip can be completed if it has at most 26 miles with the comfortable SOC level at the starting and finishing the trip with 20 percent SOC left [107] . So, the minimum SOC level is assumed 40 percent of total capacity to allow for completion of the return trip.

The initial SOCs of all the LDEVs are chosen randomly and assumed to be 50-80% of the total SOC. When the solar is available in 1084, there is no need to discharge the LDEVs and the LDEVs discharge in the early morning. They follow the same characteristics with the addition of the depreciation cost but discharge at slower rates. If all the LDEVs are connected to the 1200 building, they get charged at the early hours of the day when the electricity price is low. All the LDEVs take part in reducing the net load and the discharging rates are slower during the overall cost (energy cost+ battery degradation cost) optimization. For 1200 building, the maximum total discharging power reduces to approximately one-sixth of capable V2G in off-board configurations whereas the amount

of reduction is nearly half for the on-board configurations with the inclusion of degradation cost as shown in Figure 3.34 and Figure 3.35. This shows that the V2G availability largely depends on the number of LDEVs in the fleets and their configurations

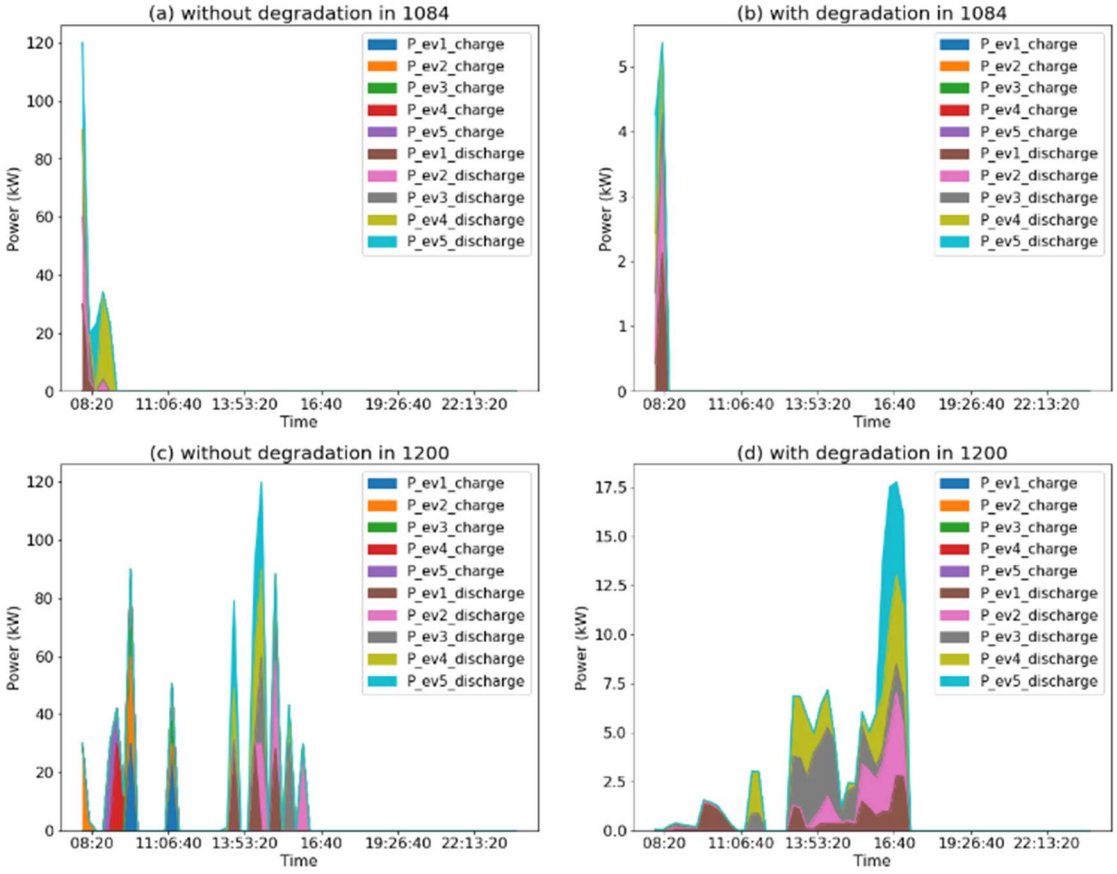

Figure 3.34 Case II: LDEV Activities in Different Buildings with Off-board Charging; LDEV was Unavailable Between 12:00 and 13:00; and After 17:00

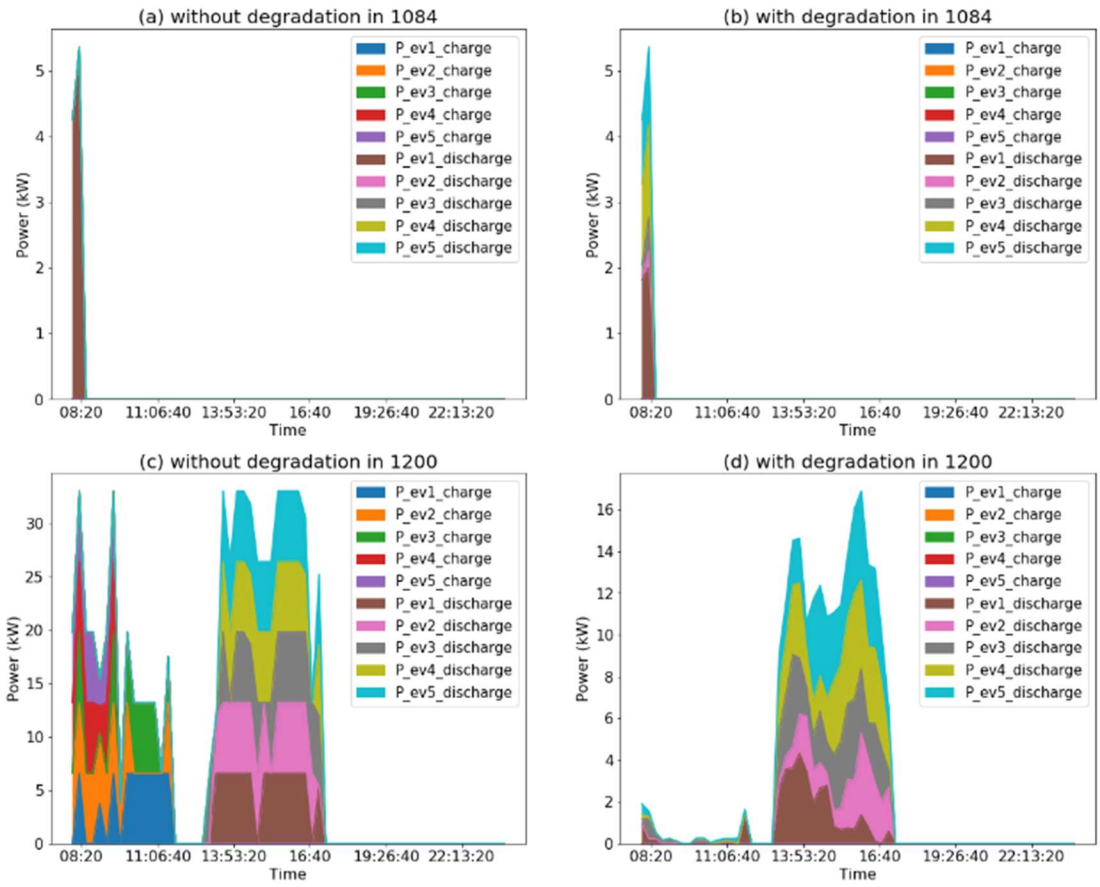

Figure 3.35 Case II: LDEV Activities in Different Buildings with On-board Charging; LDEV was Unavailable Between 12:00 and 13:00; and After 17:00

Case III: Both LDEV and HDEV are Present

The last case study includes both LDEVs and HDEVs for optimization with two scenarios: a) net metering and b) no net metering. Figure 3.36 shows the optimal scheduling of LDEVs and HDEVs when all of them try to minimize the overall energy cost of two buildings. If net metering is available, then it is possible to optimize the net load by the LDEVs and HDEV. The presence of net metering helps to utilize the curtailed solar energy of the 1084 building. The LDEVs also discharge and utilize their remaining energy during the on-peak hours. The degradation cost constraint leads to the controlled lower

discharging rates of the vehicles. Figure 3.37 shows the LDEVs and HDEV activities with on-board charger configurations.

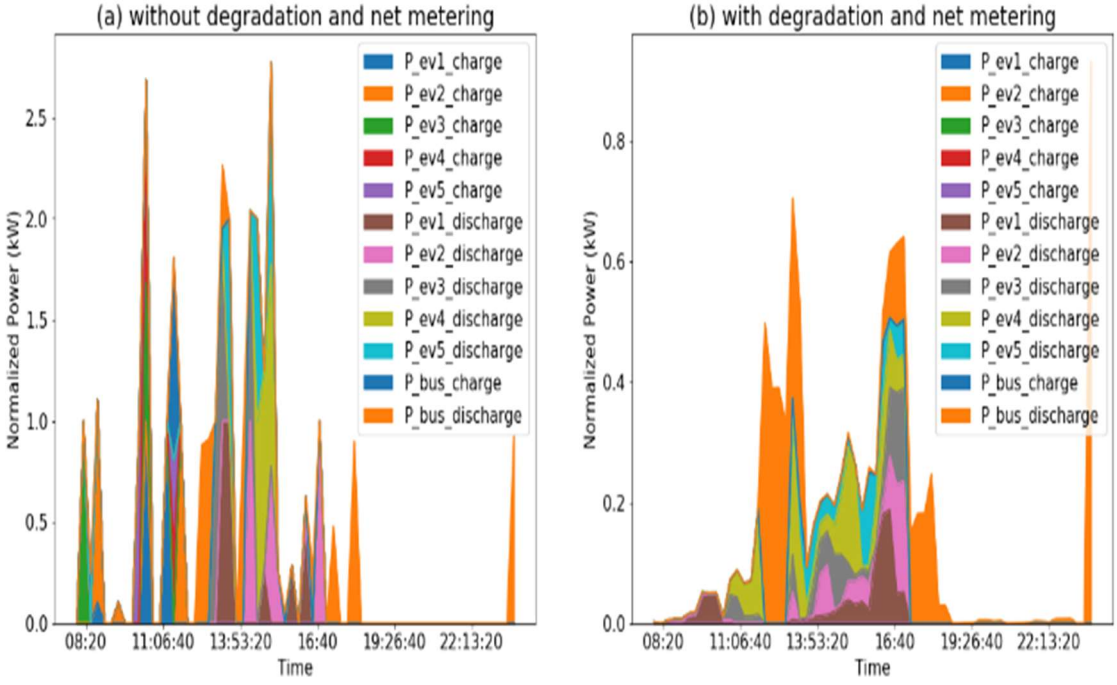

Figure 3.36 Case III: LDEV and HDEV Activities in Different Buildings with Net Metering and Off-board Charging

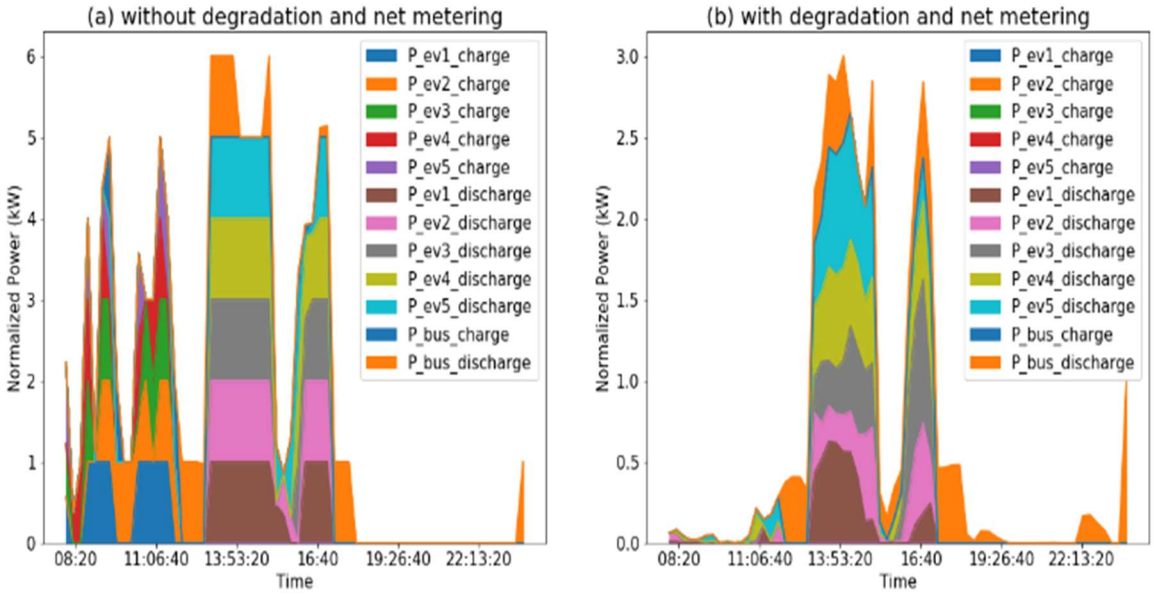

Figure 3.37 Case III: LDEV and HDEV Activities in Different Buildings with Net Metering and On-board Charging

3.4.4.2 Cost Savings

The regular energy cost without any EV is calculated for the buildings where the Time of Use (ToU) energy rate shown in Table 3-13 is applied. The energy costs for the buildings along with the uncoordinated LDEV and HDEVs are also calculated. When implementing uncoordinated EV charging, it means that all the EVs start charging when they are plugged in regardless of the TOU energy rates or the availability of solar energy. They recharge again after any trip that happened during the day to make up the used energy. Table 3-14 and Table 3-15 show the cost savings for off-board and on-board configurations in comparison to the no EV and uncoordinated EV cases respectively. The electric trolley provides the maximum cost saving opportunity due to its availability at night time and fixed number of trips. LDEVs generate lower savings due to their fixed presence at the worksite and are unavailability after 5 pm. Net metering always provides higher savings in

comparison to no net metering available. Inclusion of degradation cost reduces the amount of savings. The cost savings don't vary much and do not depend on charger configurations (i.e., on-board or off-board). Higher savings are more likely in buildings like 1084 and net metering provides the highest cost benefit for the off-board charger configurations. It is noted that no savings is possible with LDEVs compared to no EV situation when degradation cost is added.

Table 3-13 Time of Use Energy Cost [106]

Time	Price ($/kWh)
Off-Peak (11 pm - 8 am)	0.0773
Mid-Peak (8 am -12 pm), (6 pm-11 pm)	0.0898
On-Peak (12 pm - 6 pm)	0.1104

Table 3-14 Cost Savings for Off-board EVSE

		Infrastructure Cost vs with Optimization		EV Uncoordinated and Coordinated	
Cases	Building	No degradation	degradation	No degradation	degradation
Case I	1084	73.9%	42.1%	79.3%	54.1%
	1200	7.2%	5.2%	10.4%	8.6%
Case II	1084	1.5%	-	35.2%	34.3%
	1200	4.2%	-	9.4%	5.4%
Case III	net metering	13.2%	5.8%	21.6%	14.9%
	no net metering	6.7%	4.8%	13.4%	11.7%

Table 3-15 Cost Savings for On-board EVSE

		Infrastructure Cost vs Optimization		Uncoordinated and Coordinated	
Cases	Building	No degradation	degradation	No degradation	degradation
Case I	1084	73.9%	11.2%	79.3%	29.6%
	1200	6.8%	4.9%	10.1%	8.3%
Case II	1084	1.5%	-	35.2%	34.3%
	1200	4.2%	-	9.4%	5.5%
Case III	net metering	12.4%	5.5%	20.9%	14.6%
	no net metering	6.4%	4.5%	13.2%	11.4%

3.4.4.3 Peak Reduction

Table 3-16 shows the change in peaks for optimized operation in comparison to uncoordinated EV charging. Off-board configuration provides higher peak reduction compared to on-board configurations. The inclusion of degradation cost leads to higher peak savings in almost all cases. The capability of reducing the peak in 1200 building is

lower for off-board chargers. Net metering provides a higher peak reduction for on-board or level II charging capabilities in comparison to no net metering available.

Table 3-16 Peak Reduction with Optimized Operation

		Off-board		On-board	
Cases	Building Number	No degradation	degradation	No degradation	degradation
Case I	1084	67.2%	79.6%	16.5%	17.9%
	1200	15.2%	35.4%	12.2%	18.0%
Case II	1084	75.8%	75.8%	2.6%	2.6%
	1200	26.2%	44.7%	0.0%	15.5%
Case III	net metering	34.8%	43.8%	19.5%	24.3%
	no net metering	36.6%	49.6%	10.8%	15.7%

3.4.4.4 Payback Period

The payback period is another important parameter for the building owners to make a decision on EV infrastructure investments. Table 3-17 shows the cost of different EVCS equipment for different charger configurations.

Table 3-17 Cost of EVCS Equipment [108]

Type	On-board ($)	Off-board ($)
Charging Infrastructure	25,000	60,000
Installation per site	10,000	10,000
Vehicle upgrades	12,000	8,000

The payback periods for all the cases are tabulated in Table 3-18 and Table 3-19. It is possible to reach break-even in 1.24 years in building 1200 for the case I with off-board configurations. Maximum 9 years are required for case II whereas 3.88 years are needed to get the initial investment back for net metering.

Table 3-18 Payback Period in Years for Off-board EVSE

		Infrastructure Cost vs with EV		Uncontrolled vs Optimized	
Cases	Building Number	No degradation	degradation	No degradation	degradation
Case I	1084	1.59	2.80	1.18	1.73
	1200	1.54	2.11	1.02	1.24
Case II	1084	320.25	-	8.75	8.98
	1200	10.53	-	4.43	7.65
Case III	net metering	4.60	10.39	2.54	3.67
	no net metering	7.34	10.20	3.38	3.88

On the other hand, less time is required with on-board charger configurations to make a profit. It takes less than a year to make a profit in case I and a maximum of 4 years to make a profit in case II. Almost 2 years are needed in case III which is almost half than case III in off-board configurations.

Table 3-19 Payback Period in Years for On-board EVSE

		Infrastructure Cost vs with EV		Uncontrolled vs Optimized	
Cases	Building Number	No degradation	degradation	No degradation	degradation
Case I	1084	0.96	6.31	0.71	1.90
	1200	0.97	1.35	0.63	0.77
Case II	1084	139.47	-	3.81	3.91
	1200	4.59	-	1.93	3.31
Case III	net metering	2.22	5.02	1.19	1.71
	no net metering	3.49	4.93	1.57	1.80

3.4.4.5 Impacts of Fleet Size

The size of the fleet is an important factor as well to invest on the EV infrastructure. Hence, the current EV penetration scenario is compared with 10 and 20 percent EV parking spaces penetration scenarios, respectively. The maximum number of EV parking spaces can be 200 for the size of this infrastructure [109]and the HDEV and LDEV mix ratio is considered 30 to 70 percent [110] . Figure 3.38 shows the payback period for these different scenarios when net metering is available, and degradation is not considered. Though the

payback period reduces when the penetration increases, the optimal payback period can be achieved when 10 percent of the parking spaces get penetrated with PEV.

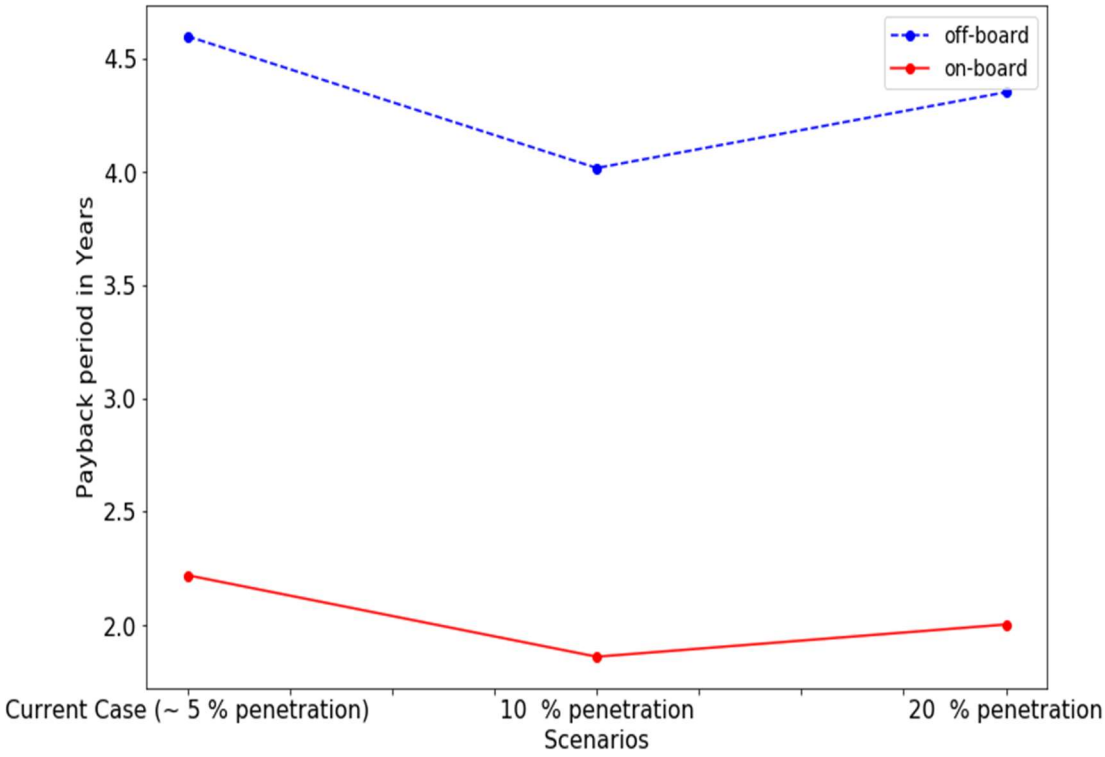

Figure 3.38 Impacts of Fleet Size on Payback Period for Net Metering

3.5 Conclusions

This chapter discusses the key factors of optimal approaches and the cost optimization strategies for bidirectional PEV operation.

In Section 3.2, the key factors to determine the optimal cost are explored by utilizing a data driven bidirectional PEV model. The study finds that the probability of PEV availability for small commercial buildings who owns PEVs do not follow any normal

distribution and expected cost optimization highly relies on PEV modeling. PEVs having higher initial SOC available for optimal cost operation provides more cost savings regardless of their distribution. Comfortable SOC priority or trying to keep enough SOC available for multiple trips results in lower savings at the end of PEV sessions. Between 2 and 3.2 percent cost savings is possible for any small commercial building load profile with a regular light duty PEV ownership. In 2018, the EV share in California is just under 5 percent of new vehicles sold [111]. State of California's proposed 2040 goal is one hundred percent zero emission vehicles [112] . This can result in 1.2 million new light duty vehicle sales per year of which 75 percent may be EVs [113] . The optimization study presented here indicates that this may lead to over $300 million savings annually. Finally, the impacts of different building loads on optimal EV charging for both unidirectional and bidirectional operation have also been examined, taking different electrical utility energy rates into consideration. This study has shown that low price differential between on-peak and off-peak electrical energy rates result in lower EV charging cost for large building loads whereas high differential electrical energy rate does the same for smaller building loads. Bidirectional operation can save up to 23.5% energy cost in comparison to unidirectional operation despite deeper discharge cycles. Bidirectional operation always gives higher percentage of savings for higher differential energy rates.

Both centralized and data driven approaches are carried out to find the optimal framework for the best PEV charging/discharging strategy and the best combination of HDEV and LDEV implementation, respectively. In Section 3.3 , a comprehensive solution incorporating the usual loads like HVAC, lighting and, plug-in loads, with newer

technologies like PV, BESS, and PEV is presented. The contributions and limitations of each of these components are represented along with battery degradation in the cost function for optimization. The results show that for buildings equipped with DERs, between 20.5% to 23.0% system cost reduction is possible depending on the type of vehicle chargers. This is valid under the Time of Use (TOU) rate schedule for the most active 12-hour period of a week-day when both the kW demand and kWh energy costs are the highest. For the slower rate of G2V/V2G activities, the maximum increase in kW peak is 39.98 percent for 40 to 60 percent variation in lighting. While for fast G2V/V2G activities, the peak demand increment is 43.07 percent. Effects of electricity price variation are explored which show that operation of BESS or PEV might not be feasible if their degradation costs are higher than the energy costs. This exhibits the need for subsidization or restructuring the utility prices in order to promote these technologies. Contrary to popular belief, it shows that level III charging causes less voltage deviation than level II, which might encourage higher adoption of level III EV charging infrastructures resulting in higher range EV purchases.

Later on, a data driven bidirectional PEV model is introduced in Section 3.4 and followed by a MIP model to minimize the overall cost of two different commercial buildings. An extensive cost-benefit analysis is completed in terms of charger configurations, payback periods, energy cost savings and peak reductions. For this specific case, the findings show that it is more economical to have an HDEV with fixed travel schedules for energy savings. The least payback period is possible by deploying an HDEV

in a large energy user building. Net metering always helps to get the initial investment back in a shorter period. The inclusion of degradation cost results in better peak reductions.

4 Plug-in Electric Vehicle User Behavior and Load Modeling

4.1 Background

Electric vehicles are being widely adopted throughout the world to ensure sustainable transportation growth. The immense popularity of PEV in recent years has impacts on both transportation and electrical distribution network. To lessen the adverse impacts of the rapid increase in PEV use requires improvements in both charging infrastructure and public policy. As mentioned earlier in Chapter 1, more than half a million PEVs were sold in the US in 2021 and the number of PEV Charging Stations (CS) according to [114] is already one hundred and nine thousand. Almost 80 percent of public charging stations are level II charging stations and having a charging rate between 6 kW and 7.2 kW [115]. User-friendly policies and lower costs are the main contributing factors to this massive PEV adoption. This chapter analyzes the spatial-temporal variety of many PEV charging sessions from a large university campus. A yearlong data analysis makes sure that the analysis properly captures the correlation of PEV charging with both seasonal and temporal variation. In addition to the interpretation of user behavior and station energy usage, it estimates the aggregated PEV load of the campus community and finds out the answers to some important key questions for policy makers: 1. PEV CS data interpretation for a large university campus community to help the policy makers and CS owners. 2. Providing a probabilistic and aggregated PEV load estimation for a large-scale PEV community and validation with an Adaptive Charging Network Simulator (ACN-Sim). 3.

Conducting feasible PEV penetration scenarios to assess the impact of overloading on the grid and possible revenues for CS owners. Later on, a comprehensive EV and grid modeling is proposed to analyze the EV impacts on the grid.

4.2 Data Collection and Analysis

University of California Riverside (UCR) is one of the ten UC campuses and is situated in southern California with more than 20 thousand students. It has a total of 18 PEV charging stations and all of them are supervised by Chargepoint [116] of which 2 of them are recently added. Hence, this data analysis is based on 16 PEV charging stations with at least a year-long data. Each of the stations has 2 charging ports. 27,746 charge sessions data were collected between Jan 2019-Jan 2020. The charging station distribution by different parking lots is tabulated in Table 4-1.

Table 4-1 Charging Station Distribution

Parking Lots	No of PEV Charging Ports
Lot 1	4
Lot 6	4
Lot 9	4
Lot 15	4
Lot 20	2
Lot 24	12
Lot 30	2
Total	32

4.2.1 Energy Usage by Station

Figure 4.1 shows the energy usage and occupancy of different charging stations during weekdays. As lot 24 has the most charging ports, it is the most frequently used PEV parking lot on the campus. Most of the charging events take place on weekdays as expected. Lot 6 station 1 (L6_S1) has used the most energy during the given timeframe. Station 1 for both lot 24 and lot 6 have used more than 17,000 kWh during the charging events over the last year. Figure 4.2 shows the seasonal variation of PEV use. The least charging events

take place in summer and fall as they involve long holidays and relatively lower campus activities.

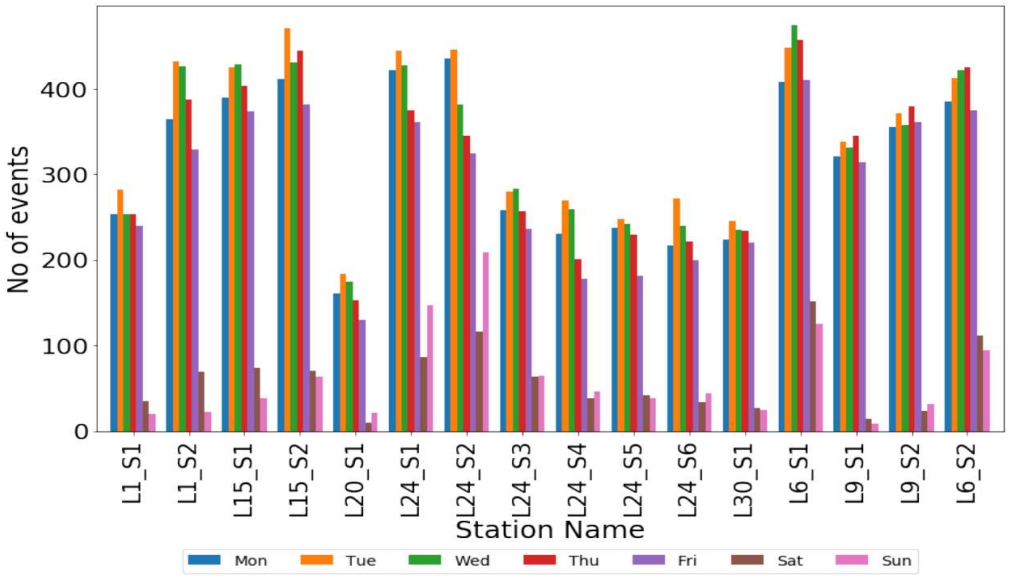

Figure 4.1 Charging Events in Different Charging Stations over a Year

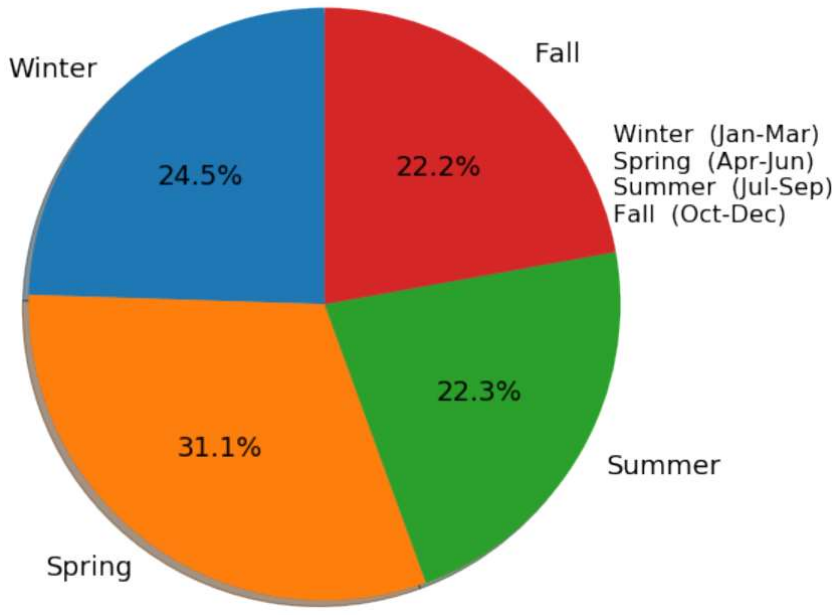

Figure 4.2 Seasonal Variation of PEV Activities

4.2.2 Distribution of Charging Sessions

The distribution of charging session starting time is the primary indicator to show the PEV station engagement scenario. In most commercial facilities that own charging stations, the main influx of charging events happens in the early morning hours (e.g. 9 am); the same happens after 5 pm for residential charging stations. The campus community covers a wide range of PEV owners, so their charging sessions do not follow a typical distribution pattern. For this study, a day is divided into 4 time periods- Late Night (12-6 AM), Morning (6 AM-12 PM), Afternoon (12-6 PM), Night (6 PM-12 AM). More than 90 percent of users charge their PEVs during morning and afternoon on a typical weekday. Overnight charging events increase on weekends. Figure 4.3 shows the distribution of charging sessions based on those four categories during different days.

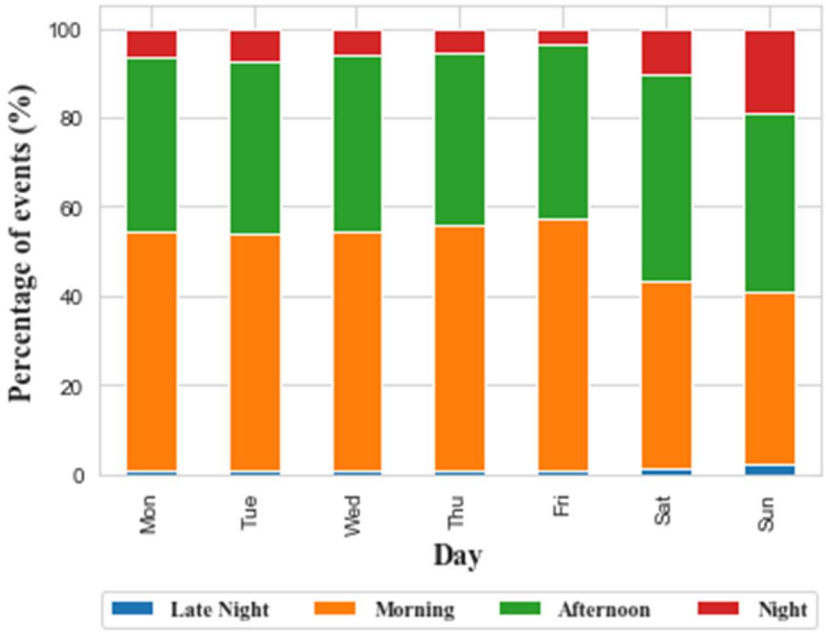

Figure 4.3 Charging Events Variability with Time and Day

4.2.3 Distribution of Charging Session Connectivity

Charging session duration is an important benchmark to analyze user behavior. Public and residential charging stations typically show four types of charging connectivity behavior. This scenario is different for any public charging station which charges people on an hourly basis for electricity usage. Charging levels also determine the length of charging sessions for any PEV user. All the charging stations on this campus are level II chargers which have a power level of between 6 kW and 7.2 kW. Most of the charging sessions end before 3 hours for the typical PEVs in use. Long charging sessions mostly happen on weekends as expected. Very few charging sessions take place lasting more than 7 hours. The charging session duration distributions are shown in Figure 4.4.

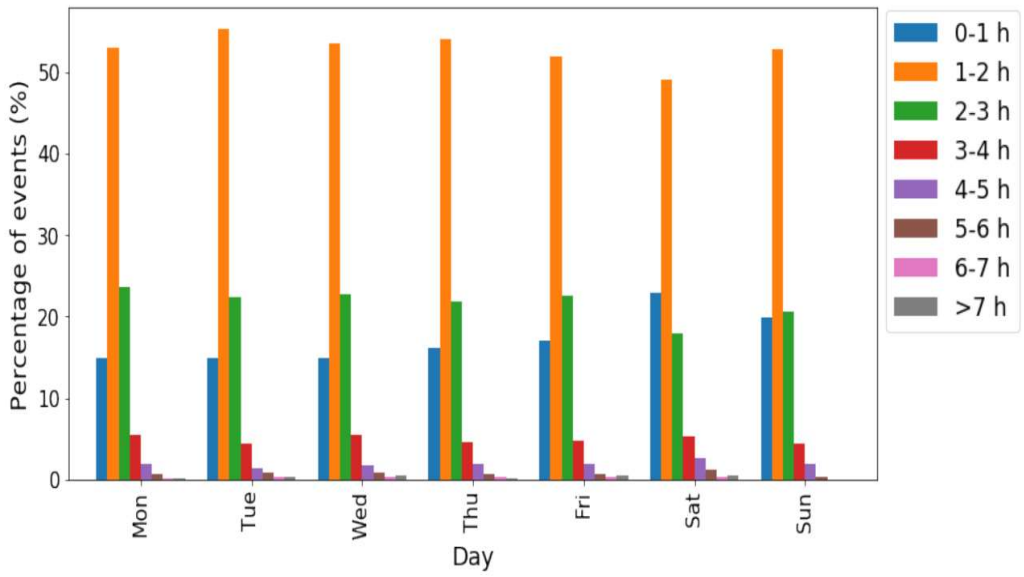

Figure 4.4 Charging Session Duration Variability

4.2.4 Distribution of Energy Usage

Figure 4.5 represents the energy usage scenario by each PEV charging session on various weekdays. The overall average energy usage is 7.46 kWh for all of the available CS data. The average energy used during any charge session is the same throughout the week. The outliers or higher energy usage for a single charging session do not happen normally on weekends. As mentioned previously, weekends mostly face long charging sessions which are validated by the Sunday energy distribution scenario.

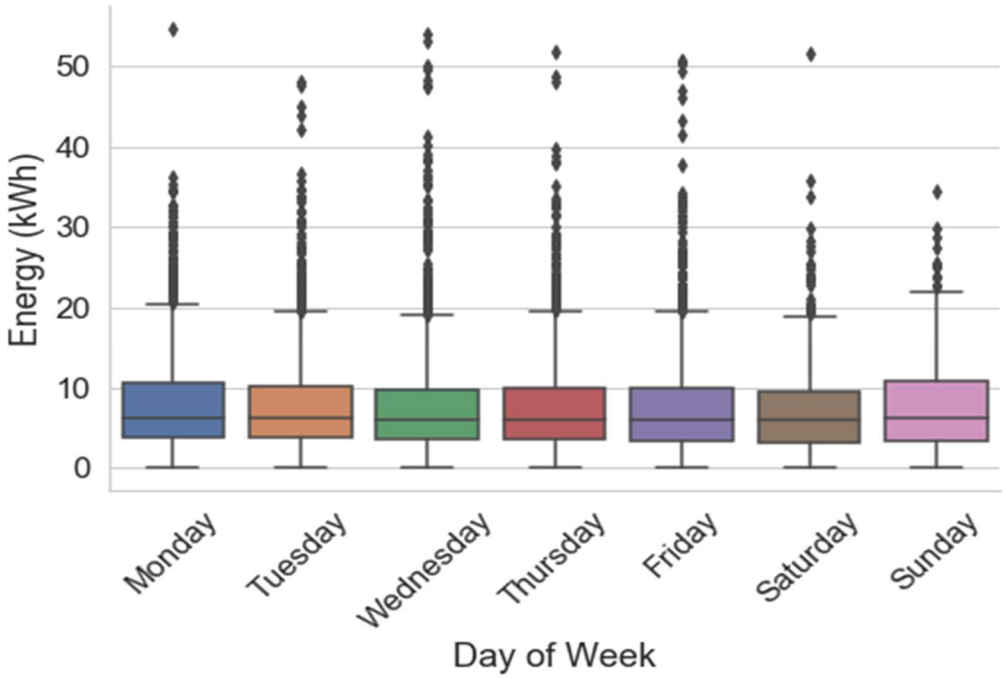

Figure 4.5 Distribution of Energy Usage

4.2.5 Utilization Factor

Charging session duration and the time needed to finish the charging are not necessarily equivalent. The utilization factor of any PEV charging station represents the proper scenario of the effectiveness of use. A higher utilization factor represents that the

charging stations are being used efficiently and having less idle time (PEV is connected but not charging). Two different Utilization Factors (UF) are analyzed.

$$\mathrm{UF_{Energy}} = \frac{Total\ Energy\ Usage\ by\ any\ Station\ (kWh)}{Maximum\ Possible\ Energy\ Usage\ (kWh)} \quad \textbf{4.1}$$

$$\mathrm{UF_{Time}} = \frac{Total\ Time\ Spent\ by\ any\ Station\ \ (h)}{Total\ Time\ Period\ (h)} \quad \textbf{4.2}$$

UF_{Energy} indicates the percentage of the maximum energy usage possible by any PEV charging station in the given timeframe. Given that all charging stations are level II, their average power level is 6.6 kW. Maximum possible energy usage can be found by using the connection duration and power level. This utilization factor shows the idling time of a charging station while a PEV is connected and helps to estimate the CS congestion. A higher utilization factor means that most of the PEVs get disconnected as soon as the charging session ends. This results in less congestion which provides higher satisfaction for the PEV owners.

UF_{Time} expresses the percentage of occupancy of any PEV charging station. The occupancy indicates that if any PEV is plugged in whether it is charging or not. This also shows the demography of PEV users in a locality. Lower UF_{Time} means that the charging stations are less used, hence the number of PEV users is also low in that given locality. Figure 4.6 shows both UF_{Energy} and UF_{Time} distribution by PEV CS. As the power level is fixed for all CS, so the distribution of UF_{Energy} is rather narrow. On the other hand, UF_{Time}

is wider as the usage of any CS also depends on other factors such as distance from the workplace and the number of CS at the same parking lot. The average values of UF_{Energy} and UF_{Time} are 58 and 33 percent, respectively.

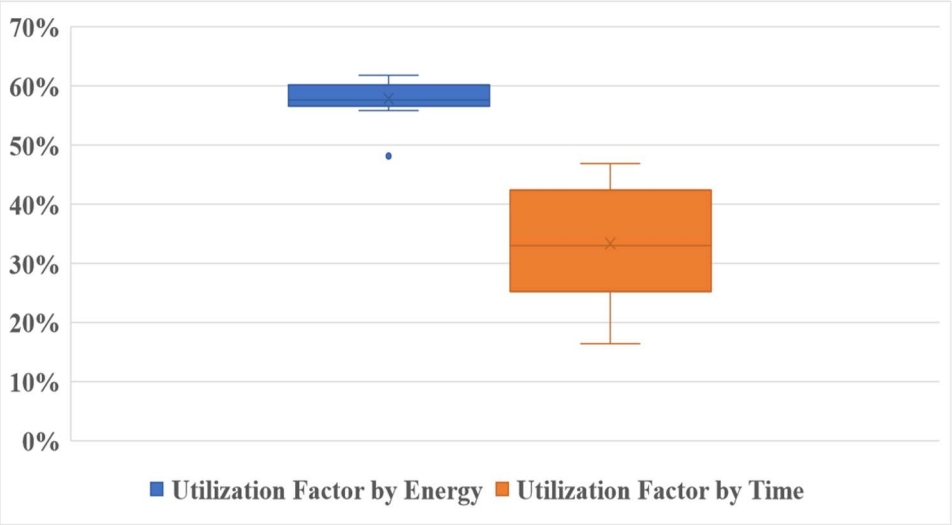

Figure 4.6 Utilization Factor Distribution for Different Charging Stations

4.3 Applications and Case Studies

4.3.1 PEV Load Modeling

The behavior of any PEV user is random and is highly dependent on the travel profile of the owner, PEV model, and charging station availability. Typically charging stations do not have access to any user's travel profile or SOC level of the PEV. Hence, it becomes more complicated to estimate the PEV demand of any charging station facility at any time. Monte Carlo simulation is a popular approach to estimate the load profile for multiple scenarios [117] [118]. This approach assumes the travelled distance and starting time of charging follows a normal probability density function given in Equation 4.3 where x is the random variable, μ is the mean and σ is the standard deviation.

$$f(x,\mu,\sigma) = \frac{1}{\sigma\sqrt{2\pi}} e^{-\frac{1}{2}\left(\frac{x-\mu}{\sigma}\right)^2} \quad \textbf{4.3}$$

In addition to the normal distribution, Poisson distribution is also used to model the independence of PEV arrival time at a charging station. As more PEV charging events happen in the morning for a workplace PEV station which violates this assumption. For a campus community, the travel profile varies widely and the starting of any charging session also does not follow any normal distribution. Instead, they follow a skewed distribution. Moreover, travel profiles are unknown here too. Hence, it will not reflect the actual scenario of PEV load estimation if typical probability density functions are used. To provide a probabilistic load estimation for the existing PEV CS infrastructure, the hourly distribution of charging sessions is used with a fixed charging power rate for the PEV ports. The maximum power level of 6.6 kW is used to model the aggregated PEV load estimation described in Equation 4.4 .

$$P_{EV\_Aggregated}(t) = \sum_{n=1}^{N} D_{EV,ch}\ (n,t) \times P_{max}\ \ for\ \forall t \in T \quad \textbf{4.4}$$

Where, $P_{EV\_Aggregated}(t)$ denotes the total expected PEV load demand (kW) at time t, N represents the total number of PEV charging ports and T is the total time period. $D_{EV,ch}\ (n,t)$ is introduced as the hourly probability distribution at time t for PEV charging port n and P_{max} is the maximum power level available for CS.

4.3.2 Current Hourly PEV Load Estimation

The distribution of weekdays' charging events highly differs from weekends or holidays. Hence, the aggregated PEV load estimation is different in both cases. Figure 4.7 shows the hourly load estimation for the available campus PEV Charging Stations on weekdays. A maximum peak of 26 kW PEV load demand can be generated at any point of time by charging activities. To validate the expected load estimation for UCR public charging stations, an open-source Adaptive Charging Network (ACN) simulator is used [55] [56] . An uncontrolled charging algorithm is deployed for the same level of charging rate to estimate the hourly load for a representative workday. The data was collected from 54 PEVCS of Caltech and the expected load is scaled down to compare with the 16 PEVCS of UCR. As, the charging stations at Caltech are mostly used by the faculties, staff, researchers of the campus; the peak happened in the early morning and the load is quite low for the rest of the day. Though the peaks closely match and happen at a similar time, the estimation for the later part of the day contrasts with UCR estimation due to the low occupancy of Caltech PEVCS during that period of the day. If level III or fast charging CS are added to the current infrastructure, the situation will be worse and will impact the existing utility distribution transformers.

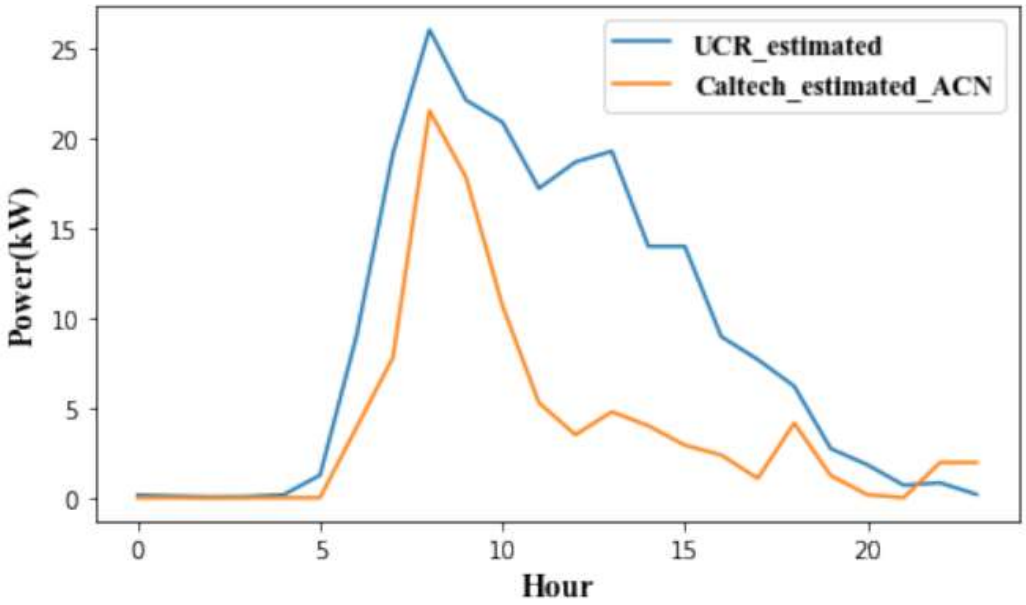

Figure 4.7 Expected Hourly PEV Load Estimation with Current CS Penetration & Validation with ACN Estimation of Caltech EVCS

4.3.3 Higher Penetration Scenarios

At present, there are approximately 4,500 parking spaces at UCR. The PEV loading scenarios for 5 percent of the parking spaces penetrated by PEV CS are shown in Figure 4.8. With the current probability distribution of charging events, the PEV load estimation is done for 5 percent and 10 percent PEV penetration scenario. All the CS are considered level II PEV CS. The aggregated load estimation is 183 and 366 kW for 5 and 10 percent penetration on any weekday whether the load estimation for weekends is 132 and 263 kW respectively. This peak can reach 3 MW if 50% of the added penetration is level III PEV CS. The average peak demand for the UCR campus is 20.7 and 12.2 MW in summer and winter, respectively. So, the estimated peak for 10 percent penetration will roughly share one-fourth of UCR peak demand on a winter day.

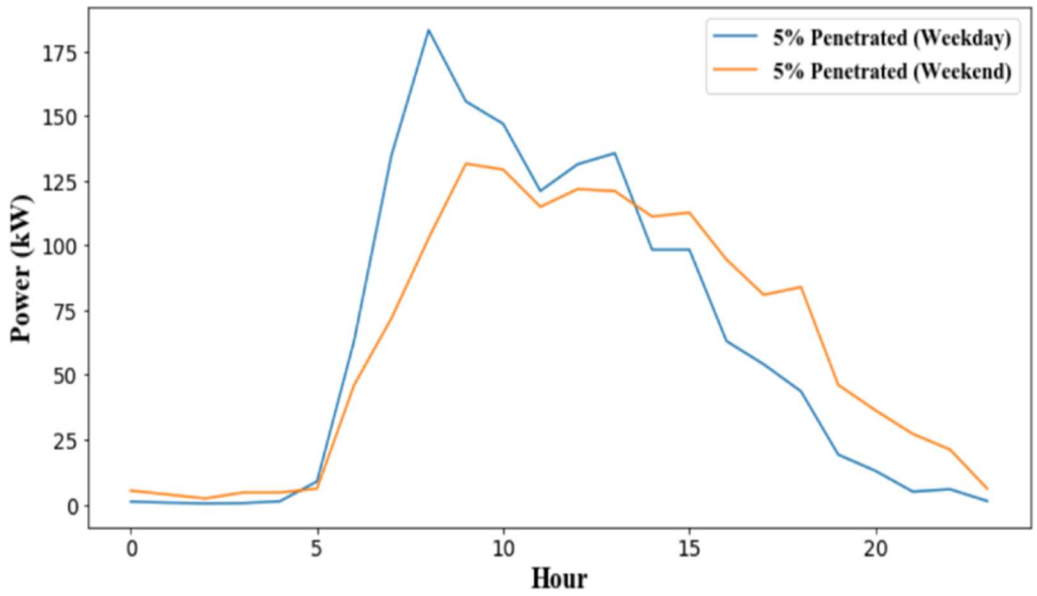

Figure 4.8 Expected Hourly EV Load Estimation on Workdays & Weekends: 5 Percent Penetration Scenarios

4.3.4 Impacts on Duck Curve

According to the Office of Energy Efficiency and Renewable Energy, the duck curve is the infamous curve that represents the shape of the electrical demand of California due to the massive difference between solar availability during mid-day and late afternoon. The abundance of solar power reduces net demand during daytime which gradually decreases with time. This results in a rapid ramp-up in net demand and takes the form of a duck and is called the duck curve. The public PEVCS are mostly occupied during the daytime and can best use the green energy available from solar. This will help flatten the dip of the duck curve. As the day goes by, the expected load for PEVCS decreases and hence will not worsen the duck curve scenario. Figure 4.9 represents the comparison between current PEV load estimation and California Independent System Operator (CAISO) net demand to show the impacts of PEV charging on net demand. But with the

higher penetration scenario, despite lower charging events by the end of the day; there will be higher ramp-ups which will need more investment in power generation infrastructure. A smart charging strategy can help to alleviate this problem to a large extent.

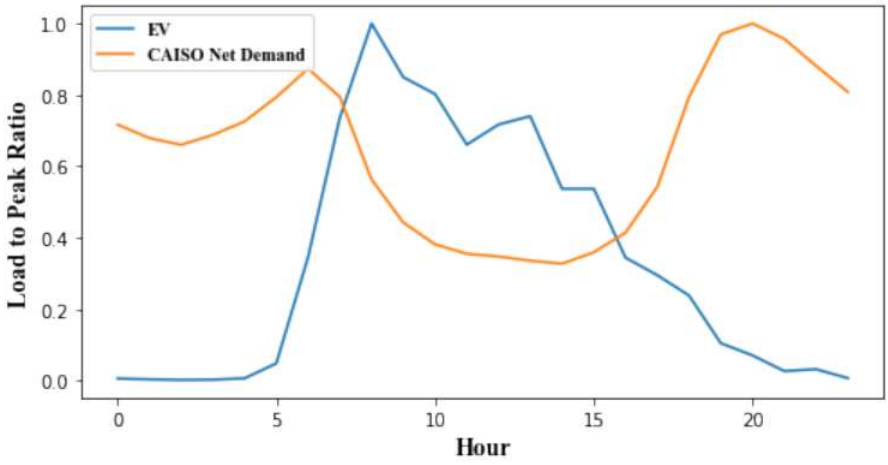

Figure 4.9 EV Load Impacts on Duck Curve

4.4 Cost Analysis

Policies regarding charging costs widely vary depending on the overall scenarios of CS locations, user behavior, and infrastructure overloading of the serving utility. The PEV owners are being charged on an hourly basis on the UCR campus. There are two sets of charges for UCR affiliates and non-UCR affiliates, respectively. The hourly based charging policy largely differs from the common charging policies based on energy (kWh) usage. The benefit of this hourly charging policy is that it reduces the congestion of PEV CS. As the PEV owners are being charged hourly with an increased rate after 2 hours, they do not leave the PEV plugged after charging is complete. This is reflected by the

connectivity distribution of all the charging sessions. 91 percent charging events are finished by 3 hours which means maximum revenue is $3.5 and $6.5 from UCR and non-UCR affiliates, respectively in most cases. The disadvantage is, plug-in hybrid EV (PHEV) owners are not very fond of this policy because of the lower charging level capacity of PHEV, typically 3 kW. Table 4-2 shows the monthly and yearly cost breakdown for both campus and PEV owners.

Table 4-2 Cost Analysis for EV Charging

	Monthly ($)	Yearly ($)
PEV Owners Charging Cost	3,020-6,894	36,241-82,738
Campus Utility Cost	1,476	17,712
Minimum Revenue	1,544	18,528

This user behavior can also be very helpful to design the optimal number of PEVCS and pricing structure elastic to geographical locations of PEVCS. Though Time of Use (TOU) pricing is popular to reduce the peak for the utilities, it might result in an unexpected peak during off-peak periods and add instability to the system. If the duration of TOU for off-peak rate is shorter, then it also might be inadequate to provide charging at a lower price for all the PEV users. TOU can be proposed for workplace PEVCS when solar or renewable energy resource is abundant. This can help to flatten the duck curve and reduce solar curtailment, the practice of intentionally reducing solar production if needed during high solar insolation time, in states such as California. Fixed charging rate schedules can

reduce the range anxiety by providing enough charging but the result may negatively impact the grid.

4.5 PEV Load Modeling

The stochasticity associated with EV arrival time, length of daily trip, and remaining capacity represented by State of Energy (SOE) has made the EV load modeling complicated. The following subsections explain the detailed EV modeling.

4.5.1 Home Arrival Time

To analyze the impacts of EV integration on a residential feeder, the home arrival times of all kinds of trips from the most recent survey of NHTS are utilized. Figure 4.10 shows the home arrival time distribution for all the trips made by vehicle owners. About 50 percent of the people get back home between 4 pm and 8 pm. Here hour 0 to 23 indicates 12 am to 11 pm of a day.

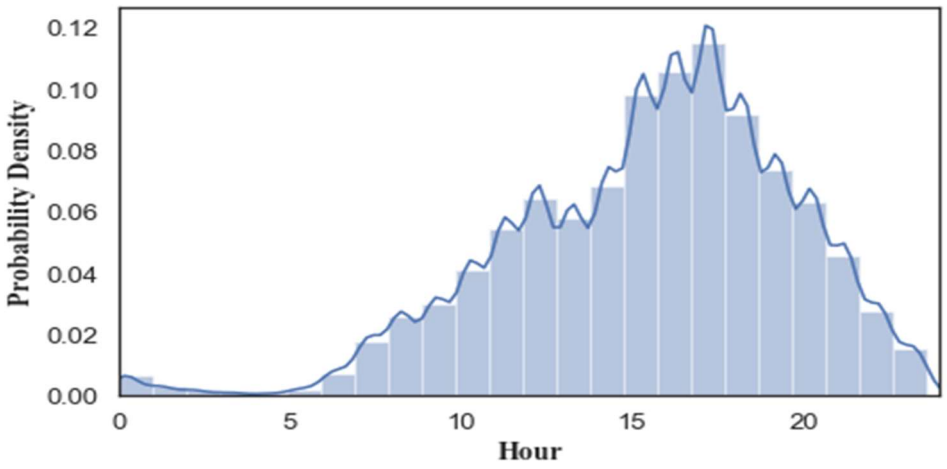

Figure 4.10 Probability Density Function of Home Arrival [119]

4.5.2 Vehicles Miles Travelled

The depletion of EV energy capacity is completely dependent on the miles traveled by the EV every day. Figure 4.11 shows the distribution of miles traveled by vehicles in the US. This distribution is used to find out the miles traveled by each EV. A very few travels continue for more than 30 miles. As traveling more than 30 miles is not a common scenario on a daily basis, these trips are excluded to model the daily travel profile for each EV. The travel profiles for the vehicles of each household are generated from the following vehicle miles traveled (VMT) distribution given in Figure 4.11.

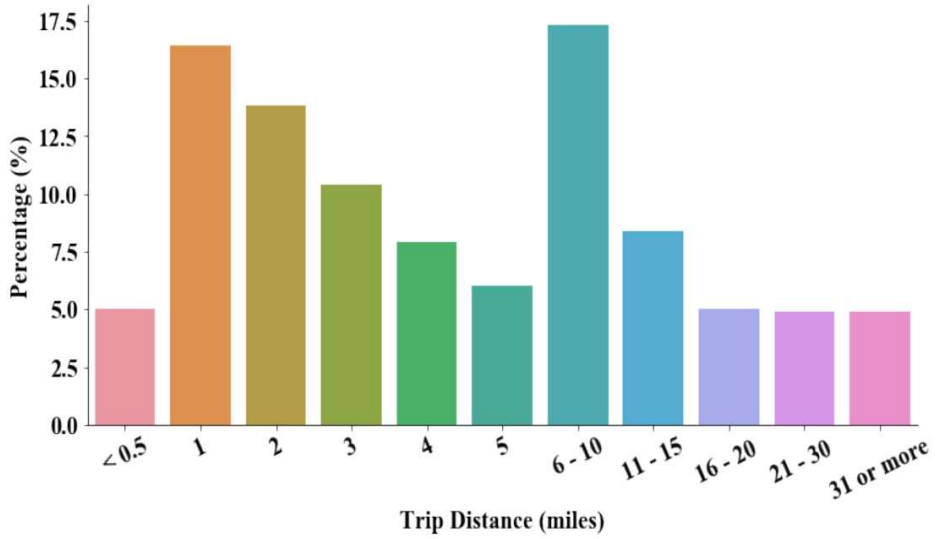

Figure 4.11 Miles traveled by vehicles [119].

4.5.3 Required Energy Calculation

The required amount of energy needed to fill in the decreased State of Charge (SOC) of EV can be calculated from its VMT so that the EV will stay fully charged for next-day trips. The required energy is calculated using the following equation.

$$Energy\ required\ for\ EV\ to\ be\ charged\ in\ full = \left(\frac{VMT}{Driving\ Range\ (miles)}\right) \times EV\ capacity\ (kWh) \quad \textbf{4.5}$$

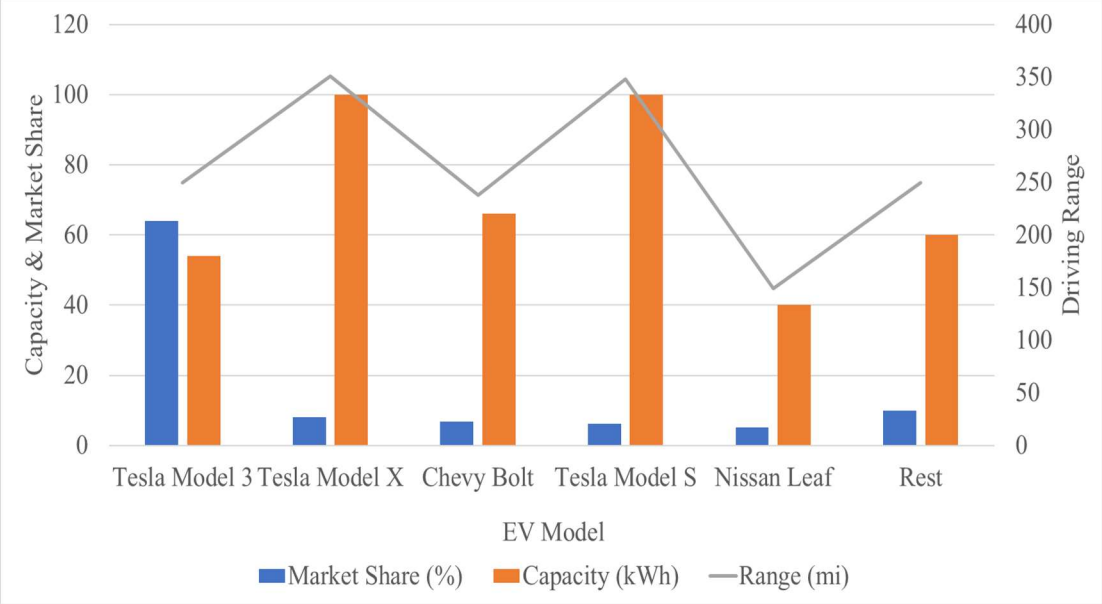

Figure 4.12 EV Sales Data for the Year 2019 in the USA [120].

Figure 4.12 shows the most recent EV sales data [120] with their driving ranges and battery capacities. Only 5 EV models shared 90 percent of the EV sales in 2019. The remaining 10 percent is represented in this study with the most common type EV of 60 kWh and 250 miles driving range. This distribution is used to generate the expected capacity and driving range for each EV of the household.

4.6 Distribution Grid Modeling

4.6.1 Count of Customers Connected to Each Node

The maximum number of EV loads relies on the number of each customer's vehicles. Hence, the number of customers connected to each node is a decisive factor to calculate the EV load. On average, 17.28-40.56 kWh energy is used every day by each residential home in the US depending on the state [121]. Based on this energy use, a 1.5 kW average load is considered for each customer to calculate the total number of customers from the total spot load of each node. The number of customers connected to each node is figured out using the following equation.

$$\text{Total No of Customers} = \frac{\text{Total Load (kW)}}{\text{Average Residential Load (kW)}} \quad \textbf{4.6}$$

4.6.2 Vehicles Count

To analyze the impacts of different levels of penetrations, the number of vehicles for each household is needed. Figure 4.13 shows the number of vehicles per household in the US, with the average being 2. This probability distribution is used to generate the number of vehicles connected to each node of the feeder.

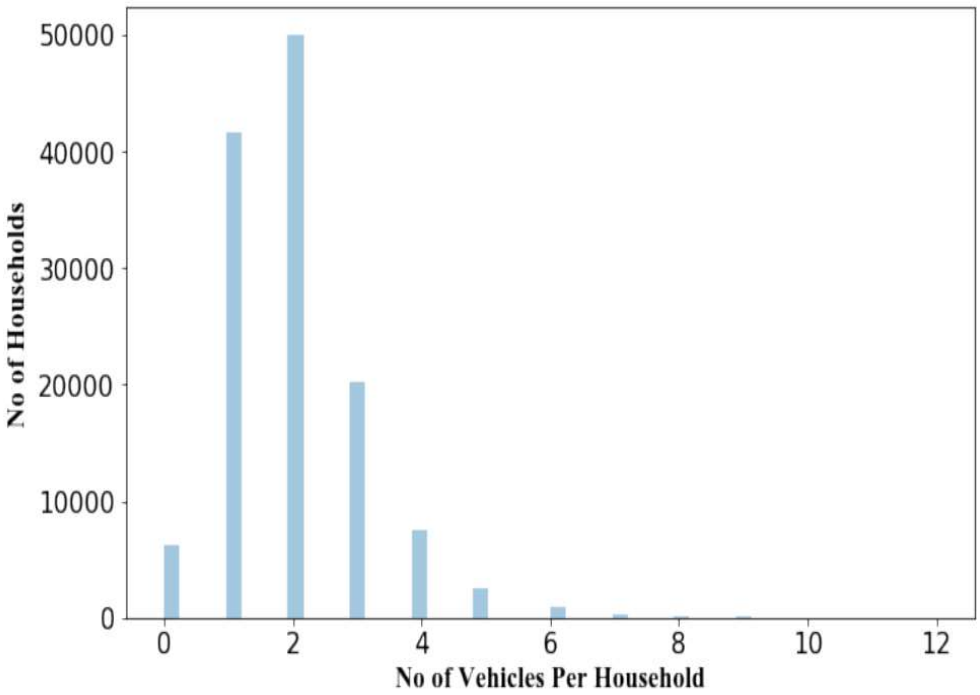

Figure 4.13 EV Distribution Per Household. [119]

4.7 Conclusions

The wide availability of public charging stations is necessary for higher penetration of PEV. Charging behavior and energy consumption analysis can provide insights to the policy makers and assist them in implementing future beneficial charging infrastructures. This chapter analyzes a wide range of public PEV customers' behavior and generates a general load profile for public parking lots to assess future impacts on the distribution grid. This study has analyzed the busiest sessions throughout one year of the chargers utilization in a university parking lot. Short term charging sessions are the most prevalent in any paid public CS where connection duration charge is present, and this helps reduce congestion. To capture the real usage scenarios, two different utilization factors are introduced for energy and duration in Section 4.2. Both CS congestion and overall occupancy are

relatively low in this university campus. As, PEV deployment is a multi-strategic game of utilities, customers, CS owners; such analysis will help in finding the most optimum solution for all the stakeholders.

In Sections 4.5 and 4.6 , a customer oriented stochastic EV modeling is presented to quantify the EV penetration impacts on voltages at the local nodes and feeder vehicle capacity. Customer-oriented EV estimation is important for the utility to decide on necessary system upgrades. The number of EVCS required at a certain locality is coherent with the EV to Customer Ratio (EVCR) for the nodes of the feeder of that locality. To analyze the requirements for the distribution system upgrading, a comprehensive and realistic detailed distributed EV load modeling in a given feeder is needed.

5 PEV Utilization and Impacts on the Grid

5.1 Background and Motivation

The fact that PEVs can provide clean transportation without emitting any pollution like fossil fuel burning vehicles is well known. However, they can potentially help both the utility and customers behind the meter by acting as a battery energy storage and providing energy back to them when needed. The benefits of this emerging concept depend on issues such as optimal charging/discharging strategy and battery degradation cost of PEV. But repeated charging and discharging activity can have adverse impacts on battery life. For the success of PEVs' energy storage capability utilization, it is crucial to find a better balance between battery degradation cost and ensuring services to the grid. The beneficial opportunity of providing EV energy back to the grid at CPP periods has not been widely explored yet. Research based on models combining CPP and EV charging is an emerging field while including bidirectional EV field implementation is relatively new.

The recent additions of Distributed Energy Resources (DERs) on the customer side have resulted in more bidirectional power flow in the distribution system. The mass adoption of EV will impact the grid and will require appropriate modeling to assess their impacts. Typically, the distribution system used to be considered as a static load for the transmission system and the impact of dynamic characteristics of DERs or EVs is not properly included in the evaluations. Co-simulation can be utilized to analyze these combined characteristics by studying different subsystems which are coupled to each other. The designated simulating environments for different subsystems are not capable enough to address the dynamics of the subsystems simultaneously. The co-simulation platform can

couple the subsystems and address the interdependencies in a coupled simulation environment. This will eventually help to identify the true impacts of EV on the grid.

5.2 PEV Utilization for Demand Response

5.2.1 Data Collection and Analysis

As mentioned in Chapter 3, UCR's CE-CERT is located off-campus in a commercial/industrial area of the city. The electric vehicles used in this testbed are light-duty model 2013 vehicles with a battery capacity of 24 kWh each. The commercially available bidirectional charger has a capacity of 30 kW charging/discharging rate for any electric vehicle plugged in it. There are 10 CPP events in the 2019 summer in Southern California Edison (SCE) territory. 22nd August was a typical hot day when the CPP event was called a day before that day. The building data was collected at 15-minute intervals through an in-house developed data acquisition system developed by using commercially available non-proprietary hardware and software based solution for building automation. It is deployed to control the load usage of the building and monitor the regular load behavior. Figure 5.1 shows the load profile of the building for a typical weekday and a CPP day. The CPP day peak is 16.7 percent higher than a regular day peak. Moreover, the CPP periods (usually 4-9 pm) electricity consumption are also higher than regular usage.

Current Nissan leaf (2020) specifications and Tesla 3 model specifications have been used for simulation purposes. The PEV can be charged up to 19.2 kW for level II EV and 50 kW for level III PEV. For this study, 15kW has been used for level II EV and 30 kW is used for level III EV due to the capacity limitation of the available V2G charger.

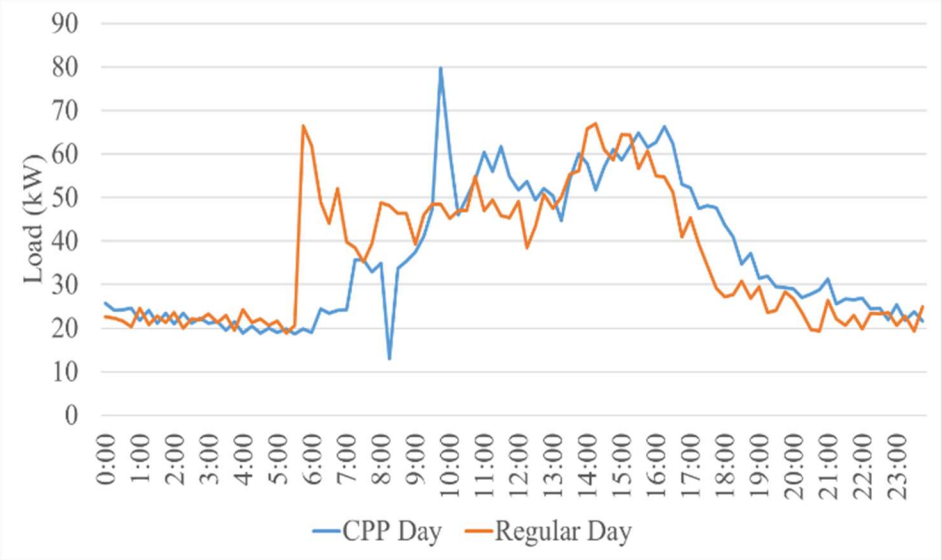

Figure 5.1 Building Load Variation in Regular and CPP Days

5.2.2 Framework for Optimization and Modeling

5.2.2.1 Optimization Framework

A novel framework is developed to ensure the optimal cost savings for the consumers behind the meter as well as for the benefit of the utility in any CPP event. Usually, the customers are notified about a CPP event through email or text messaging a day before the actual event. After the event is called, the optimization process will take place using the historical or average building load for similar days. This will result in optimal scheduling for both grid to vehicle (G2V) and vehicle to grid (V2G) operations for both of the vehicles. Next day vehicle trips can be planned accordingly after knowing the schedule for charging/discharging. Making the PEVs available during the high energy cost rate period to perform power delivery through V2G operation can help in reducing the overall energy and battery degradation cost. The detailed framework is shown in Figure 5.2.

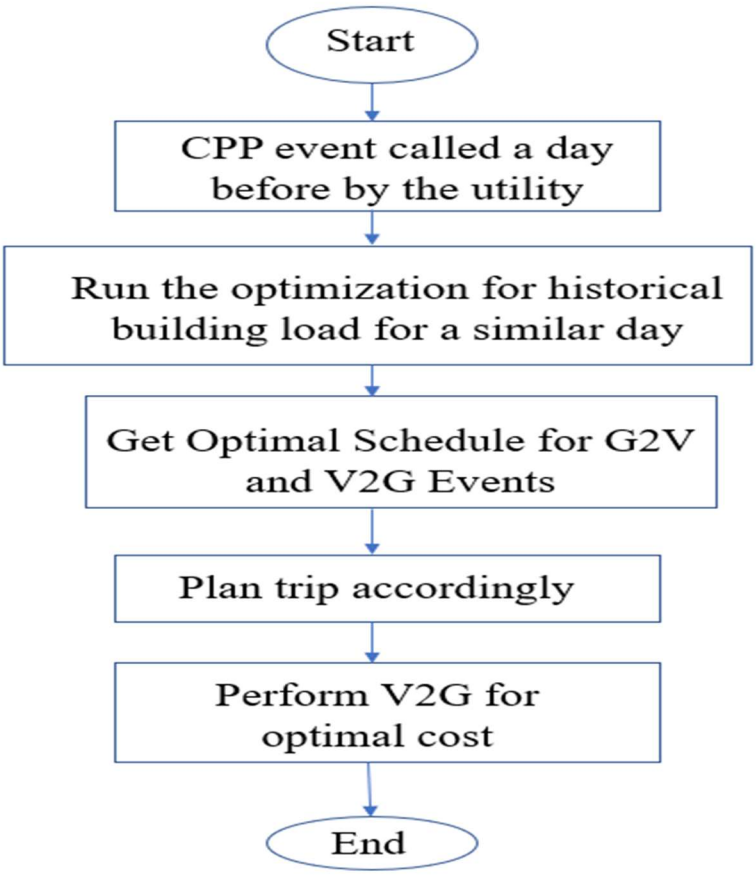

Figure 5.2 Framework for PEV in CPP Events

5.2.2.2 Notations

i =Time slot index

T=Total time period

Δt = Time interval

SOC_{EV}= State of Charge of Electric Vehicle (EV)

$\eta_{ch,EV}$= EV charging efficiency

$\eta_{disch,EV}$= EV discharging efficiency

P_{G2V2}=Power transferred from grid to level II EV

P_{V2G2}= Power transferred from level II EV to grid

P_{G2V3}=Power transferred from grid to level III EV

P_{V2G3}= Power transferred from level III EV to grid

c_1= Charging decision binary variable for level II EV

d_1= Discharging decision binary variable for level II EV

c_2= Charging decision binary variable for level III EV

d_2= Discharging decision binary variable for level III EV

$P_{G2V\ max2}$= Maximum charging power for level II EV

$P_{V2G\ max2}$= Maximum discharging power for level II EV

$P_{G2V\ max3}$= Maximum charging power for level III EV

$P_{V2G\ max3}$= Maximum discharging power for level III EV

P_{grid}= Power from grid to building

$P_{building}$ = Power used in building

E_c = Energy Cost

B_{DC} = Battery degradation Cost

SOC_{min} = Minimum State of Charge for EV

SOC_{max} = Maximum State of Charge for EV

5.2.2.3 PEV Modeling

The PEV needs to be modeled first to optimize the cost for the consumers behind the meter. The decision for discharging the electric vehicle depends on the consumers' behavior and acceptance of the beneficial concept of bidirectional energy flow in EVs. That's why it is also important to make sure that battery degradation costs for PEV activities are considered. Equations 5.1-5.11 are used to model the activities. The first equation states the state of charge of PEV at any time instant i. The second and third equations limit the maximum charging and discharging power, respectively, for level II PEV activities. The fourth constraint prevents the charging and discharging of the level II PEV to occur simultaneously. Equation 5.5 describes the state of charge similarly to equation 5.1. Equations 5.6-5.8 are similar to equations 5.2-5.4 but represent level III PEV. Equation 5.9 is for one of the two cases and ensures that two PEVs cannot be discharged at the same time due to equipment limitation. Equation 5.10 denotes that all the charging and discharging decisions are binary variables. Equation 5.11 makes sure that the state of charge is always within the acceptable range for both EVs. The specifications used for the simulations are described in Table 5-1.

For $\forall i \in T$

$$SOC_{EV}(i) = SOC_{EV}(i-1) + \left(\eta_{ch,EV} \times P_{G2V2}(i) - \frac{P_{V2G2}(i)}{\eta}_{disch,EV}\right) / \quad \textbf{5.1}$$

$$\text{Capacity} \times \Delta t$$

$$0 \leq \mathrm{P_{G2V2}(i)} \leq c_1(i) \times \mathrm{P_{G2V\,max2}} \quad \textbf{5.2}$$

$$0 \leq \mathrm{P_{V2G2}(i)} \leq d_1(i) \times \mathrm{P_{V2G\,max2}} \quad \textbf{5.3}$$

$$c_1(i) + d_1(i) = 1 \quad \textbf{5.4}$$

$$\mathrm{SOC_{EV}(i)=SOC_{EV}(i\text{-}1)+\left(\eta_{ch,EV} \times P_{G2V3}(i) - P_{V2G3}(i)/\eta_{disch,EV}\right)/ Capacity \times \Delta t} \quad \textbf{5.5}$$

$$0 \leq \mathrm{P_{G2V3}(i)} \leq c_2(i) \times \mathrm{P_{G2V\,max3}} \quad \textbf{5.6}$$

$$0 \leq \mathrm{P_{V2G3}(i)} \leq d_2(i) \times \mathrm{P_{V2G\,max3}} \quad \textbf{5.7}$$

$$c_2(i) + d_2(i) = 1 \quad \textbf{5.8}$$

$$d_1(i) + d_2(i) = 1 \quad \textbf{5.9}$$

$$c_1(i), c_2(i), d_1(i), d_2(i) \in \{0,1\} \quad \textbf{5.10}$$

$$SOCmin \leq SOC(i) \leq SOCmax \quad \textbf{5.11}$$

Table 5-1 PEV Specifications

Name	Type	Charge/ Discharge Rating (kW)	Stored Energy (kWh)		
			Initial (60% of Total)	Minimum (40% of Total)	Maximum (100% of Total)
Nissan Leaf	Level II	15	24	16	40
Tesla 3	Level III	30	60	40	100

5.2.2.4 Energy Price Modeling

Energy rate is the most decisive factor in minimizing the total energy used by any consumer. There are several energy rates for residential and commercial loads served by Southern California Edison (SCE) and the rates of interest are mostly Time of Use (TOU) rates. Critical Peak Pricing (CPP) is one of these rates which is shown graphically in Figure 5.3. It follows a flat rate of 0.08 ($/kWh) at non-CPP periods and much higher 0.4 ($/kWh) at CPP periods. Though the peak can be higher at non-CPP time periods, solar is abundant at that time. Hence, the CPP hour is considered from 4-9 pm when solar production starts becoming unavailable.

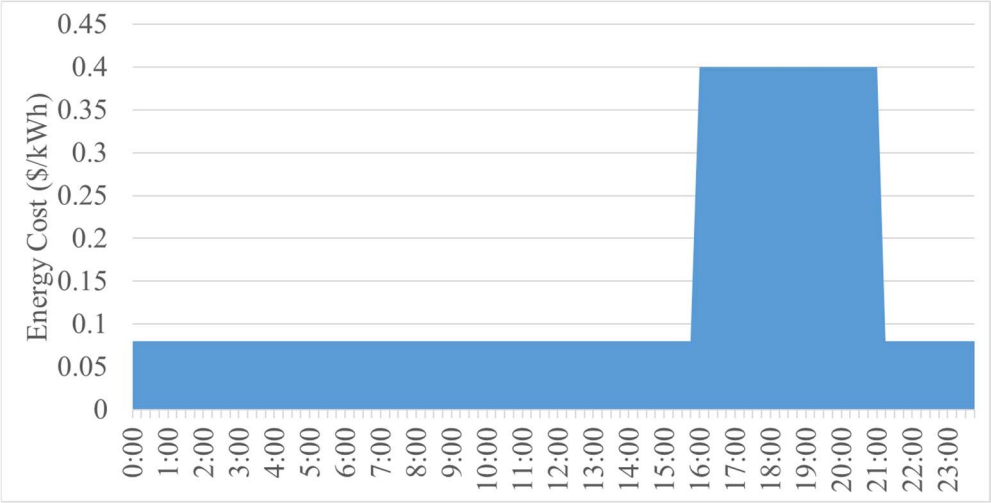

Figure 5.3 Energy Cost for CPP Event Days of SCE

5.2.2.5 Power Balance Modeling

The summation of imported grid power, charging power for level II EV and level III EV must be equal to the discharging power of both EV and total power needed for the rest of the building load. Equation 5.12 defines the power balance equation.

$$P_{grid}(\mathrm{i}) + \mathrm{P_{V2G2}}(\mathrm{i}) + \mathrm{P_{V2G3}}(\mathrm{i}) = P_{building}(\mathrm{i}) + \mathrm{P_{G2V2}}(\mathrm{i}) + \mathrm{P_{G2V3}}(\mathrm{i}) \qquad \textbf{5.12}$$

5.2.3 Problem Formulation and Constraints

5.2.3.1 Objective Function

The objective of the CPP problem is to reduce the total cost associated with PEV activities. The total cost includes both the energy cost and degradation cost due to PEV activities. The objective function is presented below.

$$\text{minimize } \sum_{i=1}^{T}\Big\{\big(P_{grid}(i)\times\Delta t\times E_c(i)\big)+\Big(\eta_{\text{ch,B}}\times \mathrm{P_{G2V2}(i)}+ \tag{5.13}$$

$$\mathrm{P_{V2G2}(i)}/_{\eta_{\text{disch,B}}}\Big)\times B_{DC}\times\Delta t+(\eta_{\text{ch,B}}\times \mathrm{P_{G2V3}(i)}+\mathrm{P_{V2G3}(i)}/_{\eta_{\text{disch,B}}})\times$$

$$B_{DC}\times\Delta t\Big\}$$

5.2.3.2 Constraints

Equation 5.1-5.12 states the constraints for the CPP problem formulated for optimization.

5.2.3.3 Optimization

The CPP cost optimization problem itself is a Mixed Integer Linear Programming (MILP) problem. It has been solved with Gurobi in python [88]. The workstation to solve the optimization problem is core i-7 with 16 GB RAM

5.2.4 Simulation Results

5.2.4.1 Case I: One EV in Bidirectional Operation

There is one bidirectional charger available right now in this testbed. With one PEV discharging at a given time, the resulting overall power transfer scenario and SOC of the battery are shown in Figure 5.4. It is more cost-effective to discharge the level III PEV at the CPP periods. In this scenario level II PEVs do not take part in any charging/discharging activities as the associated degradation cost is high which is 0.1317 $/kWh [94] [122]. Another thing that should be noted here is the minimum SOC of level III EV has been set to 40 percent of the total SOC so that the PEV is protected from being fully discharged at the time of the CPP period. Even though the building load is lower at CPP period, the overall grid experiences higher peak due to higher energy usage by the consumers at those

periods. As the building in this case study closely follows a commercial load pattern, the building load starts decreasing in the afternoon which is opposite in case of residential loads.

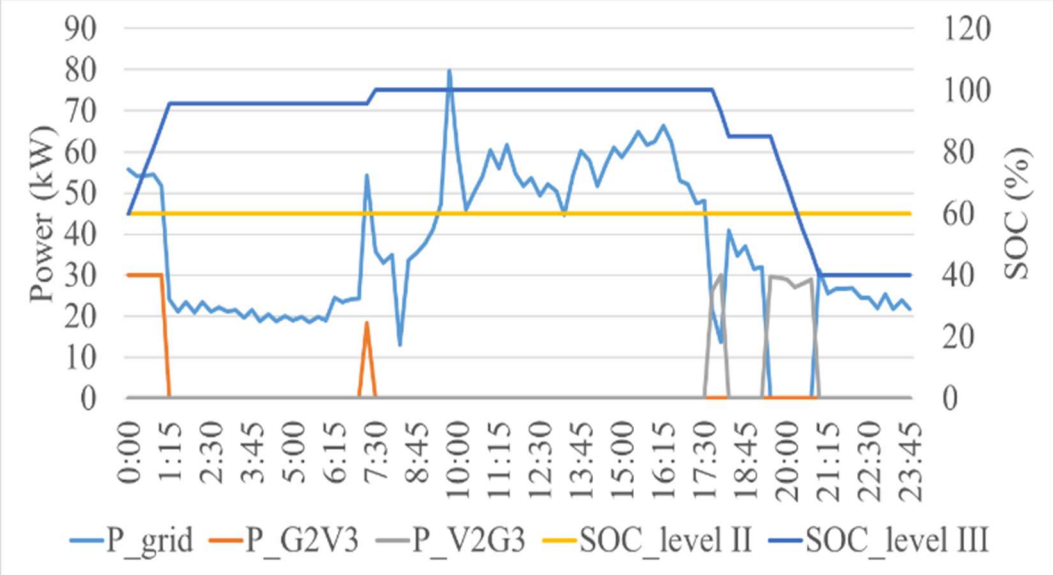

Figure 5.4 Case I: Charging Profile for PEV (SCE CPP Scenario) – One Bidirectional EV

5.2.4.2 Case II: Both EVs in Bidirectional Operation

When both the level II and level III EVs can act in bidirectional operations, then, as expected, they provide more discharging activities during CPP periods. Figure 5.5 shows the impacts of bidirectional charging while both PEVs can take part in V2G mode at the same time. In contrast with the first case, Nissan leaf is also involved with charging at off-peak periods and provides energy back to the grid at CPP event periods.

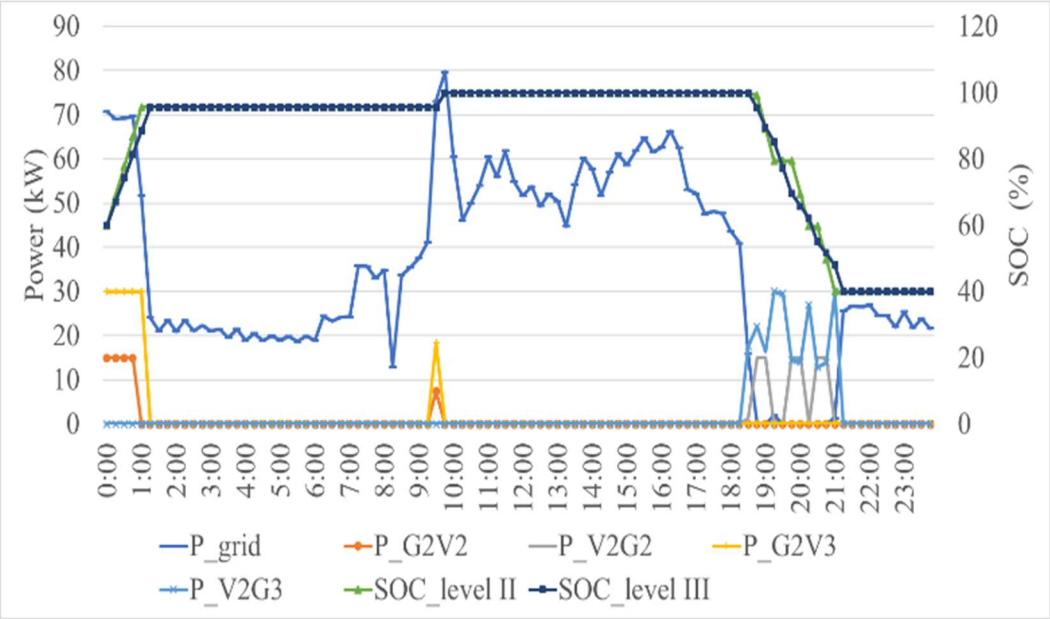

Figure 5.5 Case II: Charging Profile for PEV (SCE CPP Scenario) – Multiple Bidirectional EVs

5.2.4.3 Impacts of CPP Pricing on Purchased Grid Power

To be effective CPP prices are designed to be always higher than regular time electricity prices. Depending on the utility and it's serving territory, the CPP-off peak price ratio can vary from 3.7 to 9 [66]. Figure 5.6 shows the impacts of the CPP-off peak ratio on purchasing power from the grid. For this scenario where the location considered is within SCE territory, the CPP-Off Peak price ratio is 5. The higher the price ratio, the more discharging events take place during any CPP periods. Though with higher CPP rates peaks also happen during off-peak periods to charge the available PEVs to make sure they can discharge to their fullest during the CPP period. As degradation cost is way lower in comparison to energy price at a CPP event, this peak can also be taken care of with the adjustment of constraints on a maximum peak. Case II also provides more V2G actions during CPP.

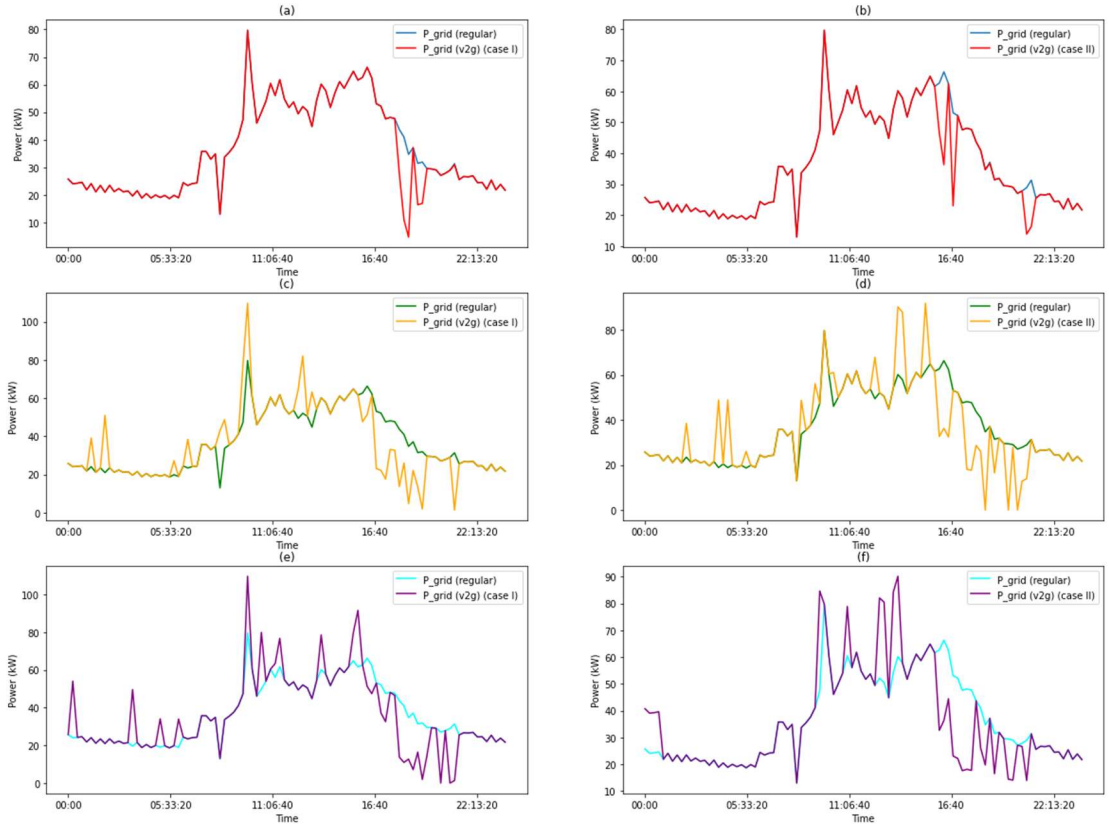

Figure 5.6 Purchased Grid Power Scenarios for Various CPP-Off Peak Price Ratios (a-b) Ratio is 3.7, (c-d) Ratio is 5, (e-f) Ratio is 9

5.2.5 Cost Analysis

5.2.5.1 Behind the Meter Cost Savings

Table 5-2 shows the cost savings for the prosumers behind the meter. As the cost reduction involves both energy reduction and battery degradation cost, the energy savings are the same for both cases for any CPP-off peak price ratio. A maximum amount of $48.68 can be saved for any single CPP event which results in $584 savings for a year of 12 CPP events. Lower CPP-Off peak ratio results in lesser V2G operation along with lower cost savings. This can benefit approximately 112,000 metered electric customers around this building in the city of Riverside [123].

Table 5-2 Customers' Savings from V2G Operation During CPP

CPP-Off Peak Price Ratio	Energy Cost ($)	Transferred Energy from Vehicle to Grid (kWh)	Cost Savings ($)	Total Savings ($)
3.7	112.93	26.6	4.95	59.4
5	130.79	79.8	23.14	277.7
9	174.30	79.8	48.68	584.1

5.2.5.2 Savings for the Utility

To provide power during critical events, utilities are now highly dependent on peaker power plants. The cost of peaker power plants during 4-9 pm operation in California with high solar generation is way more than the electricity generation of regular power plants at that time. The generation price varies from an additional $10-20/MWh more than any regular power plant operation [124]. The maximum savings possible for a utility from any single event are noted in Table 5-3. $798 can be saved for a fleet of 500 EVs with the same capacity and power ratings from any CPP event. California has a goal of 250,000 electric vehicle charging stations by 2025 [125]. If one-fourth of the EV stations participate in V2G, it can save $16,625-$33,250 in generation cost and 1,662.5 MWh per CPP event, and $49,875-$99,750 in generation cost and 4,987.5 MWh per CPP event with the lowest CPP-off Peak ratio and highest CPP-off Peak ratio, respectively.

Table 5-3 Utility Savings from V2G Introduction During CPP

CPP-Off Peak Price Ratio	Lower Bound on Savings ($)	Upper Bound on Savings ($)	For EV Fleet ($) (500 EVs)
3.7	0.266	0.532	266
5	0.798	1.596	798
9	0.798	1.596	798

5.3 Impacts on Distribution Level Microgrid

5.3.1 Testbed for PEV Charging

The testbed at UCR CE-CERT as mentioned in Chapter 3 was designed to incorporate actual EV chargers and evaluate the impacts of EV charging in a micro grid scale. The overall one-line electrical diagram of these chargers along with the rest of the electrical load in the Administration Building (1084) is shown in Figure 5.7.

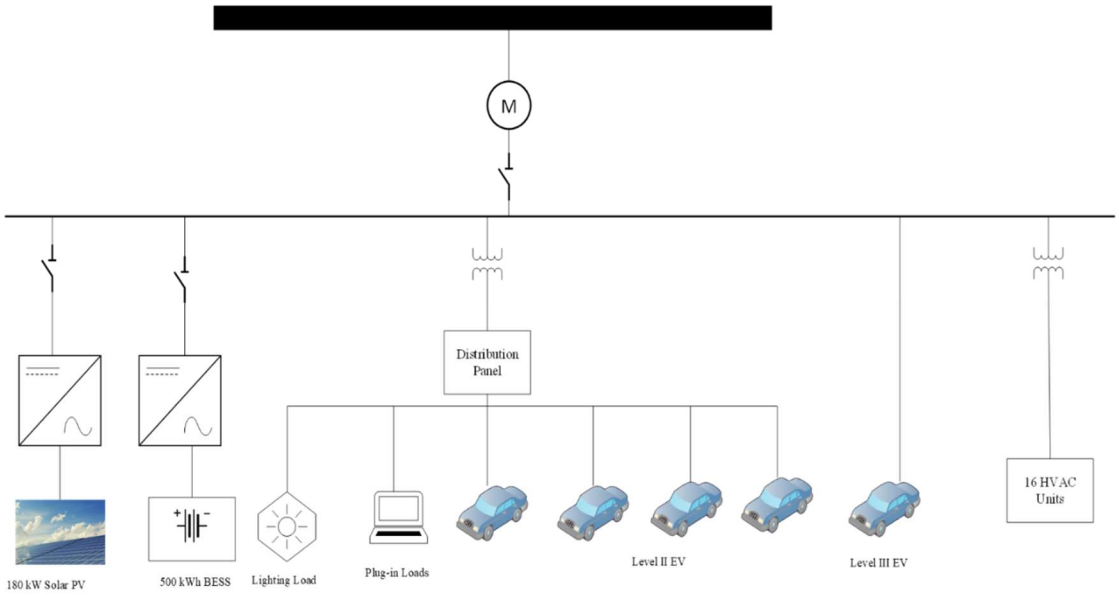

Figure 5.7 Electrical Layout: The System with EV Chargers

5.3.2 EV Characteristics

Since the charging characteristics vary depending on the vehicle type, understanding the charging patterns of each individual vehicle is essential. Based on these patterns we can eventually be able to identify, solely from the charging characteristics plots, which vehicles are charging by themselves or with other vehicles at the same time. To understand which vehicles were connected to which chargers at any given time, the vehicle make, model, license number, and charging station were logged in a spreadsheet every morning, afternoon, and late afternoon. In order to capture these charging characteristics, Fluke 435 Series II power analyzers were installed along the 3-phase 220 VAC and 480 VAC lines.

5.3.2.1 Level II Chargers

The main measurement variable that we were interested in was active power. The characteristic of each vehicle was recorded by reviewing the total kW use by the chargers while only one vehicle was plugged in. The charging characteristics of Nissan Leaf was observed and recorded. It was verified that Nissan Leaf charges at a maximum rate of 6 kW.

5.3.2.2 Level III Charger

This testbed has only one level III EV charging plugpoint. The experiments were performed on different days of November and December 2018. As there is only one charger, so individual EV characteristics have been recorded separately. Nissan Leaf and Chevy Volt have been plugged on different days. Nissan Leaf's charging level was at a constant 50 kW rate throughout the full charging period. Chevy Volt's charging protocol was different rates in different time intervals with a maximum charging rate of 50 kW for the initial half an hour. Figure 5.8 and Figure 5.9 show the charging characteristics for Nissan Leaf and Chevy Volt respectively.

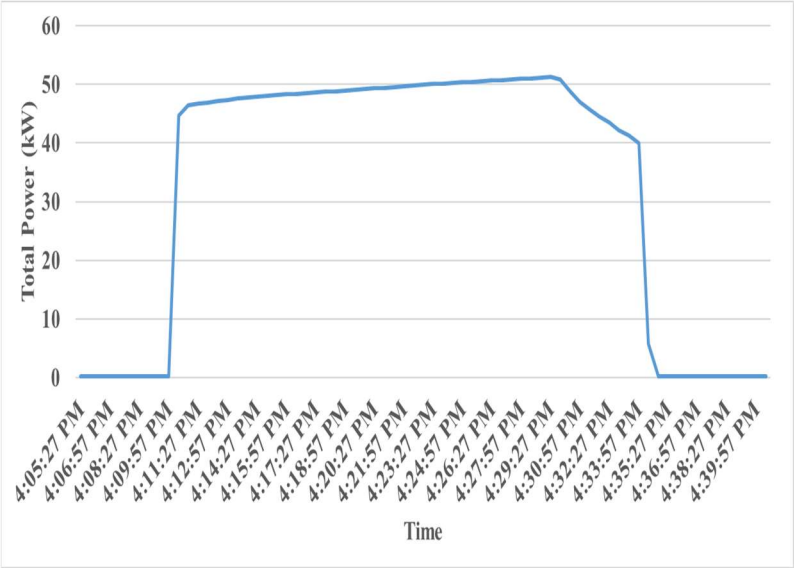

Figure 5.8 Level III EV Charger Characteristics for Nissan Leaf on 26th November, 2018

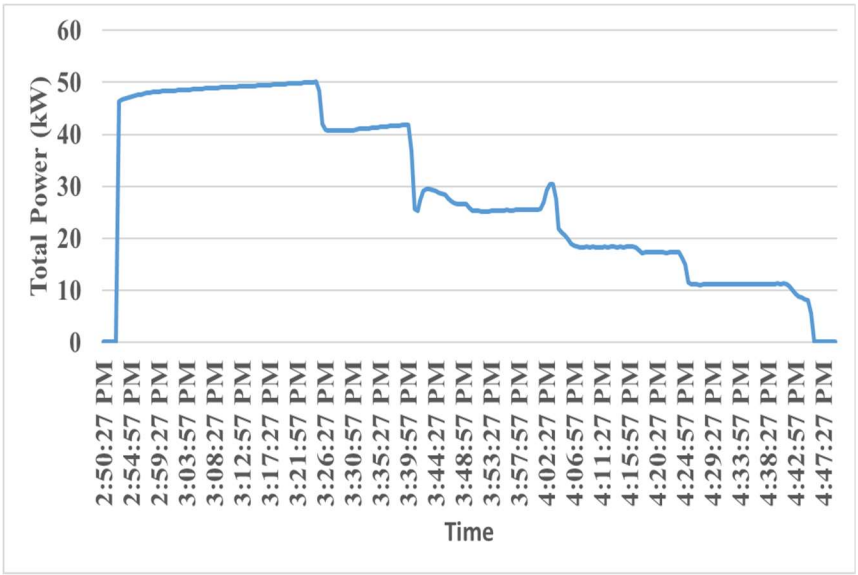

Figure 5.9 Level III EV Charger Characteristics for Chevy Volt on 30th November, 2018

5.3.3 Charging Impacts

5.3.3.1 Impacts on Administration Building

EV charging is closely associated with the overall energy management when EV shares the same meter with the building. The cost optimization strategy varies charging characteristics based on the size of the building load. In cases where only one EV level II charger is in operation, the impact on kW demand is insignificant as the charger demand value is comparable to some of the AC units in the building. But when two EVs are being charged, the peak demand of the building goes up due to the cumulative value of two chargers. In cases where the EV uses DC fast charging or level III charger, then it gets charged at a much higher rate of 50 kW which creates a huge impact on this building's total load. Figure 5.10 shows the impact of DC fast charging on this building's load profile. The peak building load increases to a great extent and results in a higher electricity bill for Time of Use (TOU) demand charges. Charging characteristics of Chevy Volt, Nissan Leaf, Ford Fusion, and Mitsubishi Miev show that charging rates vary from 3.2 kW to 6 kW per vehicle. If all four vehicles charge at the same time during any 15-minute period, the total demand over a given month will be 19.2 kW. Due to implementation of optimal HVAC peak shaving controllers, peak demand for this building was 34.4 kW at the time of experiment. If all four level II chargers are used simultaneously, the additional peak demand of 19.2 kW is equivalent to an increase of 56% in the building peak demand and the associated increase in the monthly electric bill.

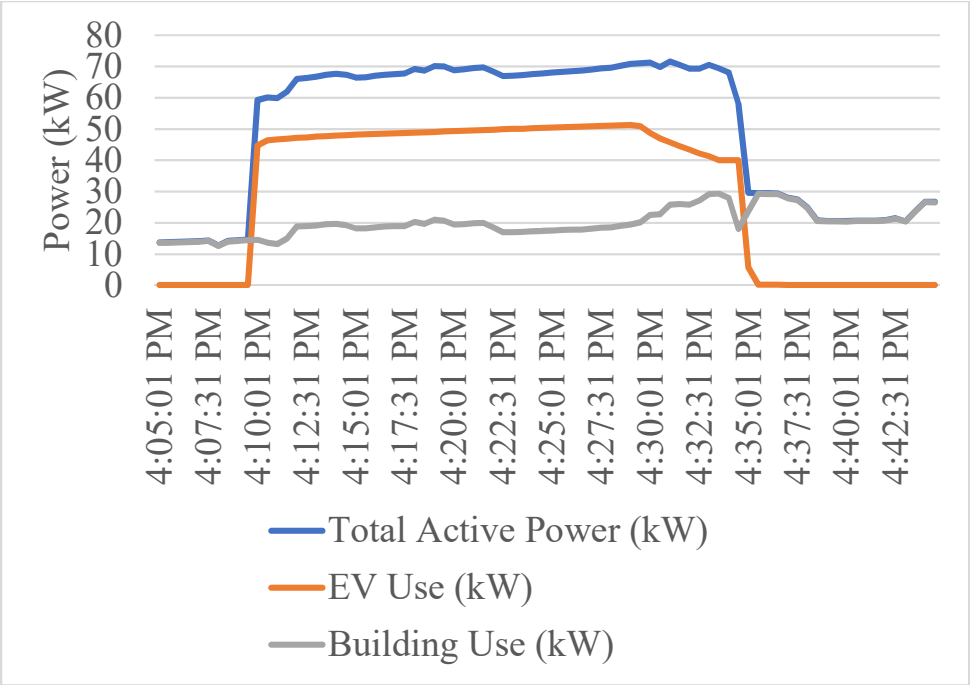

Figure 5.10 Level III EV Charging Impacts on Building Net Load on 26th November,2018

5.3.3.2 Impacts on CE-CERT Feeder

CE-CERT is situated at Columbia Avenue. Along Colombia Avenue from the I-215 Freeway to Michigan Avenue, approximately 1.7 mile long industrial/commercial sector of Riverside, California, there is a total of 2,288 parking spaces. If 10% of these parking spaces are turned into EV charging spaces, it will result in approximately 230 EV charging stations. In a 12-month period, all chargers will be simultaneously used for at least a duration of 10-15 minutes. The measurement results presented above shows an average kilowatt usage per car to be approximately 3.875 kW for level II EV chargers and 50 kW for level III EV chargers. By converting regular parking spaces into EV charging spaces, there will be significant additional maximum demands created on the distribution feeder.

Scenario 1

If 80% of these are level II chargers and 20% are level III chargers, and the vehicles have same charging characteristics as CE-CERT charging stations, then the additional maximum demand created by the charging stations will be approximately 3,000 kW. 12.47 kV feeder may have a 4,000 kW capacity, so only 10% EV penetration adds an additional 75% load to that feeder.

Scenario 2

If 20% of the available parking spaces are converted into EV charging stations, then the additional maximum demand created by the charging stations will approximately be 6 MW. A 20% EV penetration will add an additional 150% load to that feeder resulting in severe overloading.

Scenario 3

If 50% of the available parking spaces are converted into EV charging stations, then the additional maximum demand created by the charging stations will approximately be 15MW resulting in an additional 376% load to that feeder requiring distribution feeder upgrade.

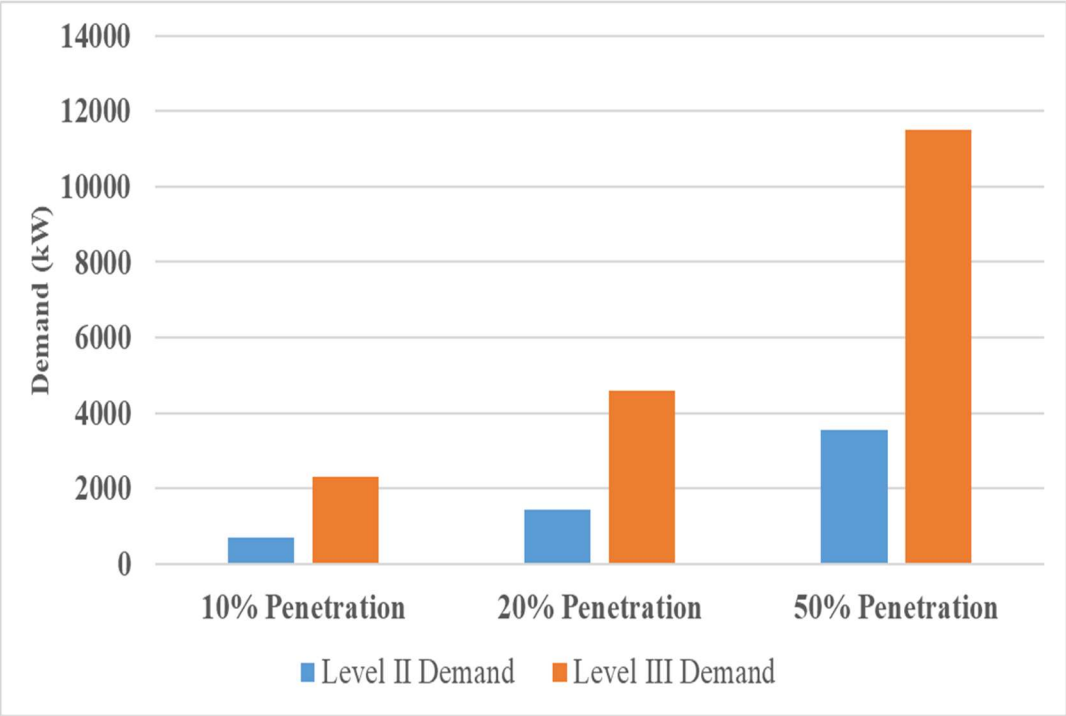

Figure 5.11 PEV Charging Impacts on CE-CERT Feeder

5.3.3.3 Impacts on California Grid

The availability of solar energy during daytime reduces the net demand to be met by non-solar generation. But solar energy starts to decrease in the late afternoon or early evening. Having the same power consumption from the commercial and industrial consumers without the solar availability requires a rapid ramp up in electricity production from non solar generators within a very short period of time. The resulting net demand profile resembles the shape of a 'duck' and is called a "Duck Curve". This is a very common scenario for a grid with intermittent renewable energy such as in California, which has abundant solar energy already integrated into the grid. Multiple generation units are needed to provide this rapid ramp up and they are needed to be in full operating mode in a very short period of time. If there are multiple EVs that are being charged at the same time

from the grid, it will increase the net demand eventually. If 10% parking space penetration scenario presented in Section 5.3.3.2 is now expanded for the California statewide grid, we can get a feel for potential future impacts of EV. For this scenario, we assume that all EVs are plugged in at the same time and look at the modified duck curve. Figure 5.12 is showing the potential net increase in demand and ramp rate due to PEV penetration.

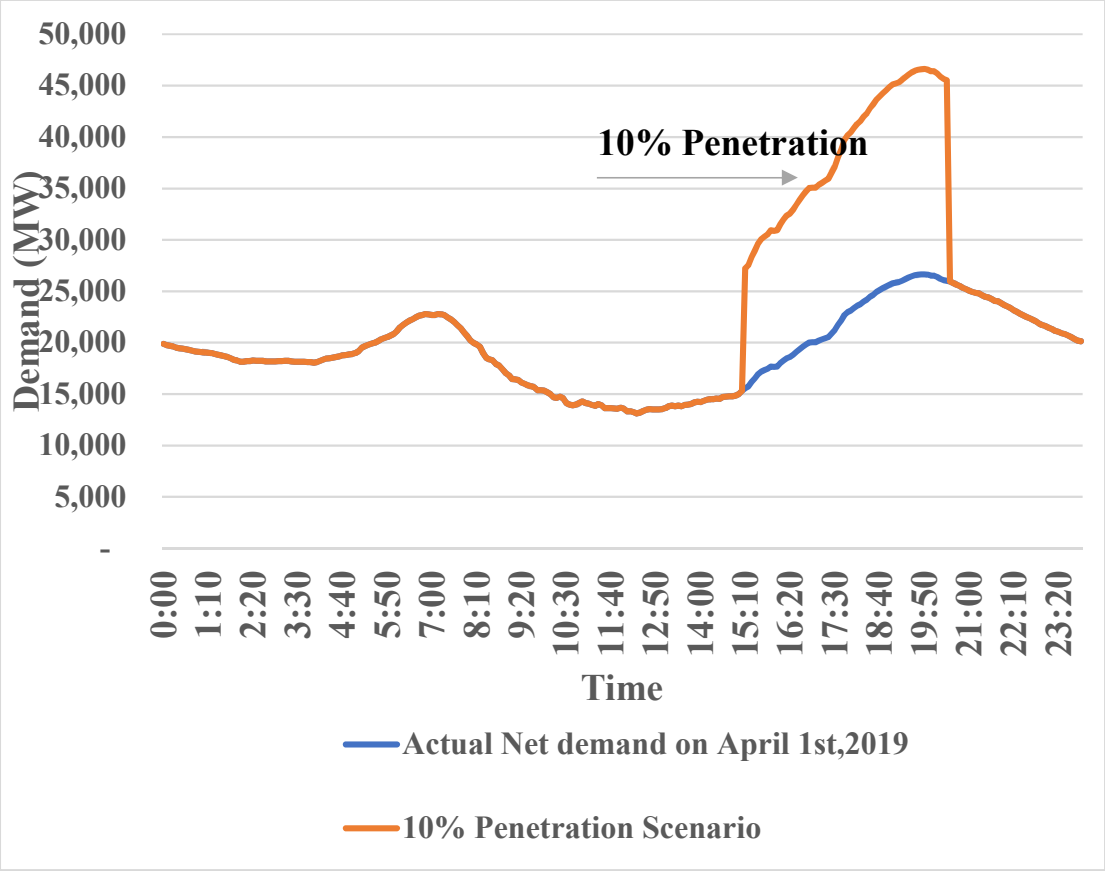

Figure 5.12 PEV Charging Impacts on California Net Demand

To look at this scenario from a different perspective, we reviewed National Renewable Energy Laboratory's (NREL) 2018 study on projected PEV load demand in California for 2025 [126]. By 2025 in any workplace, the lower estimate for Level II chargers are 99,333

and level III chargers are 9,064. The maximum charging load will be 981 MW for weekdays and 794 MW for weekends. The impact of Level III charging was not estimated properly in this analysis whereas this type of charging will become more common with the availability of the newer model of BEVs. The maximum PEV load demand will also happen in the evening according to this analysis which is the ramp up period for duck curve.

5.4 EV Penetration Impact Analysis on the Transmission System using Co-Simulation

5.4.1 Modeling

5.4.1.1 Transmission and Distribution System Modeling

The transmission system used for this study is IEEE 9 bus system [127] . There are three load buses in this transmission system. This three-phase transmission system is modeled by using sequence networks and the power flow is solved in Matlab. A residential distribution feeder such as Electric Power Research Institute (EPRI) ckt 24 [128] is considered as the distribution feeder which is connected to bus 6. The distribution circuit power flow is executed in OpenDSS [96] . Bus 6 of the transmission network is represented as a voltage source whereas the distribution network is considered as a static load at the point of common coupling. Both the systems are simulated simultaneously in their respective simulation platforms and exchange information through the co-simulation script developed in Matlab [80] [129]. The distribution circuit provides the information of real and reactive power whereas the transmission system solver provides the voltage information as shown in Figure 5.13.

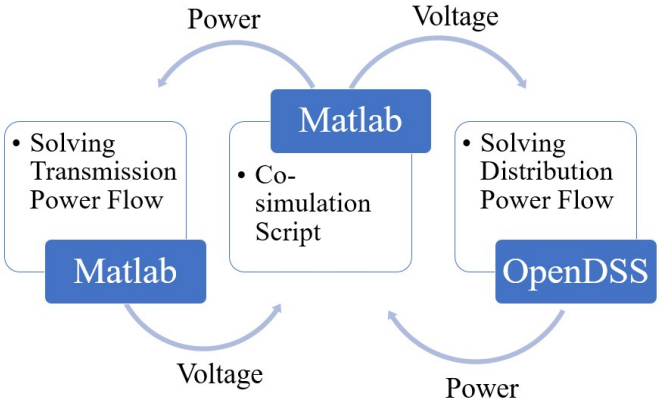

Figure 5.13 T&D Co-simulation Framework

5.4.1.2 PV Modeling

Solar Photovoltaic (PV) systems are deployed at each customer node at the distribution feeder in a distributed manner. The nodes are randomly selected and PV systems are deployed for different penetration levels. The PV scenario is generated using the Monte Carlo approach [130] and the PV sizes are adjusted according to the type of the customer. As the EPRI ckt-24 is a residential feeder and 87 percent of the loads are residential loads, hence the sizes of PV imitate the residential PV mostly. The percentage of the penetration level indicates the number of nodes equipped with PV production.

5.4.1.3 EV Modeling

Whether the EV penetration is modeled based on the percentage of total loads on the distribution feeder on many occasions, the EV to Customer Ratio (EVCR) helps to assess the impacts of EV penetration more comprehensively [131]. The number of EVs at each node depends on the customers connected to each node. As the distribution circuit is a residential feeder and consists of 87 percent residential loads, the remainder loads are

divided into two other subsections such as small and large commercial loads, respectively as follows.

- Residential load nodes (<8 kW)
- Small commercial load nodes (8≤ and $\leq 100\ kW$)
- Large commercial load nodes ($\geq 100\ kW$)

Each node below 8 kW represents a household or a residential customer. The NHTS data distribution is used to determine the permissible number of EVs at each node [119]. Figure 4.13 in chapter 4 is showing the distribution of vehicles in each household in the US. The EVs connected at the residential nodes follow an EV charging pattern which considers that the EV owners charge their EV to the fullest capacity after they get back home. The most common EV capacity is 60 kWh now a days and it is not suggested to go below 20 percent of the total capacity by the manufacturers [132]. It is assumed that people go back home after work and start charging their EVs at home. The charging activities start from 6 pm and keep continuing charging until 2 am to get fully charged (80 percent of the total capacity/48 kWh) at a 6 kW rate in this scenario. Any node consisting of a load between 8 and 100 kW is examined as a node of small commercial customers. All nodes that fall into this category are assigned a fixed load of 25 kW. It is considered that there are 4 EVs in each node that follows commercial load shapes for small commercial consumers [133] . That means all the EVs start charging at the start of office hours (8 am) and can finish charging at 3 pm. The nodes with large commercial loads (> 100 kW) largely represent the capability of having a public EV charging station. The number of EV charging ports at each node is distributed according to the size of the loads at each node. The arrival

and departures of the EVs are modeled according to the public parking lot EV charging scenario. The charging scenarios that happened in the UCR CE-CERT EV parking lot are utilized to model the EV charging for large commercial load nodes as shown in the Figure 3.30 in Chapter 3 [134]. To generate the hourly EV charging profile, un-coordinated EV charging is considered which means when any EV comes in, it can plug in and start charging immediately.

5.4.2 Results and Discussions

The objective of this study is to verify both the co-simulation approach along with the EV penetration impacts. Hence, the values of the parameters at the Point of Common Coupling (PCC) can truly address the issues. Real power (P), reactive power (Q), voltage (V), and angle (deg) are the key information that are shared between two platforms while co-simulation is running. The real and reactive power values, and voltage and angles at the T&D interface for different levels of PV and EV penetrations are shown in Table 5-4 and Table 5-5, respectively. Without having any PV penetration, the total power consumptions (both real and reactive) are increased with a higher level of EV penetrations and the voltages decrease as anticipated. Even with 100 percent EV penetration and having no renewable resources available, the voltage per phase at PCC doesn't fall below 5 percent of standard nominal voltage [135]. When the distribution circuit is simulated alone with a fixed voltage source as a source bus, voltage drops outside the allowable range are prominent at each phase as shown in the figure below.

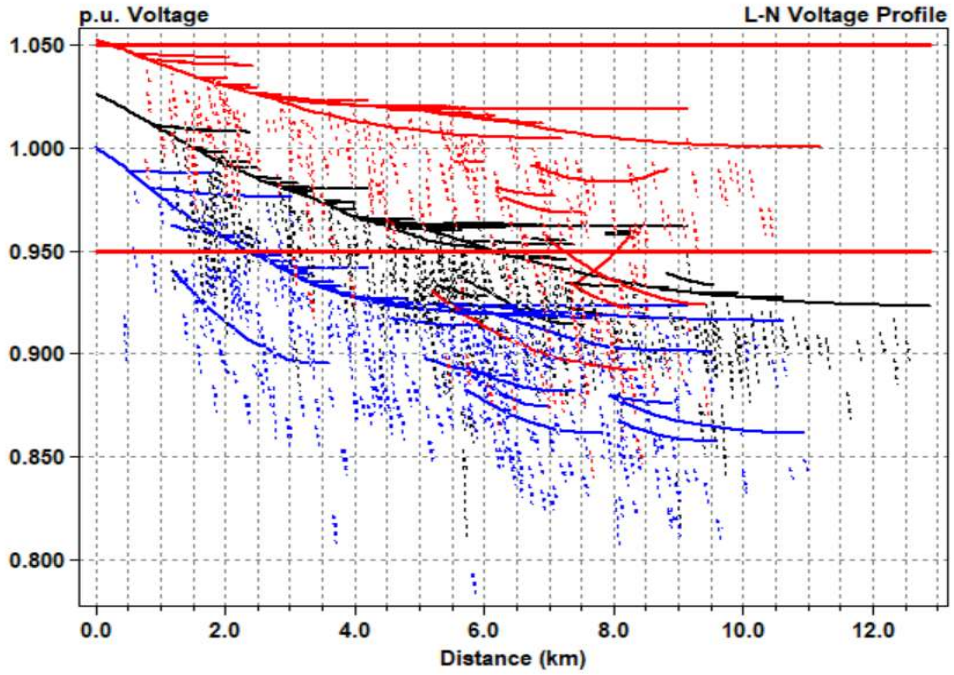

Figure 5.14 Voltage profile for the Distribution Ckt-24 with 100 Percent EV Penetration Only: Each Color Represents a Different Phase (Black: Phase 1, Red: Phase 2, Blue: Phase 3)

When PV penetrations are also considered, the PV power generation offsets the total power requirements in the system. Hence, the total power consumption is lower in comparison with no PV penetration and it decreases with the increment in PV penetration. The maximum power is consumed with 100 percent EV and having no PV available. The lowest power is required with the maximum PV (100 percent) penetration and minimum EV (20 percent) penetration as expected.

Table 5-4 Power Values at the PCC for Different Levels of EV & PV Penetrations

Penetration Level (%)		Real Power (P) (pu)			Reactive Power (Q) (pu)		
EV	PV	Phase 1	Phase 2	Phase 3	Phase 1	Phase 2	Phase 3
20	0	0.2657	0.2500	0.2493	0.0957	0.1061	0.0867
	20	0.2488	0.2340	0.2322	0.0853	0.0963	0.0774
	50	0.2220	0.2090	0.2058	0.0710	0.0823	0.0648
	100	0.1838	0.1712	0.1664	0.0541	0.0670	0.0494
50	0	0.2842	0.2979	0.2919	0.1309	0.1285	0.1394
	20	0.2704	0.2831	0.2775	0.1191	0.1171	0.1271
	50	0.2480	0.2603	0.2545	0.1032	0.1017	0.1113
	100	0.2096	0.2195	0.2149	0.0809	0.0797	0.0875
100	0	0.3023	0.3453	0.3215	0.1728	0.1714	0.2058
	20	0.2917	0.3371	0.3132	0.1627	0.1601	0.1972
	50	0.2729	0.3218	0.2983	0.1472	0.1419	0.1834
	100	0.2438	0.2933	0.2731	0.1263	0.1175	0.1614

Table 5-5 Voltages and Angles at the PCC for Different Levels of EV & PV Penetrations

Penetration Level (%)		Voltage (V) (pu)			Angle (deg) at PCC		
EV	PV	Phase 1	Phase 2	Phase 3	Phase 1	Phase 2	Phase 3
20	0	1.0219	1.0231	1.0226	-4.19	-124.22	115.65
	20	1.0269	1.0279	1.0274	-3.62	-123.66	116.23
	50	1.0337	1.0347	1.0340	-2.72	-122.77	117.12
	100	1.0418	1.0426	1.0419	-1.43	-121.48	118.43
50	0	1.0053	1.0073	1.0041	-5.37	-125.56	114.36
	20	1.0111	1.0130	1.0098	-4.87	-125.06	114.86
	50	1.0189	1.0207	1.0176	-4.07	-124.26	115.66
	100	1.0301	1.0318	1.0289	-2.71	-122.89	117.03
100	0	0.9832	0.9846	0.9793	-6.45	-126.81	113.22
	20	0.9882	0.9897	0.9842	-6.10	-126.48	113.56
	50	0.9961	0.9977	0.9917	-5.50	-125.89	114.15
	100	1.0071	1.0090	1.0028	-4.5055	-124.8975	115.1230

In case of voltages at different levels of PV and EV penetration, the maximum voltage rise happens with the same level of combined PV and EV penetration as in power scenarios. The voltage always remains within the limit despite having maximum PV and EV penetration. Due to EV penetration, the load increases which prevents the slack bus from acting as a load bus, and the voltage increases with higher PV penetration (from 0 to 100). This shows that when EV is penetrated on a large scale, the distributed PV generation is not large enough to offset all the load requirements created from EV users even with 100 percent PV penetration available.

5.5 Conclusions

In addition to contributing towards reduced carbon emission goals, electric vehicles can actively participate in demand response programs, especially in CPP events. In Section 5.2, A novel framework is proposed to solve a deterministic optimization problem including practical limitations imposed by the physical system. Battery degradation cost is included to show the actual scenario of cost-saving from the consumers' point of view. The results show that it is possible to save $48.68 of customers' cost and $1.596 of utilities' cost for each CPP event with two EVs available. Though the monetary benefits for utilities are on a lower side than the customers behind the meter, large EV fleets can provide a lot more savings for utilities. $99,750 in generation cost and 4,987.5 MWh in energy can be saved for any utility with one-fourth of the total EV stations available in California by 2025 during any CPP event.

In Section 5.3 , The charging characteristics from level II and level III chargers connected to a microgrid show 56% peak demand increment at a small commercial

building using four level II chargers. The impacts of EV charging are more alarming at feeder and grid level. Only 10% of the total parking spaces penetrated by (4:5 level II and level III mix) EV can result in an increase of 75% in peak demand for a 4 MW feeder. Finally, Section 5.4 shows a study that takes the advantage of an iterative co-simulation approach to analyze the combined EV and PV integration impacts at the Point of Common Coupling (PCC). This study analyzes the DER dynamics by running the power flow of both system simultaneously and shows that despite causing voltage drops at the distribution feeder, the voltage stays within the allowable range at PCC by the large scale EV penetration.

6 Real-Time Implementation of Vehicle to Grid

6.1 Background and Motivation

While V2G is a well-established concept and has been available for a while, it's utilization in real time and implementation is not widely adopted yet. The limited availability of V2G capable vehicles and lack of attractive utility incentives are the main reasons behind this. The growing need of energy backup at blackout/brownout events and policies toward the availability of sustainable energy have encouraged both the electric utilities and electric car makers to prepare for satisfying the increasing demand for V2G capable EVs. Hence, there are more electric vehicles becoming available that are capable of doing V2G and can support small or medium loads depending on their vehicle battery capacity and travel needs.

6.2 Grid Connected Implementation

6.2.1 Physical Installation

V2G functionality requires successful integration of several components in a manner allowing energy-based control. The microgrid at CE-CERT as mentioned in Chapters 3 and 5 has accommodation to implement V2G for both an electric trolley bus and a light duty PEV. To make the trolley capable of doing V2G, modifications are required to the trolley's DC power system, charger connector configuration, BMS data bus, and charger controls. The portable 500 kWh battery energy storage platform is utilized as the power conversion unit between the trolley batteries and the 480V AC grid power. The trailer contains the necessary BMS communication, charging controls, and a 100kW bidirectional inverter. On the other hand, for the LDEV V2G integration, a charger is

mounted on the portable energy platform to allow for Energy Management System (EMS) integrated communication and control. The line diagram for the physical power and communications layout of the portable energy platform is shown in Figure 6.1. A commercially available V2G compliant charger was selected to provide the bi-directional charging capability to any V2G capable PEVs. The external installation of this V2G unit ensures it's rated outdoor exposure. The external installation also allows for user access to control/command while still maintaining the security of sensitive equipment internal to the platform. It is noted that user can only initiate charging through the user interface of the V2G charger. Remote control is needed to make it enable for V2G activities. The vehicle must communicate the battery status, charge voltage, charge current, and other specified parameters through the charger. This communication protocol as known as ISO 15118 allows for charge/discharge operations of all CHAdeMO V2G PEV compliant platforms.

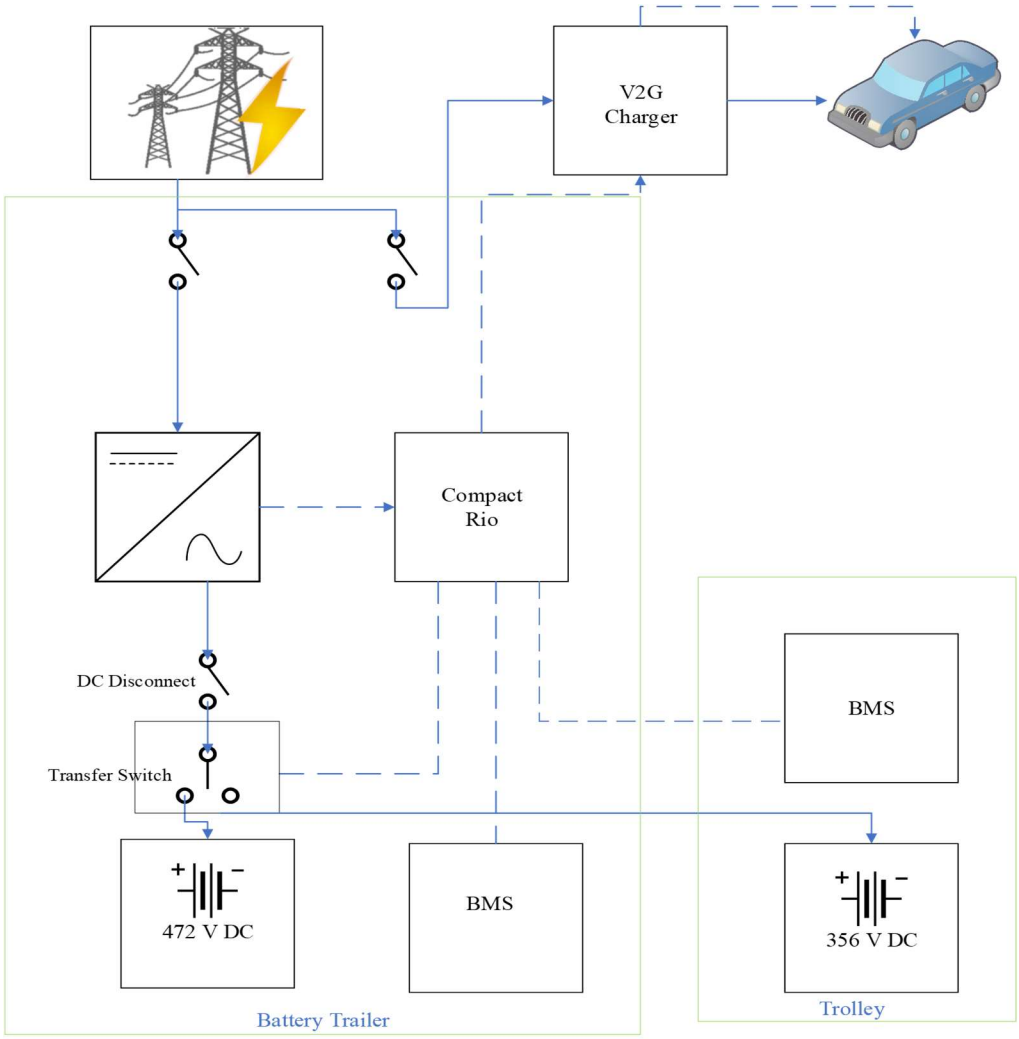

Figure 6.1 Line Diagram of the DC and AC Electrical Layout of the Portable Energy Platform: Dotted Lines are Communication Lines

6.2.2 Real Time Operation

The Nissan Leaf has been deployed and tested for bidirectional operation in real-time. Figure 6.2 shows the light-duty electric vehicle in action during bidirectional operation. The Nissan Leaf utilizes the CHAdeMO Level 3 Fast DC charging port when connecting to the V2G capable charger. The vehicle must communicate the battery status, charge voltage, charge current, and other specified parameters. The communication

protocol allows for charge/discharge operations of all CHAdeMO V2G PEV compliant platforms. Modbus control interface is used to regulate the power command of the LDEV remotely.

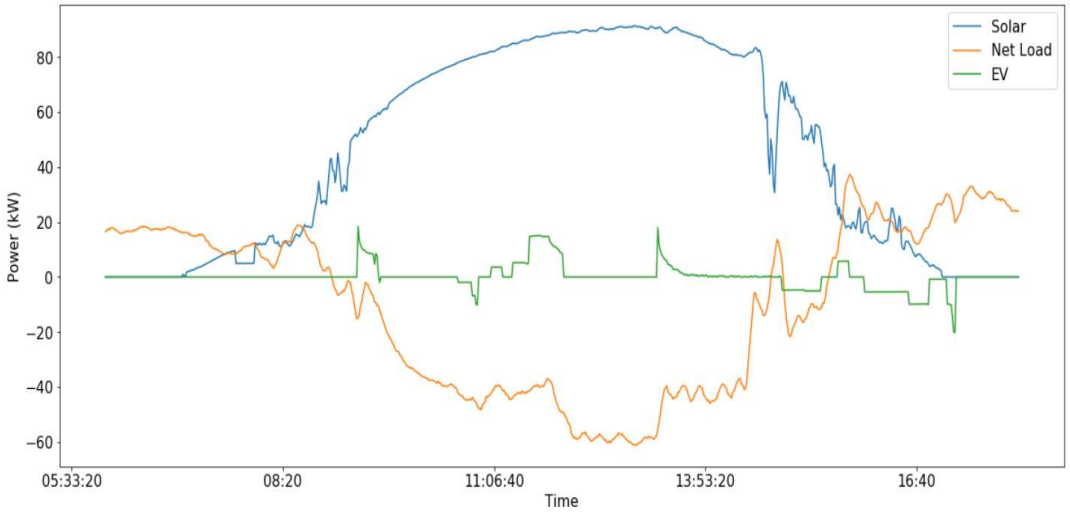

Figure 6.2 Nissan Leaf in Bidirectional Operation in 1084 Building on 1/24/2020; Negative EV Power is Referring V2G Operation

6.3 Islanded Mode Implementation

6.3.1 Supporting Building Load

To support the building load in an islanded mode, the 1084 building was disconnected from the grid. A grid forming commercial inverter located in the 500 kWh battery trailer is used to maintain the necessary grid frequency of the system while doing V2G with the LDEVs available at CE-CERT. The battery capacity of the EVs are 24 kWh as mentioned in Chapters 3 and 5. The LDEVs can not discharge at a higher rate at higher SOCs due to limitations imposed by the old software. The charger prevents SOC of the vehicle to go below 20 percent of the capacity to avoid deep discharge. At the start of the islanding, one LDEV was activated in discharging at 2.5 kW rate (at 30 percent SOC). This

energy from vehicle coupled with additional energy from BESS satisfies the required kW demand of the building which was approximately 5 kW at that time. The V2G discharge rate was then increased to 10 kW to make the islanded microgrid with surplus electrical energy. This high rate of discharging makes the BESS absorb surplus energy by charging the battery after satisfying the building load requirement. When, the first LDEV drains it's battery capacity and reaches 20 percent SOC level, the second LDEV is connected to the microgrid for V2G power delivery. As this microgrid testbed is hardware limited to a single V2G charger, the BESS charger maintains energy supply to the microgrid during the vehicle switch over. Figure 6.3 is showing the power plots for the islanded system

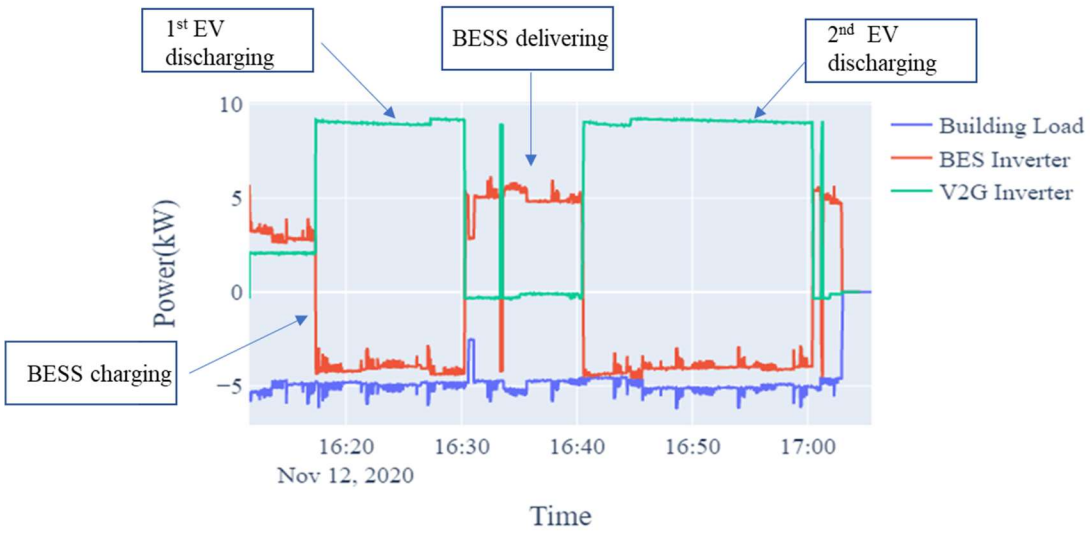

Figure 6.3 Power Plots for the System Including V2G, BES, Building Load and Islanding

6.4 Conclusions

A real-time implementation of smart V2G charging and discharging strategies are presented in this chapter. The physical setup is a sophisticated plug-and-play testbed to

implement V2G in real-time and can be tested for different LDEV and HDEV combinations. The necessary modifications and challenges for successfully implementing both G2V and V2G in real-time are documented and discussed in Section 6.2. In Section 6.3, an islanded V2G operation is presented where two Nissan Leaf EVs provided all the required power to run a commercial building. The successful demonstration of V2G in both grid connected and islanded mode will encourage the EV owners to participate in V2G activities and the utility operators can utilize it by engaging a large EV fleet in V2G operation with the help of EV aggregators.

7 Conclusions and Future Work

7.1 Conclusions

This dissertation focuses on the challenges faced by the distribution grid and the building's common point of coupling due to increased EV penetration and develops innovative frameworks to address these challenges. The impacts of EV integration from different perspectives are also presented to solve the interdependent challenges of EV owner, EV charging infrastructure and the grid.

In Chapter 3 , an innovative framework is developed for selecting the best bidirectional PEV strategy in a commercial building integrated microgrid. This study reveals that between 20.5% to 23.0% system cost reduction is achievable depending on the type of vehicle chargers for buildings equipped with DERs. Later on, an optimal cost framework is proposed for the combined HDEV and LDEV infrastructure implementation. The results show that it is more economical to have an HDEV with fixed travel schedules for energy savings in comparison to LDEV infrastructure implementation. Net metering and/or HDEV implementation in a large energy user building always helps to get the initial investment back in a shorter period. In Section 3.2, the study shows that between 2 and 3.2 percent cost savings is possible for any small commercial load profile along with a regular light duty PEV ownership. Finally, the impacts of different building loads on optimal EV charging for both unidirectional and bidirectional operation have shown that low price differential between on-peak and off-peak electrical energy rates result in lower EV charging cost for large building loads whereas high differential electrical energy rate does the same for smaller building loads.

In Chapter 4, the behavior of public PEV customers' are analyzed and a general load profile is generated to analyze the impacts on the distribution grid. Two different utilization factors are introduced for energy and duration to help predicting the real usage scenarios. Later on, a customer oriented stochastic EV modeling is proposed to quantify the EV penetration impacts on voltages at the local nodes and feeder vehicle capacity. A comprehensive and realistic detailed distributed EV load modeling in a given feeder can be useful to assess the necessary distribution system upgrades.

In Chapter 5, a novel framework is introduced to ensure PEV participation in a CPP event. The results show that $48.68 of customers' cost and $1.596 of utilities' cost savings are possible for each CPP event with two EVs available (40 kWh with 15 kW and 100 kWh with 30 kW rate of charging/discharging). In Section 5.3 , the impacts of EV charging on a distribution level microgrid are presented. Only 10% of the total parking spaces penetrated by EV, 80 percent level II and 20 percent level III mix can result in an increase of 75% in peak demand for a 4 MW feeder. Finally, an iterative co-simulation algorithm is implemented to analyze the combined EV and PV integration impacts at the PCC that shows the voltage stays within the allowable range at PCC.

In Chapter 6, real-time G2V implementation is shown for both HDEV and LDEV in a distribution level microgrid. Later on, V2G implementation is carried out to support the microgrid in both grid-connected and islanded mode of operation. It is shown that a small LDEV can support a 10 kW microgrid in islanded mode, and provide 30 kW during grid connected mode and help manage the peak.

7.2 Selected Publications from This Research

- **J Yusuf**, ASMJ Hasan, S Ula, "EV Penetration Impact Analysis on Transmission System using Co-Simulation" in *IEEE Transportation Electrification Conference and Expo*, Anaheim, CA, 2022, in press

- ASMJ Hasan, L Enriquez-Contreras, **J Yusuf**, MJ. Barth, S Ula, "Demonstration of Microgrid Resiliency with V2G Operation" in *IEEE Transportation Electrification Conference and Expo*, Chicago, IL, 2021.

- **J Yusuf**, ASMJ Hasan, S Ula, "Impacts Analysis of Electric Vehicles Integration to the Residential Distribution Grid*"* in *IEEE Kansas Power & Energy Conference,* Manhattan, KS, 2021

- **J Yusuf**, R Watanabe, S Ula, M Todd, H Gomez, "Data Driven Stochastic Energy Cost Optimization with V2G Operation in Commercial Buildings" in *IEEE 52nd North American Power Symposium,* Phoenix, AZ, 2021

- **J Yusuf**, ASMJ Hasan, S Ula, "Impacts Analysis & Field Implementation of Plug-in Electric Vehicles Participation in Demand Response and Critical Peak Pricing for Commercial Buildings*"* in *IEEE Texas Power & Energy Conference,* College Station, TX, 2021

- **J Yusuf**, S Ula, ASMJ Hasan, "Analyses and Applications of Plug-in Electric Vehicle Charging Stations User Behavior in a Large University Campus Community" in *International Conference on Smart Grids and Energy Systems*, Perth, Australia, 2020

- **J Yusuf**, S Ula, "A Comprehensive Optimization Solution for Buildings with Distributed Energy Resources and V2G Operation in Smart Grid Applications" in *IEEE Innovative Smart Grid Technologies,* Washington, DC, 2020

- **J Yusuf**, ASMJ Hasan, S Ula, "Impacts of Plug-in Electric Vehicles on a Distribution Level Microgrid*"* in *IEEE 51st North American Power Symposium,* Wichita, KS, 2019

- **J Yusuf**, S Ula, "Impact of Building Loads on Cost Optimization Strategy for a Plug-in Electric Vehicle Operation*"* in *IEEE Transportation Electrification Conference and Expo,* Detroit, MI, 2019

- **J Yusuf,** ASMJ Hasan, J Garrido, S Ula, MJ. Barth, "A Comparative Techno-Economic Assessment of Bidirectional Heavy Duty and Light Duty Plug-in Electric Vehicles Operation : A Case Study" in Sustainable Cities and Society, under review

- **J Yusuf,** ASMJ Hasan, L Enriquez-Contreras, S Ula, “A Centralized Optimization Approach for Bidirectional PEV Impacts Analysis in a Commercial Building-Integrated Microgrid” in Sustainable Energy, Grids and Networks, under review

7.3 Future Work

Though this dissertation answers most of the key questions that can facilitate wider adoption of electric vehicles, there are still some open research questions that need to be addressed as follows.

1. We have assessed the techno-economic benefits of the combination of HDEV and LDEV integrations. While LDEVs have been present in the market for a long time, MDEV and HDEVs are becoming more available with higher capacity and charging rates up to 300 kW. This extreme fast charging might have a huge impact on the distribution grid and necessary upgrades will be needed to withstand these HDEV and MDEV integrations. The impacts on the grid with the influx of advanced MDEV and HDEV availability in market and their optimal operations need to be investigated.

2. We have explored the opportunities for the utilities to utilize EVs in the critical events. The coordinated V2G charging on a large EV fleet can help the utility to meet the demand at peak periods. A detailed analysis on the advantages of large-scale EV fleets for the utilities to support the grid are required and needs to be validated with system implementation.

3. We have investigated the EV impacts on the distribution level microgrid and T&D interface with co-simulation. Innovative grid modeling can utilize the current infrastructure to adopt more EVs while withstanding the increased demand for hosting capacity. The concerns regarding the facilitation of more EVs into the grid by the grid operators and the capabilities of grid modeling helping to avoid the necessary upgrades and grid reinforcement cost need to be answered.

4. The real time V2G implementation as shown in this dissertation is still limited by different factors. Though V2G can help the utility and buildings in case of critical events, a common standard for all types of EVs is still under development that prevents the mass integration of EVs to participate in V2G activities. A common charger standard that can enable all EVs to plug-in and activate V2G is necessary for future PEV utilization. The development of a universal interconnection standard to make V2G possible for all types of EVs is so important for wide V2G implementation.

Bibliography

[1] "Number of motor vehicles registered in the United States from 1990 to 2020," [Online]. Available: https://www.statista.com/statistics/183505/number-of-vehicles-in-the-united-states-since-1990/#:~:text=How%20many%20registered%20motor%20vehicles,11%20million%20units%20in%202020.

[2] [Online]. Available: https://www.eia.gov/energyexplained/.

[3] [Online]. Available: https://www.eia.gov/.

[4] [Online]. Available: https://www.energy.gov/energysaver/articles/new-plug-electric-vehicle-sales-united-states-nearly-doubled-2020-2021.

[5] [Online]. Available: https://www.iea.org/gevo2018/.

[6] [Online]. Available: https://www.npr.org/2018/09/10/646373423/california-sets-goal-of-100- percent-renewableelectric-power-by-2045.

[7] [Online]. Available: https://www.globalfleet.com/en/safety-environment/north america/features/5-million-zeroemission-vehicles-california.

[8] [Online]. Available: https://electrek.co/2018/01/29/california-electric-cars-charging-stations/.

[9] [Online]. Available: https://ir.tesla.com/press-release/tesla-q4-2021-vehicle-production-deliveries.

[10] [Online]. Available: https://electrek.co/2016/09/02/tesla-20-stall-supercharger-world-largest-fast-charging-station/.

[11] [Online]. Available: https://teslatap.com/articles/supercharger-superguide/.

[12] F. Sehar, M. Pipattanasomporn and S. Rahman, "Demand management to mitigate impacts of plug-in electric vehicle fast charge in buildings with renewables," *Energy,* vol. 120, pp. 642-651, 2017.

[13] F. Sehar, M. Pipattanasomporn and S. Rahman, "An energy management model to study energy and peak power savings from PV and storage in Demand Responsive buildings," *Applied Energy,* vol. 173, pp. 406-417, 2016.

[14] K. Baek, W. Ko and J. Kim, "Optimal Scheduling of Distributed Energy Resources in Residential Building under the Demand Response Commitment Contract.," *Energies,* vol. 12, 2019.

[15] D. Zhang, S. Evangelisti, P. Lettieri and L. Papageorgiou, "Economic and environmental scheduling of smart homes with microgrid : DER operation and electrical tasks," *Energy Convers Manag,* vol. 110, p. 113–24, 2016.

[16] J. A. Pinzon, P. P. Vergara, L. C. P. Silva and M. J. Rider, "An MILP model for optimal management of energy consumption and comfort in smart buildings," in *IEEE Power & Energy Society Innovative Smart Grid Technologies Conference (ISGT)*, Washington, DC, 2017.

[17] J. A. Pinzon, P. P. Vergara, L. C. P. Silva and M. J. Rider, "Optimal Management of Energy Consumption and Comfort for Smart Buildings Operating in a Microgrid," *IEEE Transactions on Smart Grid,* vol. 10, no. 3, pp. 3236-3247, 2019.

[18] J. Yusuf and S. Ula, "A Comprehensive Optimization Solution for Buildings with Distributed Energy Resources and V2G Operation in Smart Grid Applications," in *IEEE Power & Energy Society Innovative Smart Grid Technologies Conference (ISGT)*, Washington, DC, 2020.

[19] D. Thomas, O. Deblecker and C. Ioakimidis, "Optimal operation of an energy management system for a grid-connected smart building considering photovoltaics' uncertainty and stochastic electric vehicles' driving schedule.," *Appl Energy,* vol. 210, 2018.

[20] S. Nan, M. Zhou and G. Li, "Optimal residential community demand response scheduling in smart grid," *Appl Energy,* vol. 210, 2018.

[21] V. Coelho, I. Coelho, B. Coelho, M. Weiss, A. Reis and S. Silva, "Multiobjective energy storage power dispatching using plug-in vehicles in a smart-microgrid," *Renew Energy,* vol. 89, p. 730–42, 2016.

[22] F. Hafiz, A. Queiroz and I. Husain, "Coordinated Control of PEV and PV-Based Storages in Residential Systems Under Generation and Load Uncertainties," *IEEE Transactions on Industry Applications,* vol. 55, no. 6, pp. 5524-5532, 2019.

[23] A. Duman and H. Erden, "A home energy management system with an integrated smart thermostat for demand response in smart grid," *Sustainable Cities and Society,* vol. 65, 2021.

[24] L. Gong, W. Cao, K. Liu and J. Zhao, "Optimal charging strategy for electric vehicles in residential charging station under dynamic spike pricing policy," *Sustainable Cities and Society,* vol. 63, 2020.

[25] H. Zhao, X. Yan and H. Ren, "Quantifying flexibility of residential electric vehicle charging loads using non-intrusive load extracting algorithm in demand response," *Sustainable Cities and Society,* vol. 50, 2019.

[26] A. Aris, R. Habibifar, M. Moradi and M. Khoshjahan, "Robust optimization of renewable-based multi-energy micro-grid integrated with flexible energy conversion and storage devices," *Sustainable Cities and Society,* vol. 64, 2021.

[27] X. Gao, Y. Akashi and D. Sumiyoshi, "Installed capacity optimization of distributed energy resource systems for residential buildings," *Energy and Buildings,* vol. 69, pp. 307-317, 2014.

[28] J. Pan, X. Wu, Q. Feng and Y. Ji, "Optimization of electric bus charging station considering energy storage system," in *2020 8th International Conference on Power Electronics Systems and Applications: Future Mobility and Future Power Transfer, PE*, 2020.

[29] C. Zhang, " Charging schedule optimization of electric bus charging station considering departure timetable.," in *IET Conference Publications*, 2019.

[30] H. Basma, C. Mansour, M. Nemer, M. Haddad and P. Stabat, "Optimization of battery electric bus charging under varying operating conditions," in *2020 IEEE Vehicle Power and Propulsion Conference, VPPC 2020 - Proceedings.*.

[31] R. Beekman and R. Van Den Hoed, "Operational demands as determining factor for electric bus charging infrastructure.," in *IET Conference Publications*, 2016.

[32] M. Jiang, Y. Zhang, C. Zhang, K. Zhang, G. Zhang and Z. Zhao, "Operation and Scheduling of Pure Electric Buses under Regular Charging Mode," in *IEEE Conference on Intelligent Transportation Systems,*, 2018-Novem.

[33] M. A. Gormez, E. Haque and Y. Sozer, " Cost Optimization of an Opportunity Charging Bus Network," *IEEE Transactions on Industry Applications,* 2021.

[34] H. Chen, Z. Hu, Z. Xu, J. Li, H. Zhang, X. Xia, K. Ning and M. Peng, "Coordinated charging strategies for electric bus fast charging stations.," in *Asia-Pacific Power and Energy Engineering Conference*, 2016.

[35] A. Houbbadi, R. Trigui, S. Pelissier, T. Bouton and E. Redondo-Iglesias, " Multi-Objective Optimisation of the Management of Electric Bus Fleet Charging," in *2017 IEEE Vehicle Power and Propulsion Conference*.

[36] A. Zahedmanesh, K. M. Muttaqi and D. Sutanto, "A Cooperative Energy Management in a Virtual Energy Hub of an Electric Transportation System Powered by PV Generation and Energy Storage," *IEEE Transactions on Transportation Electrification,* pp. 1-11, 2021.

[37] Y. Zhou, X. C. Liu, R. Wei and A. Golub, "Bi-Objective Optimization for Battery Electric Bus Deployment Considering Cost and Environmental Equity," *IEEE*

Transactions on Intelligent Transportation Systems, vol. 22, no. 4, p. 2487–2497, 2021.

[38] W. B. Heredia, K. Chaudhari, A. Meintz, M. Jun and S. Pless, "Evaluation of smart charging for electric vehicle-to-building integration: A case study," *Appl. Energy,* vol. 266, November 2019.

[39] N. B. G. Brinkel, W. L. Schram, T. A. AlSkaif, I. Lampropoulos and W. G. J. H. M. van Sark, " Should we reinforce the grid? Cost and emission optimization of electric vehicle charging under different transformer limits," *Appl. Energy,* vol. 276, 2020.

[40] R. Koubaa, Y. Yoldas, S. Goren, L. Krichen and A. Onen, "Implementation of cost benefit analysis of vehicle to grid coupled real Micro-Grid by considering battery energy wear: Practical study case," *Energy Environ,* 2020.

[41] M. Yang, L. Zhang and W. Dong, "Economic Benefit Analysis of Charging Models Based on Differential Electric Vehicle Charging Infrastructure Subsidy Policy in China," *Sustainable Cities and Society,* vol. 59, 2020.

[42] A. O. David and I. Al-Anbagi, "EVs for frequency regulation: Cost benefit analysis in a smart grid environment," *IET Electr. Syst. Transp.,* vol. 7, no. 4, p. 310–317, 2017.

[43] S. Tamura, "A V2G strategy to increase the cost–benefit of primary frequency regulation considering EV battery degradation," *Electr. Eng. Japan (English Transl. Denki Gakkai Ronbunshi),* vol. 212, no. 1-4, pp. 11-22, 2020.

[44] J. Singh and R. Tiwari, "Cost Benefit Analysis for V2G Implementation of Electric Vehicles in Distribution System," *IEEE Trans. Ind. Appl.,* vol. 56, no. 5, pp. 5963-5973, 2020.

[45] M. B. Tookanlou, M. Marzband, A. A. Sumaiti and A. Mazza, "Cost-benefit analysis for multiple agents considering an electric vehicle charging/discharging strategy and grid integration," in *20th IEEE Mediterr. Electrotech. Conf. MELECON 2020* , 2020.

[46] J. Fan and Z. Chen, "Cost-Benefit Analysis of Optimal Charging Strategy for Electric Vehicle with V2G," in *51st North Am. Power Symp. NAPS 2019*, 2019.

[47] J. Rodríguez-Molina, P. Castillejo, V. Beltran and M. Martínez-Núñez, "A Model for Cost–Benefit Analysis of Privately Owned Vehicle-to-Grid Solutions," *Energies,* vol. 13, no. 21, p. 5814, 2020.

[48] R. v. d. Hoed, J. R. Helmus, R. d. Vries and D. Bardok, "Data analysis on the public charge infrastructure in the city of Amsterdam," *World Electric Vehicle Journal,* vol. 6, no. 4, p. 829–838, 2013.

[49] A. Almaghrebi, S. Shom, F. A. Juheshi, K. James and M. Alahmad, "Analysis of User Charging Behavior at Public Charging Stations," in *IEEE Transportation Electrification Conference and Expo (ITEC)*, Detroit, MI, USA,, 2019.

[50] A. Almaghrebi, F. A. Juheshi, J. Nekl, K. James and M. Alahmad, "Analysis of Energy Consumption at Public Charging Stations, a Nebraska Case Study," in *2020 IEEE Transportation Electrification Conference & Expo (ITEC)*, Chicago, IL, USA, 2020.

[51] M. Coban and S. S. Tezcan, "Analysis of Impact of Electric Vehicles on Distribution Grid Using Survey Data," in *2019 3rd International Symposium on Multidisciplinary Studies and Innovative Technologies (ISMSIT)*, Ankara, Turkey., 2019.

[52] Z. Fotouhi, M. R. Hashemi, H. Narimani and I. S. Bayram, " A General Model for EV Drivers' Charging Behavior," *IEEE Transactions on Vehicular Technology,* vol. 68, no. 8, pp. 7368-7382, Aug. 2019.

[53] J. Mies, J. Helmus and R. v. d. Hoed, " Estimating the Charging Profile of Individual Charge Sessions of Electric Vehicles in The Netherlands," *World Electric Vehicle Journal,* vol. 9, no. 2, p. 17, Jun. 2018.

[54] R. Wolbertus, M. Kroesen, R. v. d. Hoed and C. Chorus, "Fully charged: An empirical study into the factors that influence connection times at EV-charging stations," *Energy Policy,* vol. 123, pp. 1-7, 2018.

[55] Z. J. Lee, T. Li and S. H. Low, "ACN-Data: Analysis and Applications of an Open EV Charging Dataset," in *Proceedings of the Tenth International Conference on Future Energy Systems e-Energy '19*, June 2019.

[56] Z. J. Lee, D. Johansson and S. H. Low, "ACN-Sim: An Open-Source Simulator for Data-Driven Electric Vehicle Charging Research," in *2019 IEEE International Conference on Communications, Control, and Computing Technologies for Smart Grids (SmartGridComm)*, Beijing, China, 2019.

[57] I. S. Bayram, V. Zamani, R. Hanna and J. Kleissl, "On the evaluation of plug-in electric vehicle data of a campus charging network," in *2016 IEEE International Energy Conference (ENERGYCON)*, Leuven, 2016.

[58] E. Ucer, M. C. Kisacikoglu and A. C. Gurbuz, "Learning EV Integration Impact on a Low Voltage Distribution Grid," in *2018 IEEE Power & Energy Society General Meeting (PESGM)*, Portland, OR, 2018.

[59] M. Spitzer, J. Schlund, E. Apostolaki-Iosifidou and M. Pruckner, "Optimized Integration of Electric Vehicles in Low Voltage Distribution Grids," *Energies,* vol. 12, no. 21, Oct. 2019.

[60] H. Abdullah, R. M. Kamel and A. Gastli, "EV Impact on the Residential Distribution Network with Smart PV Inverters," in *2020 IEEE Power & Energy Society Innovative Smart Grid Technologies Conference (ISGT)*, Washington, DC, USA, , 2020.

[61] S. Hes, J. Kula and J. Svec, "Analysis of Smart Technical Measures Impacts on DER and EV Hosting Capacity Increase in LV and MV Grids in the Czech Republic in the Czech Republic in Terms of European Project InterFlex," in *2019 International Conference on Smart Energy Systems and Technologies (SEST)*, Porto, Portugal, 2019.

[62] D. e. al. and S., "Charging Coordination of Plug-In Electric Vehicle for Congestion Management in Distribution System Integrated With Renewable Energy Sources," *IEEE Transactions on Industry Applications,* vol. 56, no. 5, pp. 5452-5462, Sept.-Oct. 2020.

[63] A. T. Al-Awami, E. Sortomme, G. M. A. Akhtar and S. Faddel, "A Voltage-Based Controller for an Electric-Vehicle Charger," *IEEE Transactions on Vehicular Technology,* vol. 65, no. 6, pp. 4185-4196, June 2016.

[64] M. Gamit, A. Shukla, R. Kumar and K. Verma, "Supplementary frequency control in power systems via decentralised V2G/G2V support,," *The Journal of Engineering,* vol. 18, no. 7, pp. 5287-5291, 2019.

[65] [Online]. Available: https://eetd.lbl.gov/sites/all/files/publications/report-lbnl-1252d.pdf.

[66] S. Fenwick, L. Getachew, C. Ivanov and J. Smith, "Demand impact of a critical peak pricing program: opt-in and opt-out options, green attitudes and other customer characteristics," *Energy,* vol. 35, no. 3, pp. 1-24, 2014.

[67] [Online]. Available: https://www.flexalert.org/what-is-flex-alert.

[68] [Online]. Available: https://www.nissanusa.com/vehicles/electric-cars/leaf/features/range-charging-battery.html.

[69] R. A. Biroon, Z. Abdollahi and R. Hadidi, "Effect of Tariff on Optimal Electric Vehicle Connection to the Grid in Residential Sector," in *2019 IEEE Transportation Electrification Conference and Expo (ITEC)*, Detroit, MI, USA, 2019.

[70] A. Moradipari and M. Alizadeh, "Pricing and Routing Mechanisms for Differentiated Services in an Electric Vehicle Public Charging Station Network," *IEEE Transactions on Smart Grid,* vol. 11, no. 2, pp. 1489-1499, March 2020.

[71] Y. Yin, M. Zhou and G. Li, "Dynamic decision model of critical peak pricing considering electric vehicles' charging load," in *International Conference on Renewable Power Generation (RPG 2015)*, Beijing, 2015.

[72] L. Chen and B. Chen, "2019 IEEE Innovative Smart Grid Technologies - Asia (ISGT Asia)," in *Fuzzy Logic-Based Electric Vehicle Charging Management Considering Charging Urgency*, Chengdu, China, 2019.

[73] M. Kii, K. Sakamoto, Y. Hangai and K. Doi, "The effects of critical peak pricing for electricity demand management on home-based trip generation," *IATSS Research,* vol. 37, no. 2, pp. 89-97, 2014.

[74] Q. Huang, R. Huang, R. Fan, J. Fuller, T. Hardy and Z. H. Huang, "A Comparative Study of Interface Techniques for Transmission and Distribution Dynamic Co-Simulation," in *2018 IEEE Power & Energy Society General Meeting (PESGM)*, 2018.

[75] G. Krishnamoorthy and A. Dubey, "Transmission – Distribution Cosimulation: Analytical Methods for Iterative Coupling," *IEEE Systems Journal,,* vol. 14, no. 2, p. 2633–2642, 2020.

[76] G. Krishnamoorthy, A. Dubey and P. K. Sen, "Iteratively-Coupled Co-simulation Framework for Unbalanced Transmission-Distribution System," in *2019 IEEE Milan PowerTech*, Milan, 2019.

[77] G. Krishnamoorthy and A. Dubey, "Hybrid Transmission Distribution Co-simulation: Frequency Regulation using Battery Energy Storage," [Online]. Available: arXiv:1912.07204.

[78] K. Balasubramaniam and S. Abhyankar, " A Combined Transmission and Distribution System Co-Simulation Framework for Assessing the Impact of Volt / VAR Control on Transmission System," in *2017 IEEE Power & Energy Society General Meeting*, 2017.

[79] Q. Li and S. Abhyankar, "Evaluation of High Solar Penetration Impact on Bulk System Stability through a Transmission-Distribution," in *2019 IEEE Power & Energy Society General Meeting (PESGM)*, 2019.

[80] G. Krishnamoorthy, R. Sadnan, A. Dubey, Y. N. Velaga and P. K. Sen, "Distributed PV Penetration Impact Analysis on Transmission System Voltages using Co-Simulation," in *2019 North American Power Symposium (NAPS)*, Wichita, KS, 2019.

[81] M. M. Rezvani, S. Mehraeen, J. R. Ramamurthy and T. Field, "Interaction of Transmission-Distribution System in the Presence of DER Units – Co-simulation Approach," *IEEE Open Journal of Industry Applications,* vol. 1, pp. 23-32, 2020.

[82] R. Sadnan, G. Krishnamoorthy and A. ". Dubey, "Transmission and Distribution (T & D) Quasi-Static Co-Simulation : Analysis and Comparison of T & D Coupling Strength," *IEEE Access,* vol. 8, pp. 124007-124019, 2020.

[83] [Online]. Available: https://evrater.com/ev/nissan-leaf-long-range .

[84] [Online]. Available: https://pushevs.com/2018/07/18/nissan-confirms-that-the-2019-nissanleaf-e-plus-is-coming/.

[85] [Online]. Available: https://riversideca.gov/utilities/sites/riversideca.gov.utilities/files/pdf/rates-electric/Electric%20Schedule%20DTOU%20-%20Effective%2001-1-19%20Updated%20clean.pdf.

[86] "Michael Grant and Stephen Boyd. CVX: Matlab software for disciplined convex programming, version 2.0 beta.," [Online]. Available: http://cvxr.com/cvx, September 2013.

[87] [Online]. Available: https://www.nissanusa.com/vehicles/electric cars/leaf.

[88] "Gurobi Optimization,LLC, "Gurobi Optimizer Reference Manual"," [Online]. Available: https://www.gurobi.com.

[89] H. Gan and C. Zheng, "Operation optimization of electric vehicle based on demand side management," in *2019 34rd Youth Academic Annual Conference of Chinese Association of Automation (YAC)*, Jinzhou, China, 2019.

[90] [Online]. Available: https://www.fueleconomy.gov/feg/Find.do?action=sbs&id=40812.

[91] C. D. Korkas, "Occupancy-based demand response and thermal comfort optimization in microgrids with renewable energy sources and energy storage.," *Applied Energy ,* vol. 163, pp. 93-104, 2016.

[92] Y. Liu, Z. Lu and F. Yang, "The investigation of solar PV models.," in *2018 IEEE Power & Energy Society Innovative Smart Grid Technologies Conference (ISGT)*, Washington, DC, 2018.

[93] "Lux to Lumen Calculator: How Much Light Do You Need?," [Online]. Available: https://www.bannerengineering.com/us/en/company/expert-insights/lux-lumens-calculator.html.

[94] H. Farzin, M. Fotuhi-Firuzabad and M. A. Moeini-Aghtaie, "Practical Scheme to Involve Degradation Cost of Lithium-Ion Batteries in Vehicle-to-Grid Applications," *IEEE Transactions on Sustainable Energy,* vol. 7, no. 4, pp. 1730-1738, 2016.

[95] [Online]. Available: https://site.ieee.org/pes-testfeeders/resources/.

[96] [Online]. Available: ftp://197.155.77.3/sourceforge/e/el/electricdss/OpenDSS/OpenDSSManual.pdf.

[97] S. Ula, J. Yusuf and A. Hasan, "Development and Deployment of an Integrated Microgrid Incorporating Solar PV, Battery Energy Storage and EV Charging," in *Conference Proceedings of Applied Energy Symposium: MIT A+B*, Boston, MA, 2019.

[98] J. Yusuf, R. B. Faruque, A. S. M. J. Hasan and S. Ula, "Statistical and Deep Learning Methods for Electric Load Forecasting in Multiple Water Utility Sites," in *2019 IEEE Green Energy and Smart Systems Conference (IGESSC)*, 2019.

[99] [Online]. Available: github.com/keras-team/keras.

[100] [Online]. Available: https://keras.io/api/optimizers/adam/.

[101] [Online]. Available: https://www.riversidetransit.com/.

[102] X. Wu, D. Freese, A. Cabrera and W. Kitch, "Electric vehicles' energy consumption measurement and estimation," *Transportation Research Part D: Transport and Environment,* vol. 34, pp. 52-67, 2015.

[103] J. Yusuf, R. Watanabe, S. Ula, M. Todd and H. Gomez, "Data Driven Stochastic Energy Cost Optimization with V2G Operation in Commercial Buildings," in *2020 52nd North American Power Symposium (NAPS*, 2021.

[104] A. Ahmadian, M. Sedghi, A. Elkamel, M. Fowler and M. Golkar, "Plug-in electric vehicle batteries degradation modeling for smart grid studies: Review, assessment and conceptual framework," *Renewable and Sustainable Energy Reviews,* vol. 81, no. 2, 2018.

[105] C. Guenther, B. Schott, W. Hennings, P. Waldowski and M. Danzer, "Model-based investigation of electric vehicle battery aging by means of vehicle-to-grid scenario simulations," *Journal of Power Sources,* vol. 239, pp. 604-610, 2013.

[106] [Online]. Available: https://www.riversideca.gov/utilities/businesses/rates-electric.asp.

[107] [Online]. Available: https://www.fueleconomy.gov/feg/Find.do?action=sbs&id=40812.

[108] [Online]. Available: https://www.mass.gov/doc/mass-doer-electric-school-bus-pilot-project-evaluation.

[109] [Online]. Available: https://www.codepublishing.com/CA/Galt/html/Galt18/Galt1848.html.

[110] [Online]. Available: https://www.energy.gov/eere/vehicles/articles/fotw-1072-march-11-2019-light-duty-vehicles-accounted-majority-transportation.

[111] [Online]. Available: https://www.cncda.org/wp content/uploads/CNCDA-ZEV Handout_031119-3.pdf.

[112] [Online]. Available: https://www.coltura.org/california-gasoline-phaseout.

[113] [Online]. Available: https://www.cncda.org/wp-content/uploads/CalCovering-1Q-20-REVISED.pdf.

[114] [Online]. Available: https://evadoption.com/ev-charging-stations-statistics/charging-stations-by-state/#:~:text=As%20of%20September%2031%2C%202021,States%20and%20109%2C307%20charger%20ports.

[115] [Online]. Available: https://evadoption.com/ev-charging-stationsstatistics/.

[116] [Online]. Available: https://www.chargepoint.com/.

[117] D. Tang and P. Wang, "Probabilistic modeling of nodal charging demand based on spatial-temporal dynamics of moving electric vehicles," *IEEE Trans. Smart Grid,* vol. 7, no. 2, p. 627–636, 2016.

[118] J. Fan and Z. Chen, " Cost-Benefit Analysis of Optimal Charging Strategy for Electric Vehicle with V2G,"," in *2019 North American Power Symposium*, 2019.

[119] [Online]. Available: https://nhts.ornl.gov/.

[120] [Online]. Available: https://afdc.energy.gov/data/10567 .

[121] [Online]. Available: https://www.eia.gov/tools/faqs.

[122] "Cost Comparison of Battery Storage," [Online]. Available: https://www.bluesky-energy.eu/en/2018/08/02/cost-comparison-of-battery-storage.

[123] [Online]. Available: http://scppa.org/page/member-riverside#:~:text=Established%20in%201895%2C%20Riverside%20Public,of%20Riverside%2C%20California%2C%20serving%20a.

[124] [Online]. Available: https://www.eia.gov/todayinenergy/detail.php?id=13191.

[125] [Online]. Available: https://www.cpuc.ca.gov/zev/.

[126] "California Plug-In Electric Vehicle Infrastructure Projections: 2017-2025," [Online]. Available: https://www.nrel.gov/docs/fy18osti/70893.pdf.

[127] "Illinois Center for a Smarter Electric Grid," 2013. [Online]. Available: http://publish.illinois.edu/smartergrid/.

[128] "Smart Grid Resource Center.," [Online]. Available: https://smartgrid.epri.com/SimulationTool.aspx.

[129] G. Krishnamoorthy, "TD-Cosimulation," 2020. [Online]. Available: https://github.com/gayukrishna/TD-Cosimulation.

[130] A. Dubey and S. Santoso, "On estimation and sensitivity analysis of distribution circuit's photovoltaic hosting capacity," *IEEE Transactions on Power Systems,* vol. 32, no. 4, pp. 2779-2789, 2017.

[131] J. Yusuf, A. S. M. J. Hasan and S. Ula, "Impacts Analysis of Electric Vehicles Integration to the Residential Distribution Grid," in *2021 IEEE Kansas Power and Energy Conference (KPEC)*, 2021.

[132] E. D. Kostopoulos, G. C. Spyropoulos and J. K. Kaldellis, "Real-world study for the optimal charging of electric vehicles," *Energy Reports,* vol. 6, pp. 418-426, 2020.

[133] J. Yusuf, A. S. M. J. Hasan and S. Ula, "Impacts of Plug-in Electric Vehicles on a Distribution Level Microgrid," in *2019 North American Power Symposium (NAPS)*, 2019.

[134] J. Yusuf, R. Watanabe, S. Ula, M. Todd and H. Gomez, "Data Driven Stochastic Energy Cost Optimization with V2G Operation in Commercial Buildings," in *2020 52nd North American Power Symposium (NAPS)*, 2021.

[135] ANSI, "ANSI C84.1-2020 American National Standard For Electric Power Systems and Equipment - Voltage Ratings (60 Hz)," 2020.